Università degli Studi di Milano-Bicocca
Dipartimento di Biotecnologie e Bioscienze
Dottorato di ricerca in Biologia e Biotecnologie – XXX Ciclo

Lipopolysaccharide transport and peptidoglycan remodeling: two related processes in *Escherichia coli*.

Niccolò Morè
Matr. 716966

Anno Accademico 2016-2017

SCUOLA DI DOTTORATO
UNIVERSITA' DEGLI STUDI DI MILANO-BICOCCA

Department of

Biotechnology and Biosciences

PhD program : Biology and Biotecnology Cycle XXX

Curriculum in Morphofunctional Biology

Lipopolysaccharide transport and peptidoglycan remodeling: two related processes in *Escherichia coli*.

Surname: Morè Name: Niccolò

Registration number: 716966

Tutor: Prof. Polissi Alessandra

Coordinator: Prof. Vanoni Marco Ercole

ACADEMIC YEAR 2016/2017

Morè Niccolò

Table of contents

Abstract

The cell envelope of Gram-negative bacteria is a complex multi-layered structure consisting of a cytoplasmic and an outer membrane (CM and OM), which delimit the periplasm containing a thin layer of peptidoglycan (PG) called the sacculus. The primary function of the OM is to establish a selective permeability barrier that enables the cell to maintain favourable intracellular conditions even in hash environments and the lipopolysaccharide (LPS) layer greatly contributes to this peculiar property. The integrity of the PG mesh is essential to protect the cell from bursting due to its turgor and maintain the shape of the cell. OM and PG are synthetized and assembled by multiprotein machineries that need to be finely coordinated as imbalanced growth of these layers may compromise structural integrity of the cell. In order to gain more insight in the mechanism by which the cells coordinate the growth of these two layers, we analysed the PG composition when the biogenesis of OM is compromised due to the block of LPS transport. In this work we shown that when OM is impaired *E. coli* cells remodel PG architecture by increasing the non-canonical 3-3 cross-linkage. We can assume that this is a salvage mechanism to prevent cell lysis when OM is damaged.

Abbreviations

ABC	ATP binding cassette
ATP	Adenosine-5'- triphosphate
Bam	β-Barrel assembly machine
C_{55}-P	Undecaprenyl phospate
C-terminal	Carboxy-terminal
CP-ase	Carboxypeptidase
EP-ase	Endopeptidase
Glc*N*Ac	*N*-acetylglucosamine
GTase	Glycosyltransferase
hIM	higher density inner membrane
IM	Inner membrane
Lol	Localization of lipoproteins
Lpp	Braun's lipoptrotein
LPS	Lipopolysaccharide
Lpt	Lipopolysaccharide transport
meso-Dap	*meso*-diaminopimelic acid
Mur*N*Ac	*N*-acetylmuramic acid
NBD	Nucleotide binding domain
N-terminal	Amino-terminus
OM	Outer membrane
OML	Lighter outer membrane fraction
OMP	Integral outer membrane protein
P	Phosphate
PBP	Penicillin binding protein
PG	Peptidoglycan
PL	Phospholipid
SEC	General secretory pathway
TM	Transmembrane
TMD	Transmembrane domain
TP	Transpeptidation
TP-ase	Transpeptidase
UDP	Uridine diphosphate

1. Introduction

1.1 The bacterial cell envelope

The bacterial envelope is a complex structure that functions to protect these organisms from their unpredictable and hostile environment. There are two main types of cell envelopes easily distinguishable based on their response to the Gram-staining procedure. In Gram-positive bacteria the cell envelope is made by the peptidoglycan (murein) sacculus, which encloses the cytoplasmic membrane. On the contrary Gram-negative bacteria, in addition to the peptidoglycan (PG) layer, possess a second membrane called outer membrane (OM) different in many aspects from the cytoplasmic or inner membrane (IM). The presence of a second membrane leads to define "diderm" the Gram-negative organisms as opposed to the Gram-positive "monoderm". The multi-layered structure of the Gram-negative envelope together with its peculiar composition has several implications in growth and propagation of this group of organisms as discussed in the following sections.
Escherichia coli is one of the most studied Gram-negative bacteria and the model organism for our studies.

1.2 Cell envelope architecture in *Escherichia coli*

Gram-negative diderm bacteria typically possess a double membrane system as a part of their envelope structure. While the cytoplasmic membrane or inner membrane (IM) is a symmetrical lipid bilayer made of phospholipids, the outer membrane (OM) is an asymmetrical bilayer containing phospholipids in the inner leaflet and a complex glycolipid, lipopolysaccharide (LPS), in the outer leaflet. IM and OM are separated by an aqueous compartment, the periplasm, which contains a thin layer of peptidoglycan (PG), a polymer that protects the cell from bursting by its internal turgor and maintains the cell shape (Vollmer et al., 2008) (Fig.1).

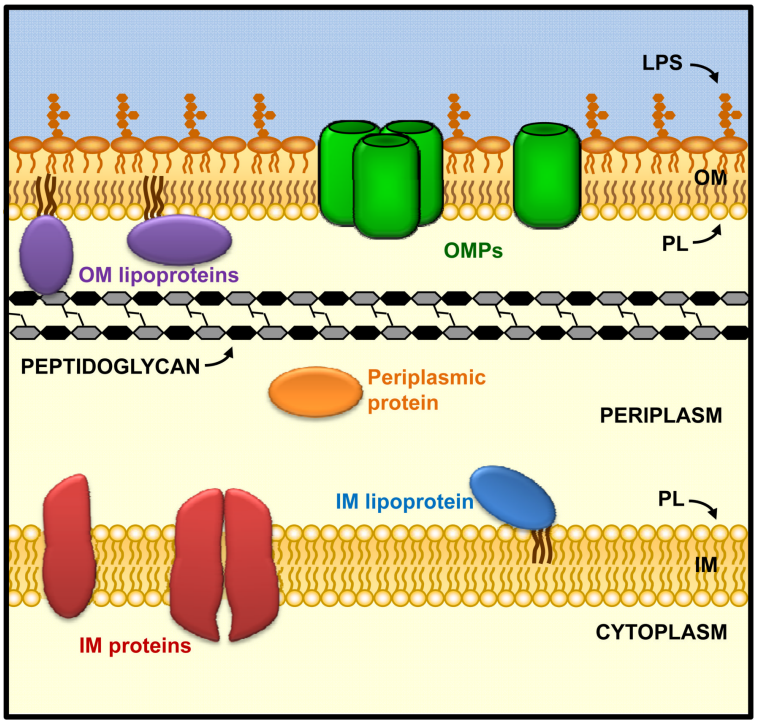

Fig.1 **Schematic representation of the Gram-negative bacteria cell envelope.**
In Gram-negative bacteria, the cytoplasm is surrounded by the inner membrane (IM), a phospholipid (PL) bilayer that contains integral IM proteins and lipoproteins (IM lipoproteins). The aqueous compartment, the periplasm, contains soluble proteins (periplasmic proteins) and a thin layer of peptidoglycan (PG). The outer membrane (OM) is an asymmetrical bilayer, with phospholipid in inner leaflet and lipopolysaccharide (LPS) in the outer leaflet. Integral OM proteins (OMPs) and lipoproteins (OM lipoproteins) are embedded or associated to the OM, respectively. (Copied from Ruiz et al. 2009)

1.2.1 The cytoplasmic membrane

The cytoplasmic or inner membrane (IM) is a classical lipid bilayer composed of phospholipids. The IM proteome of the model organism *E. coli* is composed of IM integral proteins, lipoproteins and peripherally associated proteins (Luirink et al., 2012). IM integral proteins typically span the membrane as α helices almost entirely composed of hydrophobic residues (Silhavy et al., 2010) whereas lipoproteins are located exclusively at the periplasmic side of the IM via an N-terminal N-acyl-dyacylglycerylcysteine residue (Sankaran and Wu, 1994). As the classical lipid bilayers, the IM is endowed of selective permeability and controls the directionality and the entity of the exchanges with the external compartments. Protein complexes at the IM are involved in key processes for the cell such as energy generation and conversion in the respiratory chain, cell division, signal transduction and transport processes (Luirink et al., 2012).

1.2.2 The murein sacculus

Peptidoglycan (PG), also called murein, is an essential component of the cell wall of all bacteria, forming a continuous, mesh-like structure, called the sacculus that encloses the cytoplasmic membrane (IM) (Holtje, 1998). In Gram-negative bacteria the sacculus is made of a single layer of PG with a thickness of 3-6 nm, which is associated with the OM (Vollmer and Seligman, 2010) through covalent binding to Braun's OM lipoprotein (Hantke and Braun, 1973). PG is composed of parallel glycan chains made of alternating *N*-acetylglucosamine (Glc*N*Ac) and *N*-acetylmuramic acid (Mur*N*Ac) residues linked by ß-1,4 glycosidic bonds, with a pentapeptide linked to the Mur*N*Ac moiety. In *E coli* and many Enterobacteriaceae the composition of pentapeptide is the following: *L*-Ala-*D*-Glu-*m*-Dap-*D*-Ala-*D*-Ala (*m*-Dap, *meso*-diaminopimelic acid) (Schleifer and Kandler, 1972). This short peptide ensures the crosslinking between different glycan chains to generate a matrix-like shell.

1.2.3 Outer Membrane

Gram-negative bacteria possess an additional membrane, the OM, located external to the PG layer. The OM is a peculiar asymmetric bilayer containing phospholipids in the inner leaflet and the complex glycolipid, LPS, in the outer leaflet (Silhavy et al., 2010). LPS is an unusual glucosamine-based saccharolipid, with a tripartite structure: lipid A (the hydrophobic moiety that anchors LPS to the OM), a core oligosaccharide and an O-antigen made of repeating oligosaccharide units (Raetz and Whitfield 2002). The OM acts as a peculiar permeability barrier protecting the cell from many toxic compounds such as bile salts, detergents, and antibiotics thus allowing Gram-negative bacteria to colonize many hostile environments. The LPS structure and its peculiar arrangement into the outer leaflet largely contribute to the unique permeability barrier properties of the OM. Indeed, the LPS molecules form a very tightly packed layer due to strong lateral interactions between molecules mediated by the bridging action of divalent Mg^{2+} and Ca^{2+} cations. Therefore, the LPS outer layer is the major factor accounting for the low permeability of hydrophobic solutes across the OM (Nikaido, 2003).

The vast majority of integral proteins in the OM (outer membrane proteins, OMPs) consists of amphipathic β-strands which adopt a β-barrel structure in contrast to the IM integral proteins which span the membrane as α-helices almost entirely composed of hydrophobic residues, (Fairman et al., 2011 - Schulz, 2002). The large number of OMPs is constituted by porins, a family of proteins,

which form specific and non-specific channels that orchestrate the flux of hydrophilic molecules across the OM (Zeth and Thein, 2010).

Besides integral membrane proteins the OM contains also lipoproteins which possess the canonical lipid modification at the N-terminal end for OM anchoring (Sankaran and Wu, 1994). Lipoproteins at the OM can be either exposed at the cell surface (Konovalova and Silhavy, 2015) or can be attached to the OM inner leaflet thus extending into the periplasm (Okuda and Tokuda, 2011). At the OM, lipoproteins serve to several functions including formation and maintenance of cell shape, biogenesis of the OM, transport of a variety of molecules, and signal transduction (Narita and Tokuda, 2016).

1.3. Envelope Biogenesis

The biogenesis of the multi-layered envelope represents a challenge for Gram-negative bacteria, in fact all components of the OM and PG, which are synthesised in the cytoplasm or at IM, need to be transported in compartments outside the cell (periplasm and OM) for their final assembly. This is a very difficult task for the cell, since the compartments outside the IM are devoid of ATP or other energy sources (Ruiz et al., 2006). Thus, the energy required for biogenesis of structures external to the IM such as PG and OM must be provided by exergonic reactions involving substrates energized in the cytoplasm or must be transduced by devices connected to the IM. Commonly these devices are protein machines able to use the energy released by ATP hydrolysis in the cytoplasm or the IM proton motive force (Davidson et al., 2008).

In recent years the protein systems responsible for the assembly of lipoproteins, OMPs, and LPS at the OM as well as for the growth of the PG layer have been identified and several aspects of their functioning have been elucidated.

In the following sections I will initially discuss the biosynthetic reactions that takes place in the cytoplasm and at the IM leading to the synthesis of PG disaccharide pentapeptide precursor unit and the initial polymerization reactions. Then, I will give an overview of the multiprotein complexes (envelope machineries) that orchestrate the growth of the PG sacculus and that assemble the OM layer.

1.3.1 Synthesis of peptidoglycan

The biosynthesis of bacterial cell wall peptidoglycan is a complex process that involves a series of well-conserved enzymatic reactions located in three different cellular compartments: the cytoplasm (synthesis of precursors), the inner leaflet of IM (synthesis of lipid-linked intermediates) and the periplasmic face of the IM (polymerization reactions) (Fig. 2).

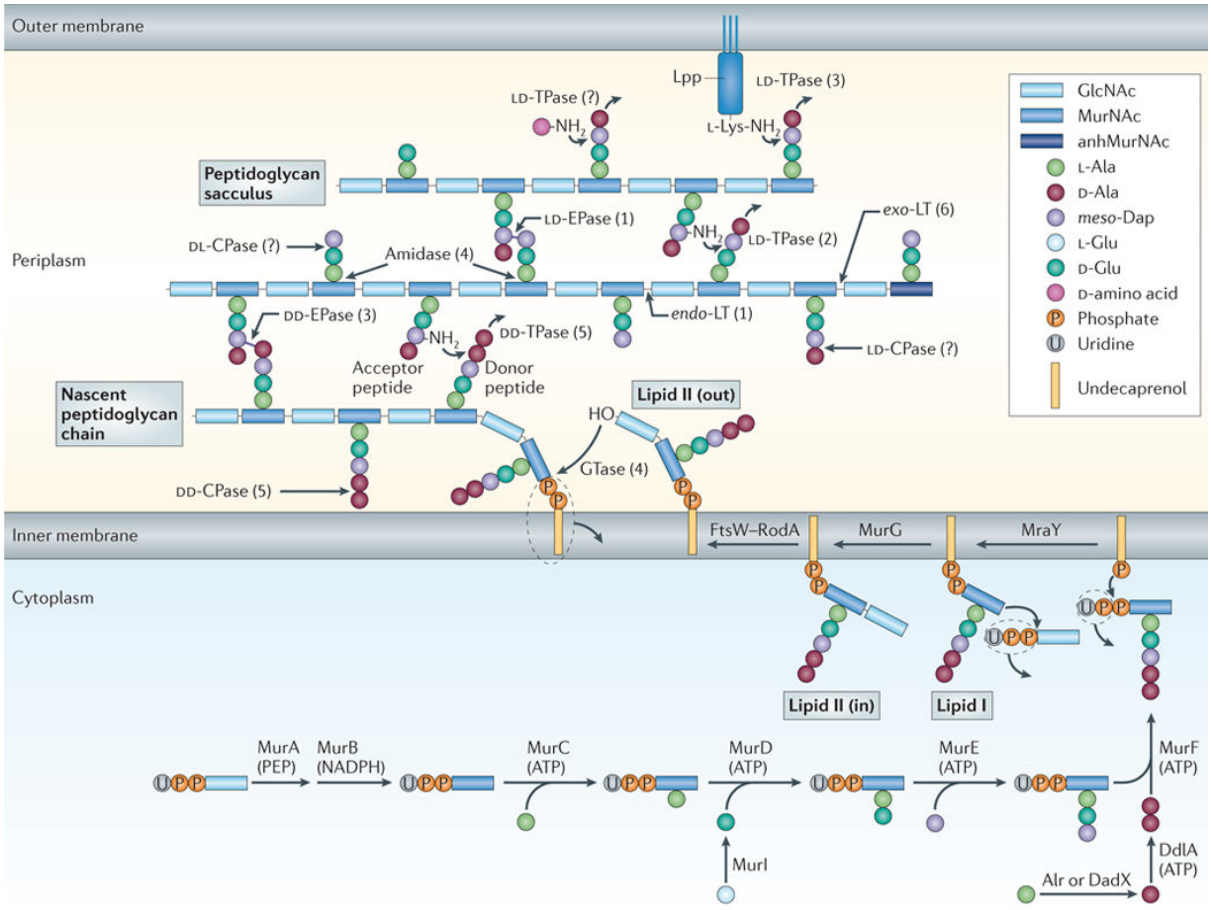

Fig.2 **Peptidoglycan synthesis**

The synthesis and attachment of a new peptidoglycan strand to the existing sacculus are shown.

Precursors are synthesized in the cytoplasm, linked to undecaprenyl phosphate and flipped across the inner membrane. A new glycan chain is synthesised from the disaccharide pentapeptide precursor (lipid II) by glycosyltransferases (GTase) and cross-linked to PG through transpeptidases (DD-, LD-TPase). Peptidoglycan is modified and hydrolysed by different hydrolases: DD-, LD- or DL- carboxypeptidases (CPases) that remove a terminal aminoacid from the peptide (DD-CPases cleave between D-Ala-D-Ala, LD- between meso-Dap-D-Ala and DL-between D-Glu-meso-Dap), and crosslinks are cleaved by the DD-, LD-, DL- endopeptidases (EPases). Lytic transglycosylases (LTs) cleave within (endo-LTs) or at the terminal (exo-LTs) of glycan strands producing 1,6-anhydro-Mur*N*Ac, and amidases remove peptides from glycan chains. (Copied from Typas et al., 2011)

Synthesis of PG begins in the cytoplasm with the synthesis of the precursors UDP-Glc*N*Ac and UDP-Mur*N*Ac. UDP-Glc*N*Ac biosynthesis from fructose-6-phosphate requires the activity of the Glm enzymes. After the formation of the UDP-Glc*N*Ac precursor, two enzymes (MurA and MurB) convert UDP-Glc*N*Ac in UDP-Mur*N*Ac. MurA (also known as MurZ) catalyses the first step of this reaction and the resulting product undergoes a reduction catalysed by MurB.

The stepwise assembly of the peptide stem of peptidoglycan is ensured by a series of four essential enzymes, known as the Mur ligases (MurC, D, E and F). These proteins catalyse the additions of *L*-alanine (MurC), *D*-glutamic acid (MurD), *m*-Dap, (MurE) and dipeptide *D*-Ala-*D*-Ala (MurF) onto the D-lactoyl group of UDP-Mur*N*Ac (Barreteau et al., 2008). The dipeptide (*D*-Ala-*D*-Ala) is synthetized by the Ddl ligases and added in a single step by MurF.

The disaccharide pentapeptide precursor is synthesised at the cytoplasmic face of the IM linked to undecaprenyl phosphate (C_{55}-P), its carrier lipid. The UDP-Mur*N*Ac-pentapeptide moiety is initially transferred to the undecaprenyl phosphate by the MraY transferase to form the lipid I moiety. Then, MurG catalyses the transfer of the Glc*N*Ac moiety from UDP- Glc*N*Ac to lipid I to generate undecaprenyl-pyrophosphoryl-Mur*N*Ac-pentapeptide-Glc*N*Ac, the disaccharide pentapeptide precursor, also named lipid II. Once the synthesis at the cytoplasmic face of the IM is complete the lipid II moiety needs to be translocated at the periplasmic face of the IM where the final steps of PG synthesis occur (Bouhss et al., 2008).

Three different proteins have been proposed to function as lipid II flippases in *E. coli* MurJ and the RodA and FtsW members of the SEDS (shape, elongation, division, and sporulation) family of proteins (Ruiz et al., 2008 - Mohammadi et al., 2011), but the more recent data support the role of MurJ instead of RodA and FtsW as the lipid II flippase in *E. coli* (Sham et al., 2014).

The two last steps that allow polymerization of the disaccharide pentapeptide moiety of lipid II into nascent glycan strands, take place in the periplasm. These steps are catalysed by membrane-bound glycosyl transferases (GTases) and transpeptidases (TPases) called penicillin-binding proteins (PBPs) so named because they are the primary target of β-lactam antibiotics (Holtje, 1998). The transglycosylation step in murein synthesis produces the glycan strands using lipid II as substrate; GTases catalyse the formation of β-1,4-glycosidic linkage between Glc*N*Ac of lipid II and Mur*N*Ac residues of the growing glycan chain, causing the release of undecaprenyl pyrophosphate. Peptides protruding from different glycan chains are then cross-linked by TPases that catalyse the transpeptidation reaction (see the following sections for details).

1.3.2 *The murein synthases*

The major enzymes implicated in PG polymerization and cross-linking, can be divided in three categories: bifunctional GTase-TPase (class A penicillin binding proteins – aPBPs), monofunctional TPase (class B penicillin binding proteins – bPBPs) and monofunctional GTase (Sauvage, et al., 2008). All murein synthases are anchored to the cytoplasmic membrane by a single transmembrane region (Vollmer and Bertsche, 2008). PBP1A, PBP1B and PBP1C constitute the aPBPs class in *E. coli*; PBP1A and PBP1B have a major and semi-redundant role in PG synthesis since either can be deleted but loss of both is lethal (Denome et al., 1999). PBP1A localises preferentially to the later wall and is one of the major components of the multiprotein complex that directs PG synthesis during cell elongation (elongasome machinery). PBP1B localises predominantly to the mid-cell and is one of the core components of the multiprotein complex that govern the synthesis of PG during cell division (divisome machinery) (See paragraph 1.4.2 below). The role of PBP1C *in vivo* is unknown at the moment (Schiffer and Holtje, 1999). PBP2 and PBP3 are monofunctional TPase belonging to class B (bPBPs); TPase activity of PBP2 is essential for cell elongation and maintenance of the rod shape (Spratt, 1975), whereas PBP3 has been shown to be essential for cell division (Spratt, 1975). Finally, there is the monofunctional GTase class, represented by MgtA, that is able to polymerize glycan strand but is not able to cross-links the peptides (Hara and Suzuki, 1984).

Transpeptidation reaction

DD-type

Peptides protruding from different glycan chains are cross-linked by TPase reaction. In *E. coli* and many Enterobacteriaceae the majority (95% to 98%) of the cross-links is of the DD-type or 4-3 type, which are formed between the carboxyl group of D-Ala (position 4) of one peptide and the amino-group of *meso*-Dap (position 3) of another stem peptide, and are catalysed by the PBPs (DD-TPases). This class of enzymes carries a serine in the active site that attacks the peptide bond between the two terminal D-Alanines of the donor to form an intermediate acyl-enzyme complex which is cleaved by the amine-group of the *meso*-Dap residue of the acceptor peptide to release the enzyme and form the cross-link (Terrak et al., 1999). The energy for this reaction is obtained from the cleavage of the D-Ala-D-Ala bond of the pentapeptide of the donor peptide (Fig. 3).

LD-type

In *E. coli* the 2%-5% of the total crosslinks are 3-3 cross-links, between *meso*-Dap residues of two different stem peptides, which are catalysed by LD-TPases (Magnet et al., 2008, Magnet et al., 2007). Five different LD-TPase have been described in *E. coli*, two of them LdtD and LdtE (formerly YcbB and YnhG) catalysed this unusual 3-3 crosslink (Magnet et al., 2008) (Fig. 3) whereas LdtA, LdtB and LdtC (formerly ErfK, YcfS, YbiS) catalyse the bond between the ε-amino group of the Braun lipoprotein Lpp and the L-carboxyl group of the *meso*-Dap residue in the murein peptide (Braun and Wolff, 1970) thus covalently linking the PG to the OM (Fig. 3). Based on the crystal structure of the *Enterococcus faecium* LD-TPase (Ldt_{fm}), Arthur's group found that the catalytic residue of these LD-TPases contains Cys residue instead of the Ser residue typical of PBPs. This Cys residue is located in a buried pocket accessible by two paths on different sides of the protein. Based on Ldt_{fm} structure it has been suggested that these paths are the binding sites for the acceptor and donor substrates of the LD-TPases (Biarrotte-Sorin et al., 2006). The reason why bacteria produce both 4-3 and 3-3 cross-links remains largely unknown. It has been proposed that the LD-transpeptidation reaction is important for the cell under conditions where no pentapeptides are present in sufficient amounts (Holtje, 1998). More recently several reports have proposed that the 3-3 linkage can act as a mechanism of resistance to β-lactam antibiotics (Goffin and Ghuysen, 2002). Indeed, *Enterococcus faecalis* mutants resistant to β-lactam antibiotics have been shown to reprogramme PG architecture by substituting the 4-3 cross-links formed by the β-lactam sensitive PBP-TPase with the 3-3 bonds formed by Ldt_{fm} a LD transpeptidase which is insensitive to β-lactam antibiotics (Mainardi et al., 2005). A similar mechanism has been shown in *E. coli* where mutants resistant to β-lactam antibiotics increase the expression of the LD-TPase LdtD and consequently the level of 3-3 crosslinks in their PG (Hugonnet et al., 2016). More in general it seems that the presence of 3-3 cross linkage has a role in strengthening the PG meshwork under stress conditions as witnessed also by the increase of the level of 3-3 bonds in "dormant" *Mycobacterium tuberculosis* cells (Lavollay et al., 2008).

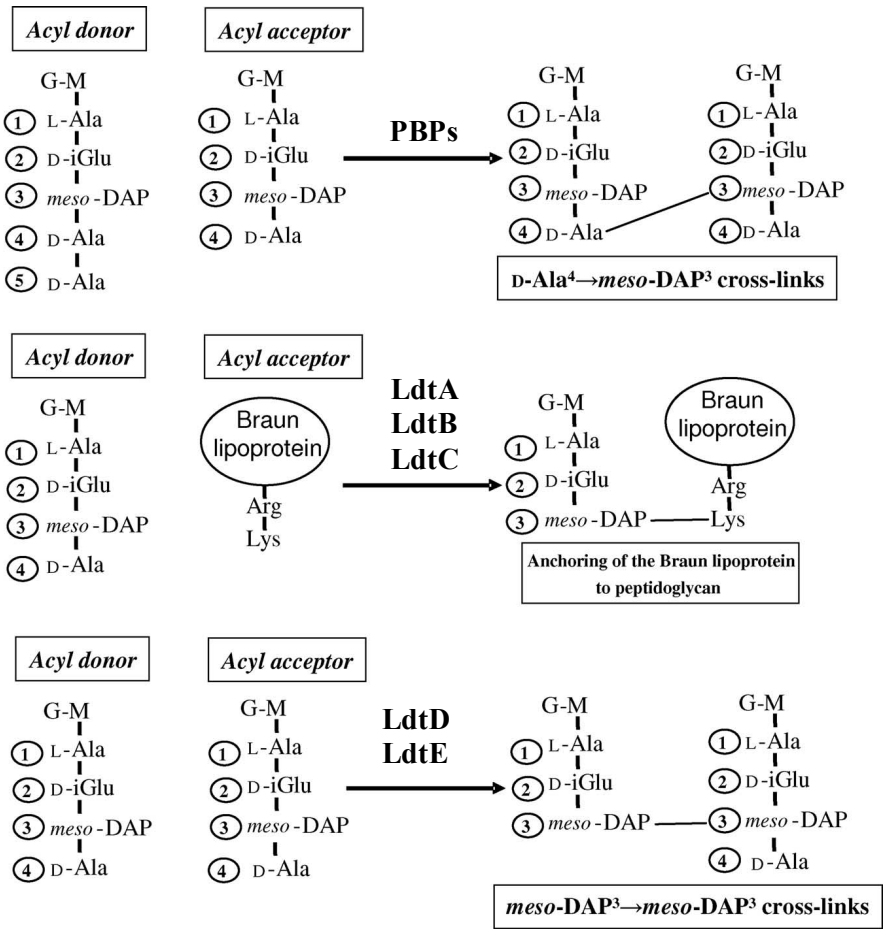

Fig.3 **DD-transpeptidases (PBPs) and LD-transpeptidases in *E. coli***

DD-TPase catalyse the 4-3 cross-links between the D-Ala in position 4 of one stem peptide to meso-DAP in position 3 of another stem peptide and use energy that comes from cleavage of the D-Ala^4-D-Ala^4 bond. LdtA, LdtB nad LdtC are LD-transpeptidases that anchor the Braun lipoprotein (Lpp) to PG. LdtD and LdtE are LD-TPase that catalysed the 3-3 cross-links between two meso-DAP residues of two different stem peptides (Modified from Magnet et al., 2008).

DD-carboxipeptidases

Beside the murein synthases, *E. coli* encodes many hydrolytic enzymes, which are able to cleave every amide and glycosidic linkage in PG. Their activity is fundamental for peptidoglycan growth, during cell cycle and for maintenance bacterial cell shape. Among them class C PBPs have an important role in PG synthesis as PG-modifying activities and are classified by their ability to hydrolyse the peptide bond between the peptide side chains and PG glycan strands through endopeptidase (DD-EPase) activity (PBP4, PBP4b and PBP7) or carboxypeptidase (DD-CPase) activity (PBP5, PBP6a and PBP6b) (Meiresonne et al., 2017).

Guided by their membrane anchors and the availability of their pentapeptide substrates, DD-CPases localise to sites of PG synthesis, where they remove terminal D-Ala residues from pentapeptides stems and reduce the number of donors for the transpeptidation reactions (Typas et al., 2011).

Newly made PG is rich in pentapeptide stems, but these are rapidly cut off by DD-CPases to tetrapeptides. Tetrapeptides cannot function as donors for transpeptidation reaction by class A and B PBPs, but are donors for LD-TPase (Glauner and Holtje, 1990). PBP5 and PBP6a are 62% identical at the amino acid level and share 47% of identity with PBP6b (Baquero et al., 1996). Based on their sequence similarity, it has been suggested that these proteins might have similar physiological functions in the maintenance of the cell shape (Nelson and Young, 2001 – Ghosh and Young, 2003). However, PBP5, PBP6a and PBP6b are primarily expressed in early exponential, stationary and mid-exponential phases, respectively (Buchanan and Sowell, 1982; Baquero et al., 1996; Santos et al., 2002), which may explain their different role in the cell. The main DD-CPase is PBP5 (encoded by the *dacA* gene), indeed cells deleted for *dacA* show aberrant cell morphologies with branches and bends; these defects can be bypassed by the ectopic expression of PBP5 but not by expression of one of the other DD-CPases (Nelson and Young, 2000) suggesting that, despite redundant, PBP5, PBP6A and PBP6b play different roles in the cell. A recent work shows that PBP6a is the only DD-CPase that is up-regulated when the growth rate is reduced under growth in minimal medium, and interestingly, in these conditions PBP6a localised at the division site (Meiresonne et al., 2017). As for the role of PBP6b, Vollmer's group recently published that this CPase is important for cell shape maintenance during growth in acid condition, consistent with the higher activity and stability of this enzyme at low pH (Peters et al., 2016).

1.4 Building the envelope layers: Multiprotein Machineries

As detailed in the previous paragraphs, OM and PG components are synthesised in the cytoplasm or at IM and therefore need to be transported in compartments outside the cell (periplasm and OM) for their final assembly. In recent years the multiprotein complexes responsible for the assembly of lipoproteins, OMPs, and LPS at the OM as well as for the growth of the PG sacculus have been identified and several aspects of their functioning have been elucidated. OMPs and lipoproteins cross the periplasm bound to soluble chaperones, LolA for the lipoproteins (Matsuyama et al., 1997) and a network of others chaperones for the OM ß-barrel proteins. Chaperones deliver their proteins to the OM acceptors; LolB for the lipoproteins (Matsuyama et al., 1997) and Bam complex (ß-barrel assembly machinery) for the OMPs (Hagan et al., 2010) (Fig. 4). The transport and assembly of LPS, at the OM is performed by the Lpt (lipopolysaccharide transport) machinery, a multiprotein complex that spans the entire cell envelope (Okuda et al., 2016) (Fig.5).

The growth of the sacculus during cell cycle is ensured by two PG synthesis machineries (Typas et al., 2012): the cell elongation machinery (elongasome), that promotes lateral growth of the cell, and the cell division machinery (divisome), that controls cell division and daughter cells separation. Importantly, both elongasome and divisome macromolecular complexes also span the entire envelope as they are composed by transmembrane and periplasmic proteins that interact with the OM components of the respective machines (Fig. 6-8).

1.4.1 Cellular machineries required for OM assembly

OMPs and lipoproteins are synthesised as pre-proteins in the cytoplasm and are then secreted across the IM by the Sec translocase, a universally conserved translocation machine that transports unfolded proteins across the IM (Du Plessis et al., 2011).

Lipoprotein sorting: Lol system

Bacterial lipoproteins are characterized by the presence of acyl groups covalently attached at the N-terminal cysteine residue of the mature protein that mediate membrane association (Sankaran and Wu, 1994).

Lipoproteins are synthesized in the cytoplasm as protein precursors with an N-terminal signal sequence and processed into the mature form at the periplasmic side of cytoplasmic membrane, where the modification of the N-terminal cysteine and the cleavage of the signal sequence occur by the sequential action of the three essential enzymes (Karimova et al., 2017). Mature lipoproteins are then sorted to the OM or retained in the IM, depending on the amino acid residue at position 2, which functions as retention or transport signal (Yamaguchi et al. 1988). In *E. coli*, aspartate (D) at position 2 acts as a "default" cytoplasmic membrane retention signal, whereas lipoproteins with other residues at position 2 are actively translocated to the OM by the lipoprotein OM localization (Lol) system, that empowers lipoproteins extraction from the IM, release into the periplasm and insertion in the periplasmic side of the OM. (Yamaguchi et al., 1988).

The Lol system is composed by five essential proteins; at the IM, LolCDE constitute an ABC transporter that mediates the detachment of lipoproteins from the IM and their transfer to the periplasmic chaperone LolA at the expense of the energy of ATP hydrolysis. The hydrophilic complex lipoprotein-LolA crosses the periplasm and LolA transfers its cargo to LolB at the OM, where lipoproteins are incorporated into the lipid bilayer (Okuda and Tokuda, 2011) (Fig. 4 panel

a). Until recently, it was assumed that in *E. coli* all the OM lipoproteins were anchored to the inner leaflet of the OM with the soluble domain facing the periplasm, thus making the LolB-mediated insertion in the OM the last known step in lipoprotein biogenesis. However, the existence of surface exposed lipoproteins in different organisms and the observation that even in *E. coli* many of the best studied lipoproteins show a quite complex topology (some of them are inserted in OMPs, others form a channel in the OM and others are effectively surface-exposed) suggests that additional components are required, beyond the Lol system, for complete lipoprotein maturation to occur (Karimova et al., 2017). However, the mechanisms involved in final assembly of lipoproteins at the cell surface are not fully understood.

OMPs assembly: Bam complex

OMPs precursors cross the IM via the Sec translocon. Once secreted in the periplasm, misfolding of β-barrel OMP precursors is prevented by molecular chaperones, such as SurA and Skp (Ricci and Silhavy, 2012) which deliver OMPs to the Bam complex, a molecular machine driving β-barrel assembly (Ricci and Silhavy, 2012) (Fig.4 -panel b).

The Bam machinery consists of the OM β-barrel protein BamA and four lipoproteins BamB, BamC, BamD, and BamE. The Bam complex is a modular molecular machine in which BamA forms the protein-lipid interface at which OMP substrates enter into the lipid phase of the membrane. BamB interacts with BamA and is proposed to form a scaffold to assist β-barrel folding. BamB, BamC, and BamD and BamE interact with BamA, either directly or indirectly, and form a module suggested to drive a conformational switch in the Bam complex that enables β-barrel insertion into the OM (Ricci and Silhavy, 2012) (Fig.4 – panel b).

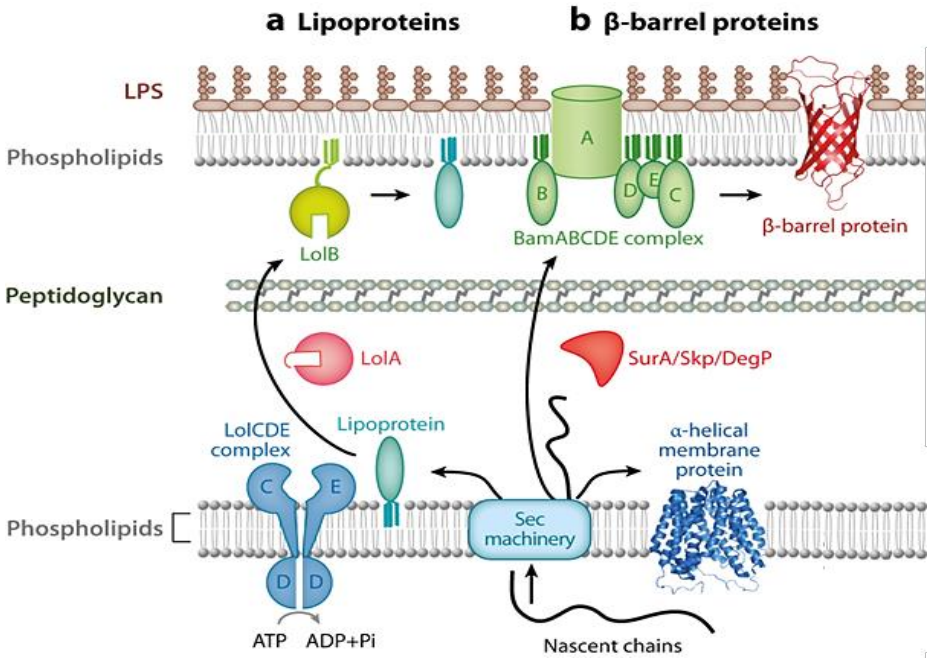

Fig.4 **Lipoproteins and OMPs biogenesis.**

Periplasmic and OM proteins are synthesized as precursors with a signal peptide at their N-terminal end in the cytoplasm and are then translocated across the IM by a Sec translocon. (a) OM lipoproteins are released from the IM in an ATP-dependent fashion and translocated to the OM by the Lol system. (b) OMPs are inserted into the OM from the periplasm by the Bam machine, consisting of the ß-barrel protein, BamA, and four lipoproteins, BamB-C-D-E. Periplasmic chaperones, SurA, Skp and DegP, are involved in the formation of the folded ß-barrel structure. (Copied from Okuda and Tokuda, 2011)

LPS assembly at the cell surface: Lpt machinery

The biosynthesis of LPS is a complex process that occurs in three different cellular compartments, cytoplasm, IM and periplasm. (Raetz and Whitfield, 2002 – Valvano, 2003 – Samuel and Reeves, 2003). The lipid A-core moiety is synthetized at the interface between the IM and the cytoplasm by a conserved pathway (Raetz et al., 2007). The lipid A-core, anchored to the IM, is then flipped across the IM by the ABC transporter MsbA, thus becoming exposed to the periplasm (Polissi and Georgopulos, 1996 – Zhou et al., 1998). O-antigen repeat units are synthesized in the cytoplasm, and then flipped to the periplasmic face of the IM linked to the lipid carrier undecaprenyl diphosphate. The mature LPS molecule is formed at the periplasmic site of the IM where O-antigen repeat units are ligated to lipid A-core by the WaaL ligase (Perez et al., 2008). The mature LPS molecule is then picked up by the Lpt (lipopolysaccharide transport) transenvelope machine that transports LPS to the cell surface. In *E. coli* the Lpt system is a multiprotein complex composed of

seven essential proteins (LptABCDEFG) located in three distinct cellular compartments of the cell envelope, IM, periplasm and OM (Fig. 5). The Lpt proteins physically interact forming a transenvelope bridge, as demonstrated by co-fractionation of all the Lpt proteins in a membrane fraction with lighter density than the OM in sucrose density gradient centrifugation experiments and by co-purification from total membranes (Chng et al., 2010). The transenvelope architecture of the Lpt complex has a functional significance as the depletion of each of the Lpt protein results in accumulation of LPS at the IM suggesting that the Lpt system operates as a single device in LPS transport (Sperandeo et al., 2008). The Lpt complex is organized in two subassemblies: the IM sub-complex $LptB_2CFG$ and the OM sub-complex LptDE, which are connected by the periplasmic protein LptA (Sperandeo et al., 2006 – Braun and Silhavy, 2002 – Wu et al., 2006 – Ruiz et al., 2008). The IM sub-complex ($LptB_2FG$) acts as an ABC transporter responsible for LPS extraction from the IM. LptB is the cytoplasmic component constituting the nucleotide-binding domain (NBD) that associates as a dimer to the IM proteins LptFG (Chng et al., 2010 – Sherman et al., 2014), which are the heterodimeric transmembrane domain (TMD) subunits of the transporter (Ruiz et al., 2008; Luo et al., 2017). LptC is a bitopic protein constituted by a single transmembrane domain and a large periplasmic domain and stably associates to the $LptB_2FG$ transporter (Sperandeo et al., 2008; Narita and Tokuda, 2009). LptA, is the periplasmic component of the machine that interacts with the C-terminal region of LptC and the N-terminal region of LptD via its N- and C-terminal ends, respectively as assessed by UV-photocrosslinking experiments (Freinkman et al., 2012). The OM translocon responsible for the final insertion and assembly of LPS in the OM is constituted by the β-barrel protein LptD (Chng et al., 2010) and the lipoprotein LptE: the two proteins form a complex with a peculiar two-protein plug and barrel architecture (Chng et al., 2010) where LptE resides within the lumen of the LptD barrel. The crystal structure of all Lpt proteins has been solved (Suits et al., 2008 – Tran et al., 2008 – Tran et al., 2010 – Sherman et al., 2014 – Dong et al., 2014 – Qiao et al., 2014 - Botos et al., 2016). Notably, Lpt proteins with periplasmic domains (LptA, LptC LptF, LptG and LptD) share a very similar β–jellyroll architecture, which is indeed used to assemble the whole transenvelope machine (Sperandeo et al., 2017). The β–jellyroll fold plays a crucial role not only in Lpt machine assembly but also in LPS transport across the peripalsm to the OM. Indeed, structural studies indicate that the interior of the Lpt proteins possessing the β–jellyroll structure is highly hydrophobic (Suits et al., 2008) and UV photocrosslinking experiments suggest that the lipid-A moiety of LPS crosses the periplasm inside the hydrophobic channel formed by LptC and LptA while leaving the hydrophilic portion of the molecule exposed in the periplasm (Okuda et al., 2012). The energy required to push LPS along the hydrophobic channel formed by the LptC and LptA is provided by ATP hydrolysis of $LptB_2FG$ complex (Okuda et al., 2012).

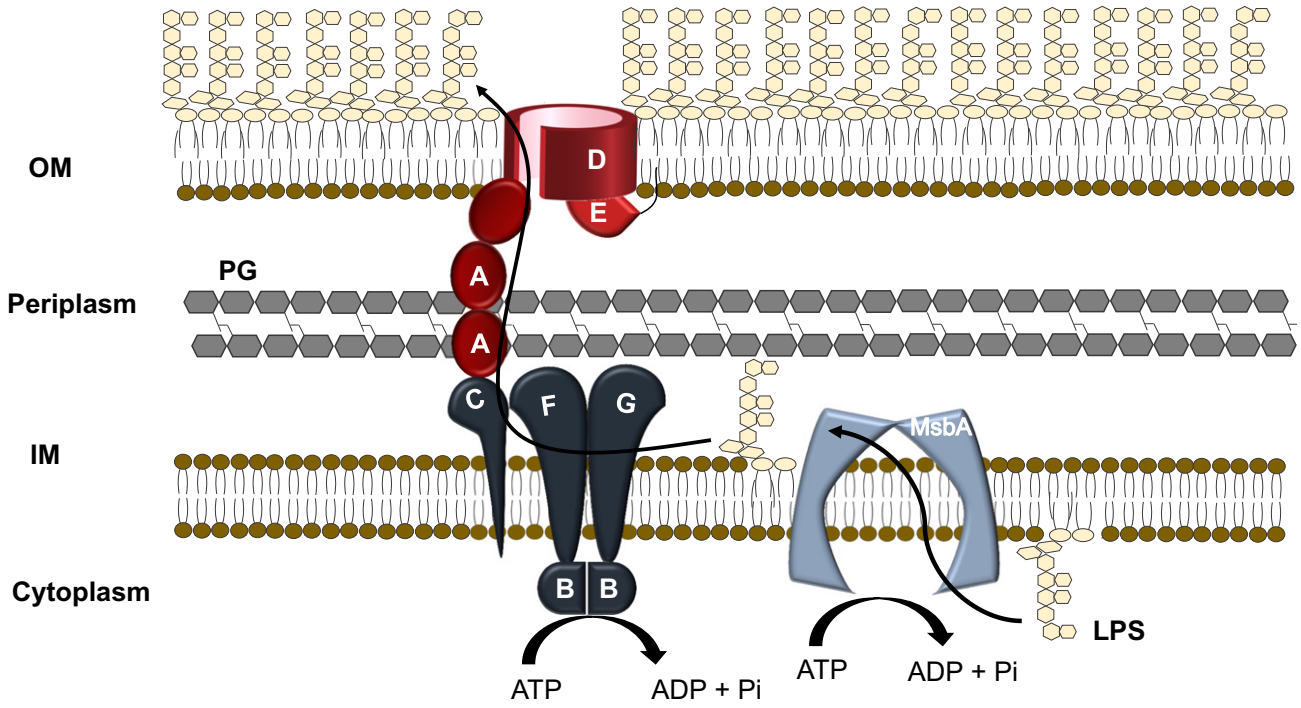

Fig.5 **Transport of LPS across the cell envelope.**

After flipping across the IM by the ABC-transporter MsbA, LPS is transported across the periplasm and assembled at the cell surface. $LptB_2FG$ form an ABC transporter that uses ATP hydrolysis to extract LPS from the IM and to push it along a periplasmic bridge built of homologous domains in LptCAD. At the OM, the LptDE translocon inserts LPS into the outer leaflet of the OM (Copied from Sperandeo et al., 2017).

Finally, the recently solved crystal structures of the LptDE complex from different organisms have revealed clues about the mechanism of final insertion of LPS into the OM lipid bilayer (Dong et al., 2014 – Qiao et al., 2014 – Botos et al., 2016). According to the current model, once delivered by LptA to the N-terminal domain of LptD, the hydrophobic portion of LPS is translocated directly into the membrane through a hydrophobic hole formed between the N-terminal domain of LptD and its β-barrel. Conversely, the sugar portion of LPS enters the lumen of the LptDE translocon and passes laterally through the gate formed in the β-barrel of LptD by the weakened interactions between the first and the last β-strands of the barrel (Dong et al., 2014 – Qiao et al., 2014).

1.4.2 Cellular machineries required for growth of PG sacculus

Murein synthesis during cell growth and division is a complex process where PG structure is continuously remodelled by PG synthases (PBPs) as well an array of PG hydrolases, capable of cleaving bonds in the PG meshwork to allow insertion of newly synthesised material (Vollmer et al., 2008). In rod-shaped bacteria such as *E. coli* building of the sacculus during cell cycle must ensure cellular integrity while maintaining cell shape and morphology. To achieve this, cells employ dynamic multi-protein complexes whose protein composition is variable depending on growth conditions (ionic strength, pH, osmolality as well as stress conditions such as the presence of antibiotics) and cell cycle state. Indeed, these multi-protein machines assemble from freely diffusing sets of PG synthases, PG hydrolases and their regulators to promote optimal synthesis depending on the cell cycle state (elongation or division) and the growth conditions. The elongasome is the machinery that drives PG growth along the longitudinal axis of the cell and the divisome is the machinery that directs PG synthesis at the septum during daughter cells separation (Pazos et al., 2017). These machineries are composed by IM integral membrane proteins, by proteins located on the outside of the IM (periplasmic hydrolases, and PBPs, which harbor large periplasmic domains), and are also intimately associated with cytoplasmic cytoskeletal proteins. Bacterial cytoskeletal elements play an important role in orchestrating PG synthesis and in the maintenance of cellular morphogenesis as witnessed by the fact that the actin homolog MreB is a key factor in elongation of the cell wall whilst the tubulin homolog FtsZ is the central player in the cell division process (Mattei et al., 2010).

1.4.2.1 Elongation machinery

The core components of elongasome include the essential SEDS protein RodA, the monofunctional PBP2 (bPBP) and the bifunctional PBP1A (aPBP). Additional components of the complex are autolysins endopeptidases and probably flippases (Laddomada et al., 2016 – Egan et al., 2017 – Errington, 2015). This complex is spatio-temporally directed by the actin-like protein MreB that localizes to the lateral cell wall of the bacterial cell (Van den Ent et al., 2001). MreB polymerizes in an ATP-dependent manner to form antiparallel filaments that are linked to the IM via the MreB amino-terminus (Salje et al., 2011). The generally accepted model (unified model) postulates that MreB serves to drive PBP1A that polymerizes the glycan strands via its GT-ase activity, while the TP domains of PBP1A and PBP2 crosslink the new polymerised strands and insert this new

material into cell wall gaps opened by the autolysins. According to this model the PG synthesis is driven also from the outside of the cell as the activity of PBP1A is controlled by the outer-membrane lipoprotein LpoA (Typas et al., 2010 – Paradis-Bleau et al., 2010) (Fig. 6- panel A). This model has been recently challenged by Bernhardt and co-workers who showed that MreB and PBP1A operate in two distinct complexes (Cho et al., 2016). This finding together with the understanding that SEDS protein RodA has itself GT-ase activity (Meeske et al., 2016) leads to proposing a new model for PG synthesis during cell elongation (interdependent model). RodA, instead of PBP1A, is the major PG polymerase that likely works with PBP2 which provides crosslinking activity. Since MreB strongly interacts with RodA and RodZ (an additional SEDS protein) and the latter mediates the interaction between MreB and PBP2, it has been proposed that MreB-RodAZ-PBP2 form the so-called Rod complex, which primarily drives cell wall synthesis during cell elongation. According to this model PBP1A works outside the Rod complex in a spatially independent sub-complex (Fig.6 – panel B). However, these two complexes appear to be functionally coupled as inactivation of one or the other leads to the same dramatic decrease in the incorporation of new cell wall material (Cho et al., 2016). Further studies are needed to understand how these two complexes cooperate for PG synthesis in the cell.

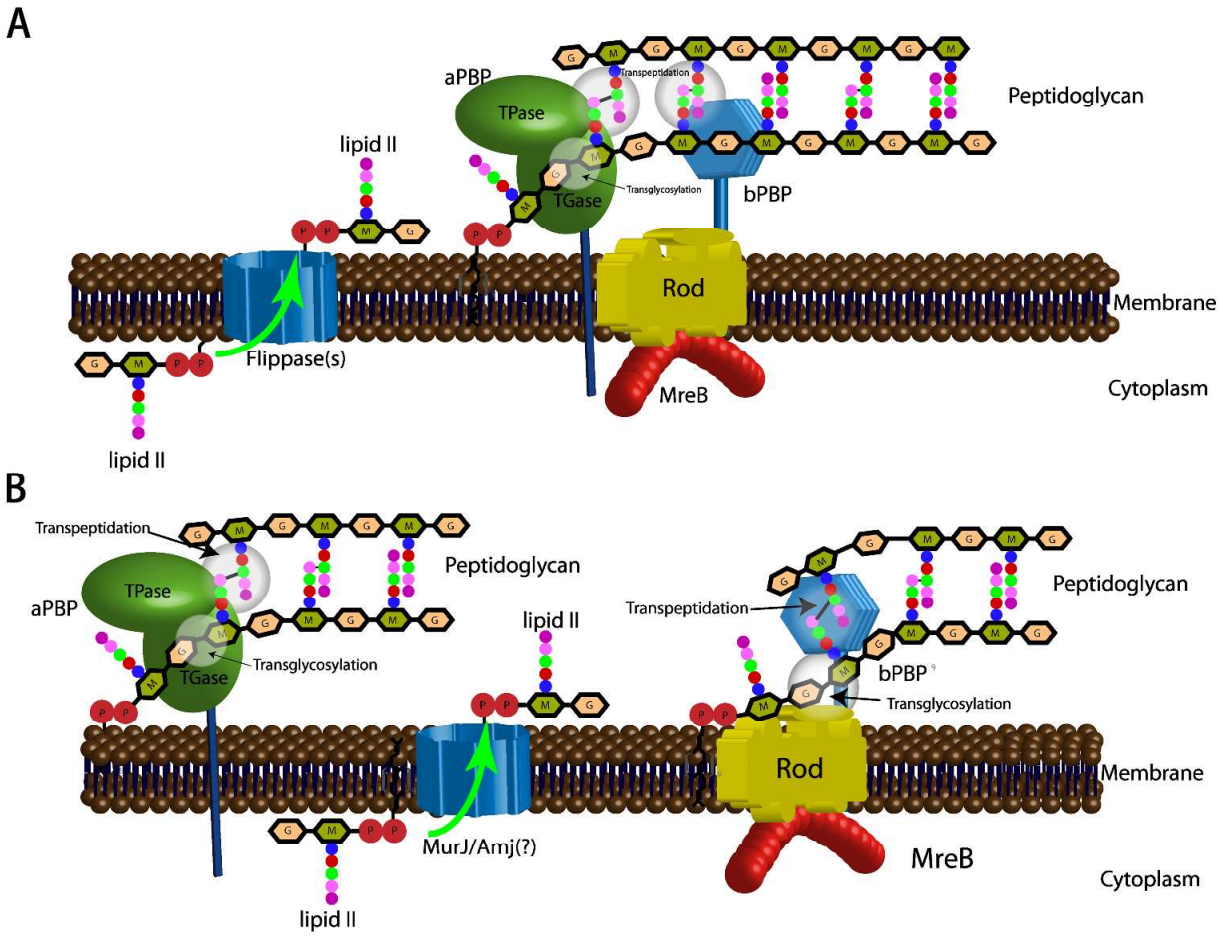

Fig.6 Unified (A) and Interdependent (B) models of PG synthesis complexes during cell elongation.
(A) In the unified model, RodA, RodZ, MreB, aPBP (PBP1A) and bPBP (PBP2) form one protein complex: guided by MreB, the PBP1A protein produces PG strands via GT domain while both PBP1A and PBP2 crosslink these strands into existing PG. (B) In the interdependent model, RodA, RodZ, bPBP (PBP2) and MreB form one unique complex, while aPBP (PBP1A) works in a different spatial and temporal frame. Glycan strands are produced by the GTase RodA and are cross-linked by PBP2 to the existing PG. (Copied from Zhao et al., 2017)

1.4.2.2 Divisome machinery

The divisome is the specialised machinery that controls septal PG synthesis and separation of daughter cells. To date around thirty proteins have been identified as components of the divisome thus highlighting the complexity of such machinery. The components of divisome are located in the cytoplasm, in the IM, in the periplasm and in the OM and communicate via dynamic protein-protein interactions (Egan and Vollmer, 2013 - Typas and Sourjik, 2015). This macromolecular

organization highlights the crucial role of such a multi-protein machine allowing coordination of septal PG synthesis with IM and OM invagination and finally daughter cells separation.

The assembly of the divisome can be divided into two temporally distinct stages. The first stage involves the formation of a Z ring at the future division site by the bacterial tubulin homologue FtsZ, with the help of ZipA and FtsA, which act as FtsZ membrane anchor (Aarsman et al., 2005 – Rowlett and Margollin, 2015) (Fig.7). Such structure formed at mid-cell underneath the IM is the so-called proto-ring (Szwedziak et al., 2014). In the second stage the downstream components FtsK, FtsBLQ, FtsW, FtsI (PBP3) and FtsN join sequentially, some as preformed sub-complexes, (Szwedziack et al., 2014 – Haeusser and Margollin, 2016) to form the mature divisome. The bifunctional PBP1B and its regulators LpoB and CpoB also associate to the mature divisome (Typas et al., 2010 - Gray et al., 2015). Recruitment of FtsN at the divisome is crucial step as its arrival at the Z ring signals the accomplishment of the divisome core assembly and activates septal PG synthesis (Liu et al., 2015 – Tsang and Bernhardt, 2015). Recently it was demonstrated that FtsAZ filaments treadmill in circumferential paths around the division ring pulling along the associated cell-wall-synthesizing enzymes (Bisson-Filho et al., 2017). The rate of FtsZ treadmilling controls both the rate of cell wall synthesis and cell division. The coupling of both the position and activity of the cell wall synthases to FtsAZ treadmilling guides the insertion of new material, synthesizing increasingly small concentric rings to divide the cell. It is not completely understood which are the PG synthases primarily responsible for synthesising septal PG. A possible candidate is FtsW for which a glycosyltransferase activity has been proposed: according to this model FtsW may work in conjunction with PBP3 (a class b PBP), which provides TP activity (Derouaux et al., 2008). However, the bifunctional PBP1b and its LpoB and CpoB regulators also associate to the divisome, and it has been shown that FtsW, PBP3 and PBP1b form a ternary complex in vitro. It is therefore possible that these three proteins work in concert for proper PG synthesis during the last stages of cell division (Leclercq et al., 2017).

The synthesis of septal PG leads to the recruitment and activation of amidases, hydrolytic enzymes that cleave off peptide stem thus splitting cell wall material shared by developing daughter cells to facilitate their separation (Haeusser and Margolin, 2016).

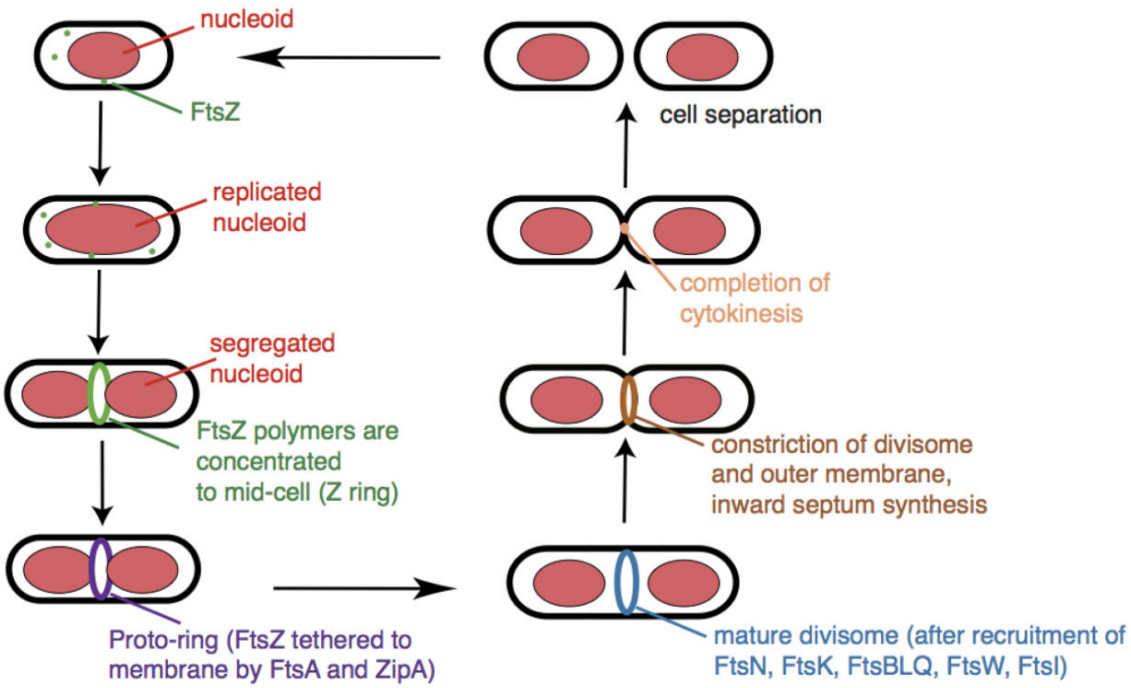

Fig.7 **General overview of bacterial cytokinesis**

After *Escherichia coli* cells replicate and segregate their chromosomes, which are organized as nucleoids, FtsZ and FtsA-ZipA, are concentrated at the mid-cell and organize into the Z-ring, forming the essential proto-ring, which is linked to the membrane. After the recruitment of additional proteins (FtsN, FtsK, FtsBLQ, FtsW, FtsI) the proto-ring progresses to a mature divisome. Mature divisome coordinates the constriction of IM and OM via Tol-Pal system with the functions of specific hydrolases and ingrowing septal PG. After this step the cells are ready to separate in two daughter cells of approximately equal size. (Copied from Haeusser and Margolin, 2016)

Septal cleavage needs to be closed after the cell separation by the OM invagination. OM constriction is ensured by the Tol-Pal (PG-associated lipoprotein) complex, which connects physically the IM with the OM and coordinates the spatio-temporally series of events during membrane invagination (Gerding et al., 2007) (Fig. 8).

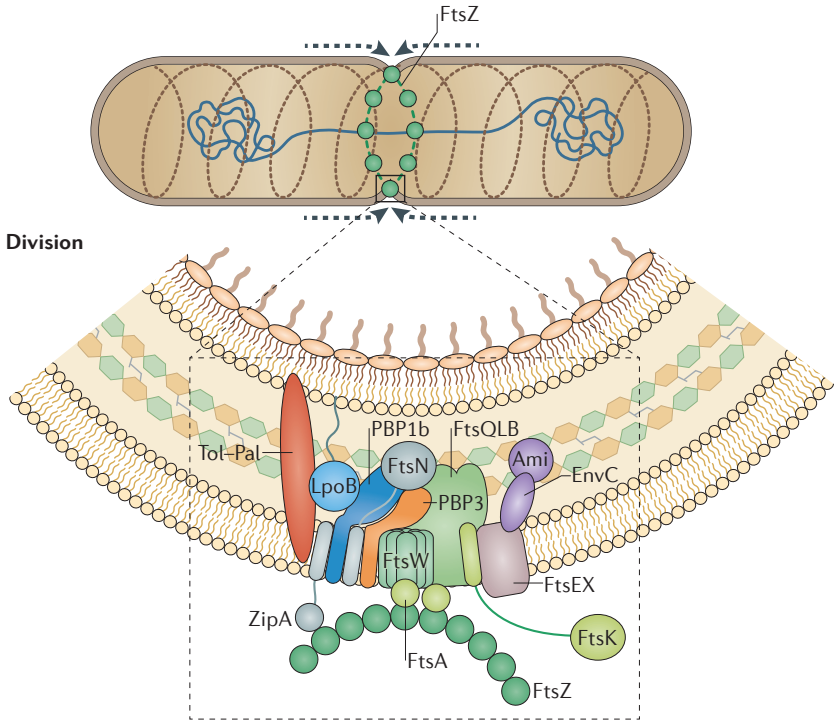

Fig. 8 **Model of PG synthesis complex during cell division.**

The cell division complex assembles at the mid-cell for the synthesis and cleavage of septal PG to produce new cell poles of the daughter cells. FtsZ, a tubulin-like protein, recruits the proto-ring (FtsA-ZipA) at the future division site. Maturation of divisome takes place by the recruitment of proteins in a hierarchical manner with a precise spatio-temporal coordination. (Copied from Typas and Sourjik, 2015)

1.4.2.3 Models for the growth of the sacculus

During the cell growth, the surface of the sacculus is enlarged by addition of new PG material and, as highlighted previously, new incorporation needs the action of PG hydrolases that open the "old" PG layer allowing the insertion of nascent chain (Vollmer et al., 2008). Clearly, PG lytic and synthetic processes need to be tightly regulated to maintain the structural integrity of the sacculus. Initially, it was suggested a "*make before break*" model in which new bonds need to be formed before that the hydrolases cleave the old bonds in the PG (Koch, 1995). Several years later, based on the results of pulse-labelling experiments, Holtje proposed a "*3 for 1*" model in which three new glycan chains are generated and linked in a single "old" docking strand which is at the same time hydrolysed and removed ensuring the space for the insertion of the three new glycan strands (Holtje, 1998). This model explains the high amount of PG turnover observed in growing cells.

The recent discovery that two interdependent complexes may work together in the elongasome machinery (Cho et al., 2016) leads to the proposal of a new model named "*break before make*". According to this model, endopeptidases associated the elongasome machinery cleave the existing crosslinks in the "old" PG creating a space for the insertion of new PG generated by the action of RodA and cross-linked to the existing PG via bPBPs. To ensure the maintenance of structural integrity of the cell wall, aPBP (PBP1A) is supposed to "follow" the RodA machine to generate additional strands of new PG, which are crosslinked with new PG on one side and "old" PG on the other (Zhao et al., 2017) (Fig. 9).

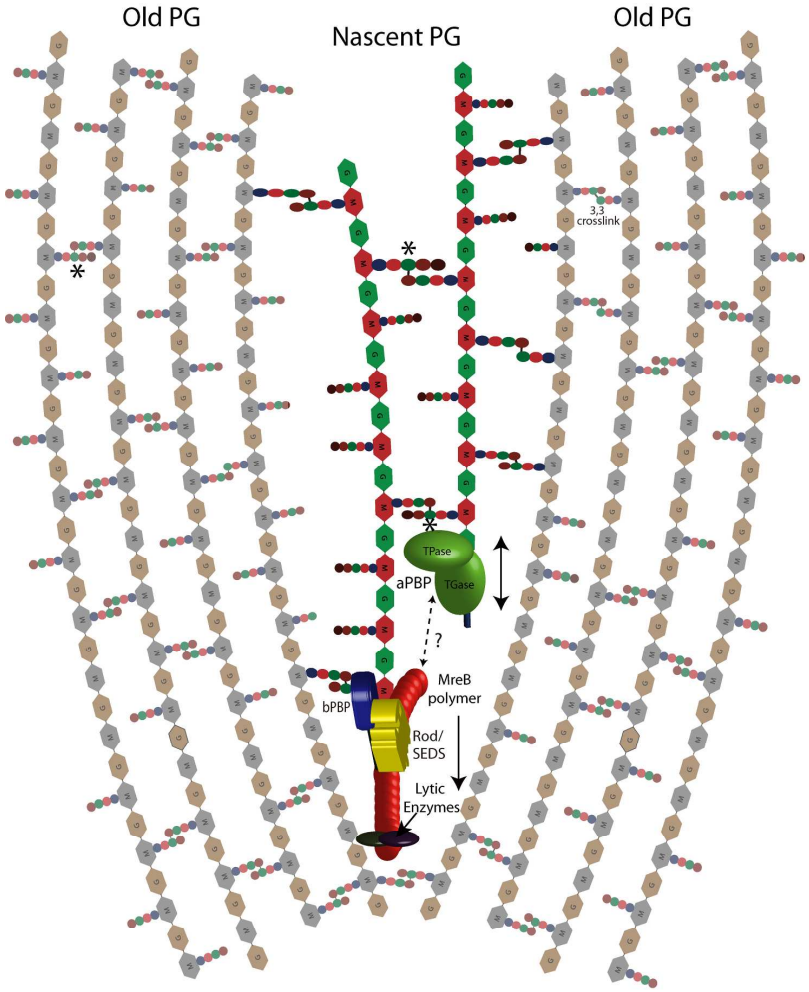

Fig.9 **PG Synthesis complexes in the "break before make" model.**

Lytic enzymes, associated to the Rod-SEDS-MreB complex (elongasome machinery), cleave the cross-links in the existing PG, later RodA synthetizes a new PG template strand, which is linked to the PG via bPBP. At the same time, aPBP, that works in a differential frame, generates additional strand of new PG with the GTase domain and links them, with TPase domain, to the existing PG (Copied from Zhao et al., 2017).

1.4.2.4 How bacteria coordinate PG and OM layers growth?

Our knowledge of how Gram-negative bacteria coordinate the growth of their multi-layered envelope is very limited. Since the bacterial envelope is built by multiprotein machineries it is very likely that their activity is finely coordinated. Two seminal works showed that the activity of two major aPBPs, PBP1A and PBP1B components of elongasome and divisome, respectively, is controlled by the OM cognate lipoproteins LpoA and LpoB (Typas et al., 2010 - Paradis-Bleau et al., 2010). These findings suggest that the synthesis of the PG in controlled not only from the inside via cytoskeletal elements but also from the outside via OM lipoproteins. A link between OM and PG biogenesis has also emerged from two recent papers. Grabowicz et al., (2014) showed that point-mutation in the gene for O-antigen ligase (WaaL) in *E. coli* generates a modified LPS (LPS^{*}) decorated by PG subunits; Martorana et al., (2014) showed that block of LPS transport modulates the level of several proteins involved in PG synthesis/turnover. The results obtained in these two works nicely intersect in different ways PG and OM biogenetic pathways. Finally, in a recent paper it has been shown that the envelope machine facilitating septal PG synthesis (PBP1B-LpoB complex) interacts with the Tol-Pal system to ensures proper OM constriction during cell division (Gray et al., 2015). The coordination between these two complexes requires the protein CpoB (Coordinator of PG synthesis and OM constriction associated with PBP1B), which interact with both PBP1B and the Tol-Pal complex. The PBP1B protein produces new cell wall material to fill the gaps in the PG of the two daughter cells, while Tol-Pal system provides the energy necessary for the invagination of the OM. CpoB takes part in this process regulating the activity of PBP1B in response to signal coming from the Tol system.

Clearly, we are at the beginning in understanding how OM biogenesis and PG growth are coordinated and additional studies are required to deeply explore this field.

2. Bibliography

1. Aarsman, M.E., Piette, A., Fraipont, C., Vinkenvleugel, T.M., Nguyen-Disteche, M., den Blaauwen, T. (2005) Maturation of the *Escherichia coli* divisome occurs in two steps. *Mol.Microbiol*. 55, 1631-1645
2. Adams, D. and Errington, J. (2009) Bacterial cell division: assembly, maintenance and disassembly of the Z-ring. *Nat.Rev.Microbiol.* 7, 642-653
3. Banzhaf, M., van den Berg., van Sparoea, B., Terrak, M., Fraipont, C., Egan, A., Philippe, J., ZApun, A., Breukink, E., Nguyen-Disteche, M., den Blaauwen, T., Vollmer, W. (2012) Cooperativity of peptidoglycan synthases active in bacterial cell elongation. *Mol. Microbiol.* 85, 179-194
4. Baquero, M.R., Bouzon, M., Quintela, J.C., Ayala, J.A., Moreno, F. (1996) *dacD*, an *Escherichia coli* gene encoding a novel penicillin-binding protein (PBP6b) with DD-carboxypeptidase activity. *J. Bacteriol.* 178, 7106-7111
5. Barreteau, H., Kovac, A., Boniface, A., Sova, M., Gobec, S., Blanot, D. (2008) Cytoplasmic steps of peptidoglycan biosynthesis. *FEMS Microbiol.Rev.* 32, 168-207
6. Benz, R. Structure and function of porins from Gram-negative bacteria. (1988) *Annu. Rev. Microbiol.* 42, 359-393
7. Biarrotte-Sorin, S., Hugonnet, J.E., Delfosse, V., Mainardi, J.L., Gutmann, L., Arthur, M., Mayer, C. (2006) Crystal structure of a novel beta-lactam-insensitive peptidoglycan transpeptidase. *J. Mol. Biol.* 359, 533-538
8. Bisson-Filho, A.W., Hsu, Y.P., Squyres. G.R., Kuru, E., Wu, F., Jukes, C., Dekker, C., Holden, S., VanNieuwenhze, M.S., Brun, Y.V., Garner, E.C. (2017) Treadmilling by FtsZ filaments drives peptidoglycan synthesis and bacterial cell division. *Science* 355, 739-743
9. Bos, M.P., Robert, V., Tomassen, T. (2007) Biogenesis of the Gram-negative bacterial uter membrane. *Annu. Rev. Microbiol.* 61, 191-214
10. Botos, I., Majdalani, N., Mayclin, S.J., McCarthy, J.G., Lundquist, K., Wojtowicz, D., Barnard, T.J., Gumbart, J.C., Buchanan, S.K. (2016) Structural and functional characterization of the LPS transporter LptDE from Gram-negative pathogens. Structure. 24, 965-976
11. Bouhss, A., Trunkfiel, A.E., Bugg, T.D.H., Mengin-Lecreulx, D. (2008) The biosynthesis of peptidoglycan lipid-linked intermediates. *FEMS Microbiol.Rev*. 32, 208-233
12. Braun, M., Silhavy, T.J. (2002) Imp/OstA is required for cell envelope biogenesis in *Escherichia coli*. *Mol.Microbiol*. 45, 1289-1302
13. Braun, M. and Wolff, H. (1970) The murein-lipoprotein linkage in the cell wall of

Escherichia coli. Eur. J. Biochem. 14, 387-391

14. Buchanan, C.E. and Sowell, M.O. (1982) Synthesis of penicillin-binding protein 6 by stationary-phase *Escherichia coli. J. Bacteriol.* 151, 491- 494
15. Chng, S.S., Gronenberg, L.S. and Kahne, D. (2010) Proteins required for lipopolysaccharide assembly in *Escherichia coli* form a transenvelope complex. *Biochemistry* 49, 4565-4567
16. Chng, S.S., Ruiz, N., Chimalakonda, G., Silhavy, T.J., Kahne, D. (2010) Characterization of the two-protein complex in *Escherichia coli* responsible for lipopolysaccharide assembly at the outer membrane. *Proc.Natl.Acad.Sci.USA* 107, 5363-5368
17. Cho, H., Wivagg, C.N., Kapoor, M., Barry, Z., Rohs, P.D., Suh, H., Marto, J.A., Garner, E.C. and Bernhardt, T.G. (2016) Bacterial cell wall biogenesis is mediated by SEDS and PBP polymerse families functioning semi-autonomously. *Nat.Microbiol.* 16172
18. Davidson, A.L., Dassa, E., Orelle, C., Chen, J. (2008) Structure, function and evolution of bacterial ATP binding cassette system. *Microbiol. Mol. Biol. Rev.* 72, 317-364.
19. Denome, S.A., Elf, P.K., Henderson, T.A., Nelson, D.E., Young, K.D. (1999) *Escherichia coli* mutants lacking all possible combinations of eight penicillin binding proteins: viability, characteristics, and implications for peptidoglycan synthesis. *J. Bacteriol.* 181, 3981-3993
20. Derouaux, A., Wolf, B., Fraipont, C., Breukink, E., Nguyen-Distèche, M., Terrak, M. (2008) The monofunctional glycosyltransferase of *Escherichia coli* localizes to the cell division site and interacts with penicillin-binding protein 3, FtsW, and FtsN. *J. Bacteriol.* 190, 1831-1834
21. Dong, H., Xiang, Q., Gu, Y., Wang, Z., Paterson, N.G., Stansfeld, P.J., He, C., Zhang, Y., Wang, W., Dong, C. (2014) Structural basis for outer membrane lipopolysaccharide insertion. *Nature*. 511, 52-56
22. Du Plessis, D.J., Nouwen, N., Driessen, A.J. (2011) The Sec traslocase. *Biochim Biophys. Acta* 1808, 851-865
23. Egan, A. J. F., Biboy, J., Veer, I., Breukink, E. and Vollmer, W. (2015) Activities and regulation of peptidoglycan synthases. *Phil. Trans. R. Soc. B.* 370:20150031
24. Egan, A.J. and Vollmer, W. (2013) The physiology of bacterial cell division. *Ann.N.Y. Acad.Sci.* 1277, 8-28
25. Egan, A.J., Cleverley, R.M., Peters, R., Lewis, R.J. and Vollmer, W. (2017) Regulation of bacterial cell wall growth. *FEBS J.* 284, 851-867
26. Errington, J. (2015) Bacterial morphogenesis and the enigmatic MreB helix. *Nat.Rev. Microbiol.* 13, 241-248

27. Fairman, J.W., Noinaj, N. and Buchanan, S.K. (2011) The structural biology of beta-barrel proteins: a summary of recent reports. *Curr.Opin.Struc.Biol.* 21, 523-531
28. Freinkman, E., Chng, S.S. and Kahne, D. (2011) The complex that inserts lipopolysaccharide into the bacterial outer membrane forms a two-protein plug and barrel. *Proc.Natl.Acad.Sci.USA* 108, 2486-2491
29. Freinkman, E., Okuda, S., Ruiz, N., Kahne, D. (2012) Regulated assembly of the transenvelope protein complex required for lipopolysaccharide export. *Biochemistry.* 51, 4800-4806
30. Gerding, M.A., Ogata, Y., Pecora, N.D., Niki, H. amd de Boer, P.A. (2007) The trans-envelope Tol-Pal complex is part of the cell division machinery and required for proper outer-membrane invagination during cell constriction in *E. coli. Mol. Microbiol.* 63, 1008-1025
31. Glauner, B. and Holtje, J.V. (1990) Growth pattern of the murein sacculus of *Escherichia coli. J. Biol. Chem.* 265, 18988-18996
32. Ghosh, A.S. and Young, K.D. (2003) Sequences near the active site in chimeric penicillin binding proteins 5 and 6 affect uniform morphology of *Escherichia coli. J. Bacteriol.* 185, 2178-2186
33. Goffin, C. and Ghuysen, J.M. (2002) Biochemistry and comparative genomics of SxxK superfamily acyltransferases offer a clue to the Mycobacterial paradox: presence of Penicillin-susceptibile target proteins versus lack of efficiency of Penicillin as therapeutic agent. M*icrobiol. Mol. Biol. Rev.* 66, 702-738
34. Gray, A.N., Egan, A.J., Van't Veer, I.L., Verheul, J., Colavin, A., Koumoutsi, A., Biboy, J., Altelaar, A.F., Damen, M.J., Huang, K.C., Simorre, J.P., Breukink, E., den Blauween, T., Typas, A., Gross, C.A., Vollmer, W. (2015) Coordination of peptidoglycan synthesis and outer membrane constriction during *Escherichia coli* cell division. *Elife.* 4, doi: 10.7554/eLife.07118.
35. Grabowicz, M., Andres, D., Lebar, M.D., Malojcic, G., Kahne, D., Silhavy, T.J. (2014) A mutant *Escherichia coli* that attaches peptidoglycan to lipopolysaccharide and displays cell wall on its surface. *Elife.* 3:e05334. doi: 10.7554/eLife.05334.
36. Haeusser, D.P. and Margolin, W. (2016) Splitsville: structural and functional insight into the dynamic bacterial Z ring. *Nat.Rev.Microb.* 14, 305-319
37. Hagan, C.L., Kim, S., Kahne, D. (2010) Reconstitution of outer membrane protein assembly from purified components. *Science* 328, 890-892

38. Hantke, K., Braun, V. (1973) Covalent binding of lipid to protein. Digliyceride and amidelinked fatty acid at the N-terminal end of murein-lipoprotein of the *Escherichia coli* outer membrane. *Eur. J. Biochem.* 34, 284-296
39. Hara, H. and Suzuki, H. (1984) A novel glycan polymerase that synthesizes uncross-linked peptidoglycan in *Escherichia coli. FEBS Lett.* 168, 155-60
40. Heidrich, C., Templin, M.F., Ursinus, A., Merdanovic, M., Berger, J., Schwarz, H., de Pedro, M.A., Holtje, J.V. (2001) Involvement of N-acetylmuramyl-L-alanine amidases in cell separation and antibiotic-induced autolysis of *Escherchia coli. Mol. Microbiol.* 41, 167-178
41. Holtje, J.V. (1998) Growth of the stress-bearing and shape-maintainig murein sacculus of *Escherchia coli. Microbiol. Mol. Bio. Rev.* 62, 181-203.
42. Hugonnet, J.E., Mengin-Lecreulx, D., Monton, A., den Blaauwen, T., Carbonnelle, E., Veckerlè, C., Brun, Y.V., van Nieuwenhze, M., Bouchier, C., Tu, K., Rice, L.B., Arthur, M. (2016) Factors essential for L,D-transpeptidase mediated peptidoglycan cross-linking and β-lactam resistance in *Escherichia coli. Elife.* 5. pii: e19469. doi: 10.7554/eLife.19469.
43. Koch, A.L. (1995) Bacterial growth and form. Chapman & Hall, New York.
44. Konovalova, A. and Silhavy, T.J. (2015) Outer membrane lipoprotein biogenesis: Lol is not the end. *Philos. Trans. R. Soc. Lond. B. Biol. Sci.* 370, 1679 doi: 10.1098/rstb.2015.0030.
45. Laddomada, F., Miyachiro, M.M. and Dessen.A (2016) Structural insight into Protein-Protein interaction involved in bacterial cell wall biogenesis. *Antibiotics (Basel)* 5.
46. Lavollay, M., Arthur, M., Fourgeaud, M., Dubost, L., Marie, A., Veziris, N., Blanot, D., Gutmann, L., Mainardi, J.L. (2008) The peptidoglycan of stationary-phase *Mycobacterium tuberculosis* predominantly contains cross-links generated by L,D-transpeptidation. *J. Bacteriol.* 190, 4360- 4366
47. Leclercq, S., Derouaux, A., Olatunji, S., Fraipont, C., Egan, A.J., Vollmer, W., Breukink, E., Terrak, M. (2017) Interplay between penicillin-binding proteins and SEDS proteins promotes bacterial cell wall synthesis. Sci. Rep. 7, 43306. doi: 10.1038/srep43306
48. Liu, B., Persons, L., Lee, L., de Boer, P.A. (2015) Roles for both FtsA and the FtsBLQ subcomplex in FtsN-stimulated cell constriction in *Escherichia coli. Mol. Microbiol.* 95, 945-970
49. Luirink, J., Yu, Z., Wagner, S.,de Gier., J.W. (2012) Biogenesis of inner membrane proteins in Escherichia coli. *Biochimica et Biophysica Acta* 1817,965-976

50. Luo, Q., Yang, X., Yu, S., Shi, H., Wang, K., Xiao, L., Zhu, G., Sun, C., Li, T., Li, D., Zhang, X., Zhou, M., Huang, Y. (2017) Structural basis for lipopolysaccharide extraction by ABC transporter $LptB_2FG$. *Nat. Struct. Mol. Biol.* 24, 469-474
51. Magnet, S., Bellais, S., Dubost, L., Fourgeaud, M., Mainardi, J.L., Petit-Frère, S., Marie, A., Mengin-Lecreulx, D., Arthur, M., Gutmann, L. (2007) Identification of the L,D-transpeptidases responsible for attachment of the Braun lipoprotein to *Escherichia coli* peptidoglycan. *J. Bacteriol.* 189, 3927-3931
52. Magnet, S., Dubost, L., Marie, A., Arthur, M., Gutmann., L. (2008) Identification of L,D-transpeptidases for peptidoglycan cross-linking in *Escherichia coli. J. Bacteriol.* 190, 4782-4785
53. Mainardi, J.L., Fourgeaud, M., Hugonnet, J.E., Dubost, L., Brouard, J.P., Ouazzani, J., Rice, L.B., Gutmann, L., Arthur, M. (2005) A novel peptidoglycan cross-linking enzyme for a beta-lactam-resistant transpeptidation pathway. *J. Biol. Chem.* 28038146-38152
54. Martorana, A.M., Motta, S., Di Silvestre, D., Falchi, F., Dehò, G., Mauri, P., Sperandeo, P., Polissi, A. (2014) Dissecting *Escherichia coli* outer membrane biogenesis using differential proteomics. *PLoS One*. 9, e100941. doi: 10.1371/journal.pone.0100941. eCollection 2014.
55. Matsuyama, S.,Yokota, N., Tokuda, H. (1997) A novel outer membrane lipoprotein, LolB (HemM), involved in the LolA (p20)-dependent localization of the lipoproteins to the outer membrane of *Escherchia coli. EMBO J.* 16, 6947-6955
56. Mattei, P.J., Neves, D. and a Dessen, A. (2010) Bridging cell wall biosynthesis and bacterial morphogenesis. *Curr. Opin. Struct. Biol.* 20, 749-755
57. Meeske, A.J., Riley, E.P., Robins, W.P., Uehara, T., Mekalanos, J.J., Kahne, D., Walker, S., Kruse, A.C., Bernhardt, T.G., Rudner, D.Z. (2016) SEDS proteins are a widespread family of bacterial cell wall polymerases. *Nature.* 537, 634-638
58. Meiresonne, N.Y., van der Ploeg, R., Hink, M.A., den Blaauwen, T. (2017) Activity-related conformational changes in D,D-carboxypeptidases revealed by in vivo periplasmic Forster resonance energy transfer assay in *Escherichia coli. M. Bio.* 8, pii: e01089-17. doi: 10.1128/mBio.01089-17.
59. Michie, K.A. and Lowe, J. (2006) Dynamic filaments of the bacterial cytoskeleton. *Annu.Rev.Biochem.* 75,467-492
60. Mohammadi, T., van Dam, V., Sijbrandi, R., Vernet, T., Zapun, A., Bouhss, A., Diepeveen-de Bruin, M., Nguyen-Distèche, M., de Kruijff, B., Breukink, E. (2011) Identification of FtsW as a transporter of lipid-linked cell wall precursors across the membrane. *EMBO J.* 30, 1425-1432

61. Morgenstein, R.M., Bratton, B.P., Nguyen J.P., Ouzounov, N., Shaevitz, J.W. and Gitai, Z. (2015) RodZ links MreB to cell wall synthesis to mediate MreB rotation and robust morphogenesis. *Prot.Natl.Acad.Sci.USA* 112,12510-12515
62. Moynihan, P.J., Sychantha, D., Clarke, A.J. (2014) Chemical biology of peptidoglycan acetylation and deacetylation. *Bioorg. Chem.* 54. 44-50
63. Narita, S. and Tokuda, H. (2009) Biochemical characterization of an ABC transporter LptBFGC complex required for the outer membrane sorting of lipopolysaccharidde. *FEBS Lett.* 583, 2160-2164
64. Narita, S.I. and Tokuda, H. (2016) Bacterial lipoproteins: biogenesis, sorting and quality control. *Biochim. Biophys. Acta.* Pii.S1388-1918 16,30323-7
65. Nelson, D.E. and Young, K.D. (2001) Penicillin binding protein 5 affects cell diameter, contour and morphology of *Escherichia coli. J. Bacteriol*. 182, 1714-1721
66. Nelson, D.E. and Young, K.D. (2001) Contributions of PBP5 and DD-carboxypeptidase penicillin binding proteins to maintenance of cell shape in *Escherichia coli. J. Bacteriol.* 183, 3055-3064
67. Nikaido, H. (2003) Molecular basis of bacterial outer membrane permeability revisited. *Microbiol. Mol. Biol. Rev.* 63,593-656
68. Okuda, S., Sherman, D.J., Silhavy, T.J., Ruiz, N., Kahne, D. (2016) lipopolysaccharide transport and assembly at the outer membrane: the PEZ model. *Nat.Rev.Microbiol.* 14, 337-345
69. Okuda, S., Tokuda, H. (2011) Lipoprotein sorting in bacteria. *Annu. Rev. Microbiol.* 65,239-259
70. Okuda, S., Freinkman, E., Kahne, D. (2012) Cytoplasmic ATP hydrolysis powers transport of lipopolysaccharide across the periplasm in *E. coli. Science.* 338, 1214-1217
71. Paradis-Bleau, C., Markovski, M., Uehara, T., Lupoli, T.J., Walker, S., Kahne, D.E., Bernhardt, T.G. (2010) Lipoprotein cofactors located in the outer membrane activate bacterial cell wall polymerases. *Cell.* 143, 1110-1120
72. Park, J.T. and Uehara, T. (2008) How bacteria consume their own exoskeletons (turnover and recycling of cell wall peptidoglycan). Microbiol. Mol. Bio. Rev. 72, 211-227
73. Pazos, M., Peters, K., Vollmer, W. (2017) Robust peptidoglycan growth by dynamic and variable multi-protein complexes. *Curr. Opin. Microbiol.* 36, 55-61
74. Peters, K., Kannan, S., Rao, V.A., Biboy, J., Vollmer, D., Erickson, S.W., Lewis, R.J., Young, K.D., Vollmer, W. (2016) The redundancy of peptidoglycan carboxipeptidases

ensures robust cell shape maintenance in Escherichia coli. M. Bio. 21, pii: e00819-16. doi: 10.1128/mBio.00819-16

75. Perez, J.M., McGarry, M.A., Marolda, C.L., Valvano, M.A. (2008) Functional analysis of the large periplasmic loop of the *Escherichia coli* K-12 Waal O-antigen ligase. *Mol.Microbiol.* 70, 1424-1440
76. Polissi, A. and Georgopulos, C. (1996) Mutation analysis and properties of the *msbA* gene of *Escherichia coli,* coding for an essential ABC family transporter. *Mol. Microbiol.* 20, 1221-1233
77. Qiao, S., Luo, Q., Zhao, Y., Zhang, X.C., Huang, Y. (2014) Structural basis for lipopolysaccharide insertion in the bacterial outer membrane. *Nature.* 511, 108-111
78. Raetz, C.R.H, Reynolds, C.M., Trent, M.S. and Bishop, R.E. (2007) Lipid A Modification System in Gram-Negative *Bacteria. Annu. Rev. Biochem.* 76, 295-329
79. Raetz, C.R.H. and Whitfield, C. (2002) Lipopolysaccharide endotoxins. *Annu. Rev. Microbiol.* 71, 635-700
80. Ricci, D.P., Silhavy, T.J. (2012) The Bam machine: A molecular cooper. *Biochim. Biophs. Acta* 1818, 1067-1084
81. Rowlett, V.W and Margollin, W. (2015) The bacterial divisome: ready fot its close-up. *Phil.Trans.R.Soc.B.* 370, 0150028
82. Ruiz, N., Kahne, D., Silhavy, T.J. (2006) Advances in understanding bacterial outer-membrane biogenesis. *Nature Reviews Microbiology.* 4, 57-66
83. Ruiz, N., Gronenberg, L.S, Kahne, D., Silhavy, T.J. (2008) Identification of two inner-membrane proteins required for the transport of lipopolysaccharide to the outer membrane of *Escherichia coli. Proc.Natl.Acad.Sci.USA* 105, 5537-4552
84. Ruiz, N., Kahne, D., Silhavy, T.J. (2009) Transport of lipopolysaccharide across the cell envelope: the long road of discovery. *Nat. Rev. Microbiol.* 7: 677-683
85. Salje, J., van den Ent, F., de Boer, P. and Lowe, J. (2011) Direct membrane binding by bacterial actin MreB. *Mol. Cell.* 43, 478-487
86. Samuel, G., Reeves, P. (2003) Biosynthesis of O-antigens: genes and pathways involved in nucleotide sugar precursor synthesis and O-antigen assembly. *Carbohydr. Res.* 338, 2503-2519
87. Sankaran, K., Wu, H.C. (1994) Lipid modification of bacterial prolipoprotein. Transfer of diacylglyceryl moiety from phosphatidylglycerol. *J. Biol. Chem.* 269: 19701-19706
88. Santos, J.M., Lobo, M., Matos, A.P., De Pedro, M.A., Arraiano, C.M. (2002) The gene *bolA* regulates *dacA* (PBP5), *dacC* (PBP6) and *ampC* (AmpC), promoting normal morphology in

Escherichia coli. Mol. Microbiol. 45, 1729-1740

89. Sauvage, E., Kerff, F., Terrak, M., Ayala, J.A., Charlier, P. (2008) The penicillin-binding proteins: structure and role in peptidoglycan biosynthesis. *FEMS Microbiol. Rev.* 32, 234-258
90. Schiffer, G. and Holtje, J.V. (1999) Cloning and characterization of PBP1C, a third member of the multimodular class A penicillin-binding proteins of *Escherichia coli. J. Biol. Chem.* 274, 32031-32039
91. Schleifer, K.H., Kandler, O. (1972) Peptidoglycan types of bacterial cell walls and their taxonomic implications. *Bacteriol. Rev.* 36, 407-477
92. Schulz, G.E. (2002) The structure of bacterial outer membrane proteins. *Biochim. Biophys. Acta* 1565, 308-317
93. Sham, L.T., Butler, E.K., Lebar, M.D., Kahne, D., Bernhardt, T.G. and Ruiz, N. (2014) Bacterial cell wall. MurJ is the flippases of lipid-linked precursors for peptidoglycan biogenesis. *Science.* 345, 220-222
94. Sherman, D.J., Lazarus, M.B., Murphy, L., Liu, C., Walker, S., Ruiz, N. and Kahne, D. (2014) Decoupling catalytic activity from biological function of the ATPase that powers lipopolysaccharide transport. *Proc.Natl.Acad.Sci.USA* 111, 4982-4987
95. Silhavy, T.J., Kahne, D., and Walker, S. (2010) The bacterial cell envelope. *Cold Spring Harb Perspect Biol* 2, a000414
96. Sklar, J.G., Wu, T., Kahne, D., Silhavy, T.J. (2007) Defining the roles of the periplasmic chaperones SurA, Skp and DegP in *Escherichia coli. Genes Dev.* 21, 2473-2484
97. Sperandeo, P., Lau, F.K., Carpentieri, A., De Castro, C., Molinaro, A., Dehò, G., Silhavy, T.J., Polissi, A. (2008) Functional analysis of the protein machinery required for transport of lipopolysaccharide to the outer membrane of *Escherichia coli. J. Bacteriol* 190, 4460-4469
98. Sperandeo, P., Martorana, A.M., Polissi, A. (2017) Lipopolysaccharide biogenesis and transport at the outer membrane of Gram-negative bacteria. *Biochim Biophys.Acta* 1862, 1451-1460
99. Sperandeo, P., Pozzi, C., Deho, G., Polissi, A. (2006) Non essential KDO biosynthesis and new essential cell envelope biogenesis genes in the *Escherichia coli yrbG-ynhG* locus. *Res.Microbiol.* 157, 547-558
100. Spratt, B.G. (1975) Distinct penicillin binding proteins involved in the division, elongation, and shape of *Escherichia coli* K12. *Proc. Natl. Acad. Sci. USA.* 72, 2999-3003
101. Suits, M.D., Sperandeo, P., Dehò, G., Polissi, A., Jia, Z. (2008) Novel structure of the conserved Gram-negative lipopolysaccharide transport protein A and mutagenesis

analysis. *J.Mol.Biol.* 380, 476-488

102. Szwedziak, P., Wang, Q., Bharat, T.A., Tsim, M. and Lowe,J. (2014) Architecture of the ring formed by the tubulin homologue FtsZ in bacterial cell division. *eLife.* 3, e040601

103. Szwedziak, P., Wang, Q., Freund, S.M. and Lowe, J. (2012) FtsA forms actin-like protofilaments. *EMBO J.* 31, 2249-2260

104. Terrak, M., Ghosh, T.K., Van Heijenoort, J., Van Beeumen, J., Lampilas, M., Aszodi, J., Ayala, J.A., Ghuysen, J.M., Nguyen-Distèche, M. (1999) The catalytic glycosyl transferase and acyl transferase modules of the cell wall peptidoglycan-polymerizing penicillin-binding protein 1b of *Escherichia coli. Mol.Microbiol.* 34, 350-364

105. Tokuda, H. (2009) Biogenesis of outer membranes in Gram-negative bacteria. *Biosci. Biotechnol. Biochem* 73, 465-473

106. Tran, A.X., Dong, C. and Whitefield, C. (2010) Structure and functional analysis of LptC, a conserved membrane protein involved in the lipopolysaccharide export pathway in *Escherichia coli. J.Biol.Chem.* 285, 33529-33539

107. Tran, A.X., Trent, M.S., Whitefield, C. (2008) The LptA protein of Escherichia coli is a periplasmic lipid A- binding protein involved in the lipopolysaccharide export pathway. *J. Biol.Chem.* 283, 20342-20349

108. Tsang, M.J. and Bernhardt, T.G. (2015) A role for the FtsQLB complex in cytokinetic ring activation revealed by a *ftsL* allele that accelerates division. *Mol. Microbiol.* 95, 925-944

109. Typas, A., Banzhaf, M., van den Berg van Sparoea, B., Verheul, J., Biboy, J., Nichols R.J., Zietek, M., Beilharz, K., Kannenberg, K., von Rechenberg, M., Breukink, E., den Blaauwen, T., Gross, C.A., Vollmer, W. (2010) Regulation of peptidoglycan synthesis by outer-membrane proteins. *Cell* 143. 1097-1109

110. Typas, A., Banzhaf, M., Gross, C.A., Vollmer, W. (2011) From the regulation of peptidoglycan synthesis to bacterial growth and morphology. *Nature Reviews. Microbiology* 10, 123-136

111. Typas, A. and Sourjik, V. (2015) Bacterial protein networks: properties and functions. *Nat. Rev. Microbiol.* 13, 559-572

112. Uehara, T., Parzych, K.R., Dihn, T., Bernhardt, T.G. (2010) Daughter cell separation is controlled by cytokinetic ring-activated cell wall hydrolysis. *EMBO J.* 29, 1414-1422

113. Ursell, T.S., Nguyen, J., Monds, R.D., Colavin, A., Billings, G., Ouzounov, N., Gitai, Z., Shaevitz, J.W. and Huang, K.C. (2014) Rod-like bacterial shape is mantained by feedback between cell curvature and cytoskeletal localization. *Proc. Natl. Acad. Sci. USA*

111,1025-1034

114. Valvano, M.A. (2003) Export of O-specific lipopolysaccharide. *Front. Biosci.* 8, 452-471

115. Van den Ent, F., Amos, L.A. and Lowe, J. (2001) Prokaryotic origin of the actin cytoskeleton. *Nature* 413, 39-44

116. Vats, P., Shih, Y.L. and Rothfield, L. (2009) Assembly of the MreB-associated cytoskeletal ring of *Escherichia coli. Mol.Mic.* 72, 170-182

117. Vollmer, W., Blanot, D., and de Pedro, M. A. (2008) Peptidoglycan structure and architecture. *FEMS Microbiol. Rev*. 32, 149-167

118. Vollmer, W. and Bertsche, U. (2008) Murein (peptidoglycan) structure, architecture and biosynthesis in *Escherichia coli. Biochim. Biophys. Acta.* 1778, 1714-34

119. Vollmer, W., Seligman, S.J. (2010) Architecture of peptidoglycan: more data and more models. *Trends Microbiol.* 18, 59-66

120. Wu, T., McCandlish, A.C., Gronenberg, L.S., Chng, S.S., Silhavy, T.J., Kahne, D. (2006) Identification of protein complex that assembles lipopolysaccharide in the outer membrane of *Escherichia coli*. *Proc.Natl.Acad.Sci.USA.* 103, 11754-11759

121. Yakushi, T., Yokota, N., Matsuyama, S., Tokuda, H. (1988) LolA-dependent release of a lipid-modified protein from inner membrane of *Escherichia coli* requires nucleoside triphosphate. *J. Biol. Chem.* 273, 32576-32581

122. Yamaguchi, K., Yu, F., Inouye, M. (1988) A single aminoacid determinant of the membrane localization of lipoproteins in *E. coli. Cell.* 53, 423-432

123. Zeth, K. and Thein, M. (2010) Porins in prokaryotes and eukaryotes: common themes and variations. *Biochem. J.* 431, 13-22

124. Zhao, H., Patel, V., Helmann, J.D. and Dorr, T. (2017) Don't let sleeping dogmas lie: New views of peptidoglycan synthesis and its regulation. *Mol. Microbiol* 10.1111/mmi.13853

125. Zhao, H., Sun, Y., Peters, J.M., Gross, C.A., Garner, E.C. and Helmann, J.D. (2016) Depletion of Undecaprenyl Pyrophosphatases Disrupts Cell Envelope Biogenesis in *Bacillus subtilis*. *J. Bacteriol.* 198, 2925-2935

126. Zhou, Z., White, K.A., Polissi, A., Georgopulos, C. and Raetz, C.R. (1998) Function of *Escherichia coli* MsbA, an essential ABC family transporter, in lipid A and phospholipid biosynthesis. *J. Biol. Chem*. 273, 12466-12475

3. Aim of the project

In an effort to understand how bacteria respond to severe OM biogenesis defects we recently performed differential proteome analysis of the total membranes of *E. coli* upon block of LPS transport (Martorana et al., 2014). Among the proteins whose level changes in comparison between the depleted and non-depleted strain, several proteins involved in biogenesis and remodelling of PG have been found. This finding further supports the idea that growth of OM and PG is coordinated. The aim of this project is to understand by which mechanism the block of LPS transport impacts on PG synthesis and remodelling.

Our initial results indicate that the PG architecture is modified when the assembly of OM is defective. Indeed, we observed a substantial increase of the non-canonical 3-3 cross links in sacculi purified from strains impaired in the LPS export pathway thus implicating the LdtD and LdtE LD-TPase in such PG remodeling.

Based on these initial evidences the following questions will be investigated:

1) What is the role of 3-3 cross-links when the biogenesis of OM is defective?
2) How are LD-TPases regulated during cell cycle and upon envelope stress in *E. coli*?
3) Are there additional proteins that take part in the PG remodelling programme in conjunction with LD-TPases?
4) What is the physiological role of 3-3 cross-links in the cell?

The answers to these questions are reported in the following manuscript, which includes the results I obtained during my thesis work and that has just been submitted for publication.

4. Manuscript

Peptidoglycan remodeling enables *E. coli* to survive severe outer membrane assembly defect

Niccolò Morè[1], Alessandra M. Martorana[1#], Jacob Biboy[2#], Christian Otten[2], Matthias Winkle[2], Alejandro Montón Silva[3], Lisa Atkinson[2], Hamish Yau[2], Eefjan Breukink[4], Tanneke den Blaauwen[3], Waldemar Vollmer[2*], and Alessandra Polissi[1*]

[1] Dipartimento di Scienze Farmacologiche e Biomolecolari, Università degli Studi di Milano, Milano, Italy.

[2] The Centre for Bacterial Cell Biology, Institute for Cell and Molecular Biosciences, Newcastle University, Newcastle upon Tyne, United Kingdom.

[3] Bacterial cell Biology & Physiology, Swammerdam Institute for Life Sciences, University of Amsterdam, Science park 904, 1098 XH Amsterdam, The Netherlands.

[4] Membrane Biochemistry and Biophysics, Department of Chemistry, Faculty of Science, Utrecht University, Padualaan 8, 3584 CH Utrecht, The Netherlands.

[#] contributed equally.

*For Correspondence:

Alessandra Polissi: Dipartimento di Scienze Farmacologiche e Biomolecolari, Università degli Studi di Milano, Via Balzaretti 9, 20133 Milano, Italy;

Email: alessandra.polissi@unimi.it; Phone: +39 (02) 503 18205; Fax:

Waldemar Vollmer: The Centre for Bacterial Cell Biology, Institute for Cell and Molecular Biosciences, Newcastle University, Richardson Road, Newcastle upon Tyne, NE2 4AX, United Kingdom; Email: w.vollmer@ncl.ac.uk; Phone: +44 (0) 191 208 3216; Fax: +44 (0) 191 208 3205.

Abstract

Gram-negative bacteria must tightly coordinate the growth of their tripartite envelope comprising the cytoplasmic membrane (CM), a stress-bearing peptidoglycan (PG) layer and the asymmetric outer membrane (OM) with lipopolysaccharide (LPS), to maintain cellular integrity and OM impermeability to many antibiotics. The biogenesis of PG and LPS relies on specialized macromolecular complexes that span the entire envelope. In this work we show that *Escherichia coli* cells are capable of avoiding lysis when the transport of LPS to the OM is compromised, by utilizing LD-transpeptidases (LDTs) to generate 3-3 cross-links in the PG. This PG remodeling programme mainly relies on the activities of the stress response LDT, LdtD together with the major PG synthase PBP1B, its cognate activator LpoB, and the carboxypeptidase PBP6a. Our data support a model according to which these proteins cooperate to repair gaps arising in the PG as a result of defective OM synthesis.

Introduction

The Gram-negative bacterial cell envelope contains the cytoplasmic membrane (CM), the periplasm with a thin peptidoglycan (PG) sacculus and the outer membrane (OM), and all of these components are essential to maintain cellular integrity (Silhavy *et al*., 2010; Vollmer *et al*., 2008). The OM is an asymmetrical membrane containing in the outer leaflet lipopolysaccharide (LPS) (Kamio and Nikaido, 1976), which is impermeable for many toxic compounds and is therefore the major determinant for the intrinsic resistance of Gram-negative bacteria to many antibiotics (Nikaido, 2003).

LPS is composed of the conserved membrane anchor lipid A, an inner oligosaccharide core and a variable O-antigen chain. LPS precursors are synthesized at the inner leaflet of the CM (Raetz and Whitfield, 2002) and flipped by the ABC transporter MsbA to the periplasmic leaflet (Polissi and Georgopoulos, 1996; Zhou et al., 1998) where the O-antigen chain is added (Raetz and Whitfield, 2002). The mature LPS is then transported from the CM across the periplasm to reach its final destination at the outermost surface of the cell (Sperandeo *et al*., 2017a, b).

LPS is an abundant molecule. An *Escherichia coli* cell has ~1.43×10^6 molecules of LPS that account for ~3.4% of the dry weight of the cell (Neidhardt and Umbarger, 1996). Considering a generation time of 20 min for fast growing *E. coli*, LPS transport must occur at a rate of more than 10^3 molecules per second to ensure complete coverage of the cell surface during growth. Moreover, the supply of LPS must be optimally coupled to the synthesis and assembly of other cell envelope components, such as PG, to prevent loss of OM integrity due to LPS depletion or detrimental effects by excessive LPS production. However, whilst many components of the LPS synthesis and transport machineries have been identified, and molecular

details of the transport machinery have begun to emerge, the regulation mechanisms of LPS transport during cell growth remain virtually unknown.

In *E. coli* LPS transport is facilitated by seven essential proteins, LptA-G (Braun and Silhavy, 2002; Chng *et al*., 2010a; Ruiz *et al*., 2008; Sperandeo *et al*., 2007; Sperandeo *et al*., 2008; Wu *et al*., 2006). At the CM the ABC transporter made of $LptB_2$-LptF-LptG associates with the bitopic membrane protein LptC to extract LPS from the CM and delivers it to the periplasmic LptA protein, which mediates the transit of LPS molecules through the periplasm (Narita and Tokuda, 2009; Okuda et al., 2012). LptA passes the LPS to the OM β-barrel membrane protein LptD and the OM-anchored lipoprotein LptE, which together form a heterodimeric translocon that assembles LPS into the outer leaflet of the OM (Chng *et al*., 2010b; Freinkman *et al*., 2011; Freinkman et al., 2012). The seven proteins work as a single device, forming a trans-envelope protein bridge through the periplasm and its PG sacculus, spanning from the cytoplasmic ATPase LptB to the OM translocon LptDE (Chng *et al*., 2010a; Freinkman *et al*., 2012; Sperandeo *et al*., 2011; Villa *et al*., 2013). This organization allows the coupling of ATP hydrolysis with LPS movement across the periplasm up to the cell surface, as proposed in the so-called 'PEZ' model (Okuda *et al*., 2016). Depletion of any of the Lpt components results in block of LPS transport and its accumulation at the periplasmic leaflet of the IM (Ruiz *et al*., 2008; Sperandeo *et al*., 2008).

The PG sacculus is composed of glycan strands made of alternating *N*-acetylglucosamine (GlcNAc) and *N*-acetylmuramic acid residues connected by short peptides, and protects the cell from bursting due to its turgor, maintaining the shape of the cell (Typas *et al*., 2012; Vollmer *et al*., 2008). The growth of the sacculus is orchestrated by a repertoire of PG synthases and hydrolases organized in two highly

dynamic macromolecular complexes, the elongasome and the divisome, which facilitate PG synthesis and hydrolysis at the side wall during growth and cell division site, respectively (Typas *et al*., 2012). Most PG synthases and some hydrolases belong to the penicillin-binding protein (PBP) family, which is the target of β–lactams antibiotics (Goffin and Ghuysen, 1998). PBP1A and PBP1B are major and semi-redundant PG synthases active in elongation and cell division in *E. coli*. They polymerize glycan strands by their glycosyltransferase (GTase) activity and cross-link stem peptides by DD-transpeptidase (DD-TPase) activity, forming the abundant 4-3 cross-links in PG (Supplementary Fig. S1) (Banzhaf *et al*., 2012; Bertsche et al., 2005; Born *et al*., 2006). Notably, PBP1A and PBP1B are each activated by a cognate OM anchored lipoprotein, LpoA and LpoB, respectively (Paradis-Bleau *et al*., 2010; Typas *et al*., 2010), and the activation of PBP1B by LpoB is modulated by CpoB and TolA to couple PG synthesis with OM constriction during cell division (Gray *et al*., 2015). LpoA and LpoB span the periplasm to reach their cognate PG synthase through pores in the PG layer (Egan *et al*., 2014; Jean *et al*., 2014; Sathiyamoorthy *et al*., 2017), presumably responding to the size of pores in the PG layer to couple PG growth with cell growth (Typas *et al*., 2012). DD-carboxypeptidases (DD-CPase) such as PBP5, PBP6a and PBP6b trim the pentapeptides present in new PG to tetrapeptides by removing the terminal D-Ala residue (Baquero *et al*., 1996; Nelson and Young, 2000, 2001). DD-CPases are not essential but are required for robust rod-shape maintenance. PBP5 is the major DD-CPase in the cell; its deletion causes aberrant cell morphology in strains lacking other PBPs that cannot be corrected by ectopic expression of PBP6a or PBP6b (Ghosh and Young, 2003; Nelson and Young, 2000), suggesting that seemingly redundant DD-CPases may have specific roles.

Indeed, PBP6b contributes substantially to PG remodeling and cell shape maintenance in cells growing at acidic pH (Peters *et al*., 2016).

In *E. coli* the majority (90%-98%) of cross-links in PG are of the 4-3 (or DD) type (between D-Ala and *meso*-Dap) (Glauner *et al*., 1988). However, PG from *E. coli* contains also a non-canonical (or 'minor') type of cross-link between two *meso*-Dap residues of adjacent stem peptides, called 3-3 (or LD) crosslinks (Supplementary Fig. S1), which account for 2-10% of all cross-links in exponentially growing cells and up to 16% in stationary-phase cells (Glauner *et al*., 1988; Holtje, 1998). 3-3 cross-links are produced by LD-transpeptidases (LDTs) belonging to the YkuD family of proteins (PF03734), which are structurally unrelated to PBPs. LDTs use tetrapeptide donors in the TPase reaction and are insensitive to most β–lactams (Supplementary Fig. S1) (Biarrotte-Sorin *et al*., 2006).

E. coli has five LDTs with two distinct functions. LdtD (formerly YcbB) and LdtE (YnhG) form 3-3 cross-links between two *meso*-Dap residues whereas LdtA (ErfK), LdtB (YbiS) and LdtC (YcfS) attach the abundant OM-anchored Lpp (Braun's lipoprotein) to *meso*-Dap residues in PG, providing a tight connection between the PG and OM. Deletion of all five *ldt* genes results in undetectable levels of 3-3 cross-links and PG-bound Lpp (Magnet *et al*., 2007; Magnet *et al*., 2008). Notably, *E. coli* mutants deleted in multiple or all *ldt* genes exhibit only minor phenotypes suggesting that these functions are dispensable during growth under laboratory conditions (Magnet *et al*., 2007; Magnet *et al*., 2008; Sanders and Pavelka, 2013).

Although the role of LDTs in the cell is not clear, LDTs have been implicated in a mechanism that bypasses PBPs to confer resistance to β-lactams. Certain strains of *Enterococcus faecium* can grow in the presence of β-lactam antibiotics using a β-lactam insensitive LDT, Ldt_{fm} to produce 3-3 crosslinks instead of the β-lactam

sensitive PBP TPases (Mainardi *et al*., 2005; Mainardi *et al*., 2000; Mainardi *et al*., 2002). This resistance mechanism requires a DD-CPase to trim the pentapeptides to tetrapeptides in peptidoglycan precursors, which can be utilized by LDTs. More recently, a DD-TPase independent and LDT dependent mutant strain of *E. coli* has been selected by its ability to grow at high and otherwise lethal concentration of ampicillin, at which it produces exclusively 3-3 cross-links in its PG (Hugonnet *et al*., 2016). This strain has an elevated level of the alarmone (p)ppGpp and needs LdtD, the DD-CPase PBP5, and the GTase domain of PBP1B together with its regulator, LpoB, to bypass PBPs and achieve broad spectrum β-lactam resistance (Hugonnet *et al*., 2016). However, *E. coli* strains do not readily acquire this mechanism of resistance, and it is possible that the 3-3 cross-linking activities of LdtD and LdtE have another, yet undiscovered function in *E. coli*.

In this work we show that *E. coli* cells defective in the LPS export pathway require LDTs that produce an increased level of 3-3 cross-links in the PG to avoid cell lysis. We identified LdtF (YafK) as a third LDT for 3-3 cross-link formation. The level of 3-3 cross-links, *ldt* expression profiles and phenotypic analysis of cells with LPS transport arrest suggest that LdtE and LdtF are housekeeping LDTs, whereas LdtD is expressed in response to OM damage. A PG remodeling programme is activated in response to the block of LPS transport and also involves the TGase activity of PBP1B and the DD-CPase of previously unknown function, PBP6a. Finally, based on biochemical interactions and activity assays, we propose a model whereby PBP1B, LdtD and PBP6a cooperate in a 'PG repair' machine that fills holes arising from disassembled Lpt machines. These findings implicate 3-3 cross-links in a PG protective remodeling programme during envelope stress.

Results

Defective LPS export induces the formation of 3-3 cross-links in PG

Several PG synthesizing or modifying enzymes are upregulated upon depletion of the essential LptC component of the LPS export machinery (Martorana *et al*., 2014). This observation raises the possibility that cells adapt to severe OM damage by modifying their PG structure, prompting us to analyze the composition of PG isolated from cells with compromised LPS transport.

For this purpose we cultured an *araB*p*lptC* conditional strain, in which *lptC* expression is under control of the arabinose inducible *araB*p promoter. The inhibition of LPS transport by removal of arabinose from the culture medium led to a growth arrest and the cells produced mostly short filaments (Fig. 1A and 1B). We purified PG sacculi from these cells and released the muropeptides by incubation with a muramidase, followed by analysis of the muropeptide composition by high-pressure liquid chromatography (HPLC). Interestingly, the sacculi purified from LptC-depleted cells showed a four- to six-fold increase in the relative amount of 3-3 cross-links between two *meso*-Dap residues, compared to cells grown in the presence of arabinose (Fig. 1E, Table 1, Supplementary Table 4). 3-3 cross-links increased already early in LptC-depleted cells indicating a rapid cellular response to the LPS transport arrest. Notably, we observed only a moderate decrease in the canonical 4-3 (meso-Dap to D-Ala) cross-links in LptC depleted cells (Fig. 1E, Supplementary Table 4).

3-3 cross-links are not essential under standard growth condition

It was previously reported that *E. coli* has five LDTs (LdtA-E) (Magnet *et al*., 2007; Magnet *et al*., 2008; Sanders and Pavelka, 2013), but the cellular function of 3-

3 cross-links is poorly defined. When inspecting the *E. coli* genome we identified another, hypothetical *ldt* gene, *yafK*. The predicted YafK protein has a YkuD (LDT)-domain with 33% and 41% sequence identity to the catalytic domain of LdtD and LdtE, respectively, and was herein termed LdtF. LdtF lacks a conserved arginine residue near the active site cysteine and might not be fully active. We included *ldtF* in our further studies on the role LDTs in the formation of 3-3 cross-links during defective LPS export.

To assess whether *ldtF* deletion affects the growth of *E. coli* and whether LdtF is a *bona fide* LDT, we deleted *ldtF* from the BW25113 wild type strain alone and in combination with *ldtD* and *ldtE*, and examined the growth phenotype and level of 3-3 cross-links in sacculi purified from all mutants. As summarized in Table 1 the deletion of *ldtD*, *ldtE* and *ldtF* alone and in all possible combinations did not affect growth of *E. coli*. Even the deletion of all six *ldt* genes did not result in any growth defect under standard laboratory conditions (data not shown). The muropeptide analysis revealed that only 3.0% of the PG muropeptides from strain BW25113 contained 3-3 cross-links (Table 1, Supplementary Table 4), consistent with earlier reports on the low abundance of these structures in *E. coli* (Glauner *et al*., 1988; Holtje, 1998). The Δ*ldtD* Δ*ldtE* mutant contained 2.2% of muropeptides with 3-3 cross-links, a value comparable to that of the wild type strain, and 3-3 cross-links were undetectable in the PG from the triple Δ*ldtD* Δ*ldtE* Δ*ldtF* mutant. This suggests that LdtF has LD-TPase activity and that no other cellular protein can perform this reaction in the absence of LdtD, LdtE and LdtF. Interestingly, the Δ*ldtD* Δ*ldtF* double mutant did not produce detectable levels of 3-3 cross-links suggesting that LdtE is either not active as an LD-TPase under these conditions, or it requires LdtD and/or LdtF for activity. In all other *ldt* defective strains the level of 3-3 cross-links was

comparable to that of the BW25113 wild type strain suggesting that one or more LDTs is active in these mutants (Table 1, Supplementary Table 4).

To further assess the activities of LDTs in the cell, we expressed *ldtD*, *ldtE* and/or *ldtF* from plasmids pJEH12, pAMS01 and/or pAMS02 (Supplementary Table 2) in a BW25113Δ6LDT background, which lacks all *ykuD* homologues (*ldtA-F*) (Kuru *et al*., 2017), and analysed the PG composition (Fig. 2). Expression of LdtD, but not of LdtE or LdtF resulted in the presence of 3-3-cross-links in PG. Interestingly, co-expression of LdtE and LdtF produced 3-3 cross-links, suggesting that one or both of these enzymes requires the other for activity. Co-expression of LdtF with LdtD increased the level of 3-3 cross-links (compared to LdtD alone). Consistent with previous reports we also detected typical products of side reactions in PG from cells with active LDTs (muropeptides with tripeptides and glycine at position 4 due to LD-CPase and Ala-Gly exchange reactions, respectively). Overall, our data show that LdtF has either LD-TPase activity or stimulates other LDTs, and that LDTs and 3-3 cross-links are not essential under standard growth conditions.

LDTs prevent cell lysis upon defective OM assembly

We reasoned that LDTs might be important in cells with defective LPS transport because the level of the 3-3 cross-links increased in *lptC*-depleted cells. To test this hypothesis we deleted every *ldt* gene alone and all possible combinations of gene deletions in the background of the *araB*p*lptC* conditional mutant and we examined the growth profile and level of 3-3 cross-links in the PG under permissive and non-permissive conditions.

Upon shifting to the non-permissive condition all *lptC*-depleted *ldt* mutants (with the exception of Δ*ldtE* Δ*ldtF*, see below) lysed rapidly, as seen by a decrease in

optical density of the cultures, and the cells lost viability as assessed by quantifying the colony forming units (CFU). Indeed, phase contrast and fluorescence microscopy revealed the formation of bulges at variable position on the cell surface suggesting that the cellular integrity was severely compromised (Fig. 1C and 1F, Supplementary Figs. 2 - 4). We verified that the effects were specific for LDTs responsible for the formation of 3-3 cross-links because the simultaneous deletion of *ldtA*, *ldtB* and *ldtC*, encoding the Lpp-attachment enzymes, in the *araB*p*lptC* background did not result in lysis under non-permissive condition (Supplementary Fig. 5). In the *lptC*-depleted Δ*ldtD* or Δ*ldtE* mutants, the level of 3-3 cross-links was reduced compared to the *araB*p*lptC* parental strain, and 3-3 cross-links were below the detection limit in the *araB*p*lptC* Δ*ldtD* Δ*ldtF* mutant (Table 1, Supplementary Table 4). Notably, the *araB*p*lptC* Δ*ldtD* Δ*ldtF* mutant did not produce 3-3 cross-links even when grown under permissive growth conditions, confirming the result obtained for the *lptC*$^{+}$ background (Table 1). Across all strains, the absence of lysis generally correlated with the presence of 3-3 cross-links with one exception: the *lptC*-depleted Δ*ldtF* mutant, which displayed a level of 3-3 cross-links comparable to that of the parental *araB*p*lptC* strain, lysed at non-permissive conditions (Table 1, Supplementary Fig. 3). In sharp contrast to the other strains, *araB*p*lptC* Δ*ldtF* cells showed morphological defects even when grown at permissive conditions (Supplementary Fig. 3D). However, no morphological defects were observed when *ldtF* was deleted in the *lptC*$^{+}$ background (Supplementary Fig. 3B) suggesting that the deletion of *ldtF* caused additional problems to cells with depleted *lptC* levels.

Only the *araB*p*lptC* Δ*ldtE* Δ*ldtF* mutant did not lyse under non-permissive conditions and arrested growth like the *araB*p*lptC* parental strain (Fig. 1F, Supplementary Figs. 4E and 4F). These cells displayed a high level (>8%) of 3-3

cross-links at all conditions (*i.e.*, even without depletion of *lptC*). Thus, in all mutants the growth arrest (no lysis) phenotype correlated with increased levels of 3-3 cross-links in the PG (Table 1). This suggests that in the *araB*p*lptC* Δ*ldtE* Δ*ldtF* mutant the activity of LdtD alone is sufficient to avoid cell lysis and, more generally, that cells avoid lysis upon an LPS transport defect by increased LDT-catalyzed formation of 3-3 cross-links in the PG.

The *ldtD* promoter is activated under envelope stress conditions

The growth phenotypes observed in the *ldt* mutants in both *lptC*$^{+}$ and *araB*p*lptC* backgrounds, and the accompanied changes in the level of 3-3 cross links in their PG suggest that the expression of *ldtD, ldtE* and *ldtF* is regulated in the cell. To measure the expression of these genes we constructed transcriptional fusions of the promoter region of *ldtD, ldtE* or *ldtF* to *lacZ* and the resulting p*ldtD-lacZ*, p*ldtE-lacZ* and p*ldtF-lacZ* containing plasmids were used to transform the BW25113 wild type strain, the conditional *araB*p*lptC* mutant and their derivatives deleted for *ldtD*, *ldtE* and *ldtF* alone and in all possible combinations. β–galactosidase activity was measured from cells collected at different time points during growth.

We observed that *ldtD*, *ldtE* and *ldtF* exhibited very different expression profiles depending on the genetic background, growth phase and growth condition (Fig. 3). The expression of *ldtE* and *ldtF* in the *lptC*$^{+}$ background was growth phase dependent, with maximal activation of p*ldtE-lacZ* and p*ldtF-lacZ* in stationary-phase cells of wild type and any *ldt* mutant tested (Fig. 3B and 3C). RpoS is the alternative sigma factor for stationary-phase gene expression (Battesti *et al*., 2011) and, indeed, we found that *ldtE* and *ldtF* were both RpoS-regulated genes, which lost their growth phase dependent promoter activation in a BW25113Δ*rpoS* mutant (Supplementary Fig. 6).

The *ldtE* and *ldtF* promoters followed the growth phase dependent activation profile in the *araB*p*lptC* conditional mutant under permissive and non-permissive growth conditions (Fig. 3B and 3C). However, the expression of the *ldtF* promoter fusion increased ~1.5-fold in the *araB*p*lptC* conditional mutant and the isogenic single mutants lacking *ldtD*, *ldtE* or *ldtF* compared to the corresponding *lptC*$^{+}$ background (Fig. 3C). By contrast, the growth phase dependent activation profile of the *ldtE* promoter was lost in all *araB*p*lptC ldt* mutant derivatives with the exception of the *araB*p*lptC* Δ*ldtF* mutant.

The *ldtD* promoter was not activated in the wild type *lptC*$^{+}$ strain and in *ldt* derivatives with the exception of the Δ*ldtE* Δ*ldtF* mutant, where the lack of LdtE and LdtF appeared to activate the expression of *ldtD* (Fig. 3A). Interestingly, *ldtD* was strongly activated, up to 8-fold compared to *lptC*$^{+}$ cells, in all *lptC*-depleted cells with or without the deletion of the other *ldt* genes (Fig. 3A). Finally, it was not possible assess the activation profile of p*ldt-lacZ* transcriptional fusions in the *araB*plptC conditional mutant deleted for all three *ldt*s as this strain lysed very rapidly upon shift to non-permissive condition thus preventing reliable measurements of β–galactosidase activity.

Overall, these results show that the expression of *ldt* genes in the cell follows two distinct profiles. *LdtE* and *ldtF* share a growth phase dependent activation profile under most conditions tested, with higher expression in stationary phase. The expression profile of *ldtE* and *ldtF* was unaffected by the presence or absence of arabinose in the *araB*p*lptC* conditional strain suggesting that these are the housekeeping LDTs in the cell. By contrast, *ldtD* was expressed strongly in the *lptC*$^{+}$ background in which both *ldtE* and *ldtF* were deleted, and in the *araB*p*lptC* conditional strain in the absence of arabinose. Taken together, these data suggest that

LdtD is a stress-response LDT activated under envelope stress conditions or in the absence of the housekeeping LDTs, a conclusion that is consistent with the presence of increased levels of 3-3 cross-links under these conditions.

Growth arrest without lysis requires PG synthesis and maturation

Thus far, our results suggest that cells defective in the LPS export pathway activate an important PG remodeling programme to avoid lysis due to the defective OM, and LDTs seem to play a major role in this process. LDTs can facilitate PG growth in certain β-lactam resistant strains of *E. coli* and *E. faecium* and, in this situation, they function with a GTase, but not a TPase domain of a bifunctional PG synthase, and a DD-CPase (Mainardi *et al*., 2000, 2002, 2005; Hugonnet *et al*., 2016). Together these activities produce glycan chains with tetrapeptide stems, which are the donor substrate for LDTs. Cells depleted for *lptC* have been shown previously to induce the expression of the bifunctional GTase/TPase PBP1B 3.1-fold, and that of the DD-CPases PBP5 and PBP6a 1.5- and 4.0-fold, respectively (Martorana *et al*., 2014). PBP5 is the major DD-CPase active under standard laboratory conditions (Nelson and Young, 2001). PBP6a is an additional DD-CPase with an unknown physiological function, as it does not seem to be active under standard growth conditions (Peters *et al*., 2016). We next asked if these enzymes are important to prevent lysis in *lptC*-depleted cells, as are the LDTs.

We assessed the growth phenotype of *araB*p*lptC* conditional mutants deleted for *mrcA* and *mrcB* (coding for PBP1A and PBP1B, respectively). PBP1A was not required to prevent lysis of the *araB*p*lptC* strain under non-permissive conditions (Fig. 4A and 4B). As shown in Figures 4C and 4D, however, *araB*p*lptC* Δ*mrcB* mutant cells suffered from severe lysis when grown in an arabinose-free medium, and

lysis could be prevented by ectopic expression of PBP1B. We next tested which of the two activities of PBP1B was needed to prevent lysis, by ectopic expression of PBP1B versions with inactivated GTase or TPase domains. PBP1B(S510A) has an inactive TPase domain and was fully functional in preventing lysis, showing that the TPase activity of PBP1B is not required (Fig. 4E). PBP1B(E233D) has an inactivated GTase domain and this enzyme thus also lacks TPase activity, which depends upon ongoing GTase reactions (Bertsche *et al*., 2005; Egan *et al*., 2015). PBP1B(E233D) was unable to prevent lysis upon depletion of *lptC*, suggesting that the GTase activity of PBP1B is crucial to prevent lysis (Fig. 4E). Consistent with this conclusion, lysis was also observed in cells lacking LpoB, a key activator of the GTase of PBP1B; LpoB is essential for PBP1B function in the cell (Egan *et al*., 2014; Typas *et al*., 2010) (Supplementary Fig. 7). CpoB modulates the stimulation of the TPase of PBP1B by LpoB and was not required to prevent lysis upon *lptC* depletion (Supplementary Fig. 7), consistent with our findings that the GTase, but not TPase was important for survival.

The amount of 3-3 cross-links of the *araB*p*lptC* Δ*mrcB* mutant grown under non-permissive conditions was comparable to that of the parental *araB*p*lptC* strain (Supplementary Table 4). The *araB*p*lptC* Δ*mrcB* mutant showed morphological defects even under the permissive condition (Fig 4D), phenotypically reproducing what we observed for the *araB*p*lptC* Δ*ldtF* mutant (see above; Supplementary Figure 3D) and suggesting that both mutants were not capable of preventing lysis despite having 3-3 cross-links in the PG. Finally, depletion of the DD-CPase genes *dacA* (coding for PBP5) or *dacC* (PBP6a) in *araB*p*lptC* had different impacts on cell growth: depletion of *lptC* (in *araB*p*lptC* Δ*dacA* cells) arrested growth without lysis whereas *araB*p*lptC* Δ*dacC* cells lysed (Fig. 5). Therefore, our data demonstrate that

survival upon severe LPS transport defect requires not only LDTs, but also the GTase and DD-CPase activities of PBP1B and PBP6a, respectively, presumably to synthesize and to modify the nascent PG substrate of the LDTs.

LdtD interacts with PBP1B and not with PBP1A

Our data so far support the hypothesis that LdtD may function with PBP1B to rescue sacculus integrity upon severe OM assembly defects. To test if LdtD interacted with PBP1B or its homologue PBP1A we purified the recombinant proteins and assessed direct protein-protein interactions by two methods. In the first experiment, we mixed oligohistidine-tagged PBP1A or PBP1B with untagged LdtD and assayed binding to Ni^{2+}-NTA beads. LdtD was pulled-down to the beads by oligohistidine-tagged PBP1B, and not by oligohistidine-tagged PBP1A or LpoB, or in the absence of tagged protein (Fig. 6A), suggesting a direct interaction with oligohistidine-tagged PBP1B. The pull-down was confirmed and extended by microscale thermophoresis, which revealed an interaction between LdtD and PBP1B, but not between LdtD and PBP1A. The K_D value of the LdtD-PBP1B interaction was 112 ± 33 nM (Fig. 6B).

LdtD forms 3-3 cross-links in mature and nascent PG

The LDT activity of LdtD has been demonstrated previously with a soluble disaccharide tetrapeptide substrate (Hugonnet *et al*., 2016). Considering its role in PG remodeling and its interaction with PBP1B, we hypothesized that the enzyme must be active against larger PG fragments or even sacculi, and/or nascent PG produced by PBP1B. We therefore tested these possibilities by first incubating LdtD with either soluble glycan chains carrying uncross-linked tetrapeptides (DS-tetra chains, the products of MepM, Fig. 7A) and PG sacculi purified from strain BW25113Δ6LDT,

which lacks all 6 *ldt* genes. LdtD was highly active against these substrates (Fig. 7A), utilizing almost all monomeric tetrapeptides to generate the 3-3 cross-linked dimer (disaccharide tetratripeptide, TetraTri). The high activity is particularly remarkable in the case of the sacculi, which after the reaction with LdtD contained an unusually high cross-linkage with ~84% of all muropeptides present in cross-links.

We next assayed the activity of LdtD during synthesis of PG *in vitro* using radiolabeled lipid II as substrate in the presence of an excess of unlabeled PG sacculi. After the reaction, the products were digested with the muramidase cellosyl and the resulting muropeptides were separated by HPLC using back-to-back UV and radioactivity detectors to monitor the products formed. LdtD produced a highly 3-3 cross-linked nascent PG, as seen by the abundant radiolabeled TetraTri(3-3) muropeptide present in the reaction with the TPase-inactive PBP1B(S510A) mutant, its activator LpoB and the DD-CPase PBP6a (Fig. 7B). 3-3 or 4-3 cross-links were not produced in the absence of LdtD or in the absence of PBP1B(S510A)/LpoB, showing that LdtD was responsible for the formation of 3-3 cross-links and that it preferred to act on polymeric PG and not on the tetrapeptide version of lipid II produced by PBP6a. However, LdtD preferentially acted on the nascent (radioactive) PG despite the presence of a ~10-fold excess of unlabelled PG sacculi. The UV traces showed that ~52% of the unlabeled tetrapeptides were consumed by LdtD, which was markedly less than the ~68% consumption of the radiolabeled tetrapeptides. This suggests that LdtD prefers new PG, synthesized by PBP1B and trimmed by PBP6a, as substrate. LdtD showed similar activity in reactions with PBP5 (instead of PBP6a), showing that both DD-CPases are capable of providing the tetrapeptide substrates (Supplementary Fig. 8).

In summary, the activity assays align well with the phenotypic data and muropeptide analysis showing that LdtD is highly active in producing 3-3 cross-links in PG sacculi, and it is able to cooperate with the GTase activity of PBP1B and DD-CPases to utilize nascent PG as substrate, consistent with a role in protective remodeling of PG during OM defective assembly.

Discussion

Gram-negative bacteria must coordinate the assembly of their cell envelope layers to maintain cellular integrity and protection against toxic compounds in the environment. The PG and OM layers are both enlarged by dynamic multiprotein complexes (Haeusser and Margolin, 2016; Okuda *et al*., 2016; Pazos *et al*., 2017), but it is largely unknown how exactly these complexes function, how they are regulated to synchronize the growth of PG and OM, and how the deranged synthesis of one layer affects the other. In this work we discovered a PG remodeling pathway involving LDTs that is required in cells with defective OM assembly, revealing a link between LPS export and a dedicated mode of PG synthesis. This link is essential for cell survival under severe OM assembly stress, such as depletion of the essential LptC component, and not required in unstressed cells. Nevertheless, the remodelling of PG by LDTs takes place also in unstressed cells, perhaps to repair the minor defects in PG that might arise during undisturbed growth, resulting in a low amount of 3-3 cross-links. Expanding from previous work (Magnet *et al*., 2007; Magnet *et al*., 2008; Sanders and Pavelka, 2013) we also show here that *E. coli* has three LDTs (LdtD, LdtE and the newly identified LdtF) that all contribute to the formation of 3-3 cross-links.

Role of the different LDTs.

LdtD, LdtE and LdtF appear to have different roles in the cell. LdtE and LdtF are housekeeping LDTs that are induced by RpoS when cells enter stationary phase (Fig. 3) consistent with the previously observed increase in 3-3 cross-links in stationary-phase cells (Glauner *et al*., 1988; Pisabarro *et al*., 1985). LdtE seems to require LdtF, LdtD or both for activity, as 3-3 cross-links were not detectable in the PG of mutants deleted for both *ldtD* and *ldtF*. LdtD is poorly expressed in *lptC*$^{+}$ cells (Fig. 3) and we propose that under stress-free conditions the LdtE - LdtF couple or LdtF alone forms 3-3 cross-links in the cell.

While LDTs are dispensable under standard growth conditions, their activity is essential to prevent cell lysis in cells with defective LPS transport; 3-3 cross-links increased under these conditions (Table 1 and Supplementary Table 4). The expression of *ldtD* increased strongly in *lptC*-depleted cells and *lptD* levels, as well as the level of 3-3 cross-links, were high in the absence of the housekeeping LdtE and LdtF (Fig. 3, Table 1) suggesting that LdtD plays a major role in PG remodelling during cell envelope stress. Interestingly, unlike the Δ*ldtE* Δ*ldtF* double mutant, the single Δ*ldtE* or Δ*ldtF* mutants lysed upon *lptC*-depletion despite the presence of a functional copy of *ldtD* and, in case of Δ*ldtF*, a level of 3-3 cross-links comparable to that of the parental stressed strain. We hypothesize that the *ldtE* or *ldtF* single mutants are not able to accumulate sufficient LdtD activity to avoid lysis upon *lptC* depletion, whereas the Δ*ldtE* Δ*ldtF* double mutant is already stressed and has a high level of LdtD *before* the depletion of *lptC*, allowing it to survive when *lptC* is depleted (Table 1). Hence, in *lptC*-depleted cells the housekeeping LdtE and LdtF help the cell to survive until sufficient LdtD accumulates, explaining why all three LDTs are needed to prevent lysis. Alternatively, or in addition, LdtD might not be properly recruited to

the PG synthetic machineries in a mutant lacking LdtF (see below). In sharp contrast to the other strains, the *ldtF* mutant shows impaired cell morphology even before *lptC* depletion and despite the presence of 3-3 cross-links (Supplementary Fig. 3D). Perhaps the aberrant cell morphology of *araB*p*lptC* Δ*ldtF* cells is caused by mis-localized 3-3 cross-links. Alternatively, LdtF could have additional roles in the cell because unlike the other LDTs it has been implicated in biofilm formation in enteroaggregative *E. coli* (Sheikh *et al*., 2001).

LdtD is part of a 'PG repair machine' with PBP1B/LpoB and PBP6a

Apart from the LDTs, *lptC* depleted cells also required the GTase function of PBP1B, its activator LpoB and the DD-CPase PBP6a (but not PBP1A or PBP5) to avoid lysis (Figs. 4 and 5). We propose that these proteins cooperate in a PG remodeling programme activated in response to envelope stress, based on our genetic evidence and the physical interaction of LdtD with PBP1B (Fig. 6). LptC-depleted cells lacking PBP1B produced a high level of 3-3 cross-links but still lysed (Fig. 4 and Supplementary Table 4); notably these cells showed aberrant morphologies even when grown under permissive conditions as observed for *araB*p*lptC* Δ*ldtF* mutant.

So far, the cellular function of PBP6a was not known due to the lack of phenotypes associated with its loss. We show here that PBP6a becomes important upon LPS transport defects. Our data support a model according to which a PG repair machinery containing PBP1B/LpoB, LdtD and PBP6a polymerizes PG strands (GTase of PBP1B), trims the pentapeptides (PBP6a) and utilizes the resulting tetrapeptides to form 3-3 cross-links (LdtD). Although LdtD is capable of working in isolation on different substrates, our model is consistent with its preference for

nascent PG and the induction of the genes encoding PBP1B and PBP6a in *lptC* depleted cells (Martorana *et al*., 2014).

How does PG repair rescue cells from lysis?

The PG layer is an elastic, net-like structure with relatively homogeneous pores that change with the cell's turgor. From penetration experiments with fluorescent dextran molecules with different sizes it was estimated that globular proteins with a molecular weight of up to 25 kDa can diffuse through relaxed PG (Demchick and Koch, 1996). Stretched PG (as it occurs in the cell) has larger pores depending on the turgor. Osmotic shock can release proteins with molecular weights of up to 100 kDa, due to the molecular sieving properties of the PG layer (Vazquez-Laslop et al., 2001). Maximally stretched peptide cross-links are estimated to generate pores with a diameter of 6.2 nm (Vazquez-Laslop et al., 2001), although such maximal expansion of the PG might not occur in the cell. Hence, larger trans-envelope machines such as the flagellum need to hydrolyse the PG layer locally to increase the pore size for their assembly through the PG layer (Herlihey et al., 2014). The pore size in PG is likely important also for trans-envelope export systems. The type II secretion machine of *Aeromonas hydrophila* becomes non-functional in the absence of the secretin ExeD, but function can be restored by growing cells in high glycine concentrations, which reduces PG cross-linkage and increases pore size, enabling transport through the PG (Vanderlinde *et al*., 2017). In case of LPS transport, the periplasmic Lpt 'bridge' alone without its cargo is approximately 3.5 nm wide, and just the inner core of an LPS molecule (without the bulky O-antigen chain) has dimensions of approximately 1.4×3.0 nm (Le Brun *et al*., 2013). Moreover, according to the PEZ model (Okuda et al., 2016), the LPS export machinery requires the coupled movement of several LptA

molecules together with their LPS cargo across the PG layer. Hence, we hypothesize that the LPS-transport machinery requires wider pores in the PG, and that the PG net is opened locally to allow assembly of the Lpt machinery and rapid flow of LPS to the cell surface. It is known that the Lpt complex disassembles and LptA is degraded when LPS transport is arrested due to depletion of LptC (Sperandeo *et al*., 2008; Sperandeo *et al*., 2011; Villa *et al*., 2013). Presumably, the PG has to be subsequently sealed, to close the holes that arose from the disassembly of Lpt machines. We propose a dedicated PG repair machine for this function, containing PBP1B/LpoB, LdtD and PBP6a, which synthesizes new PG to close defects in the sacculus (Fig. 8). The GTase function of this machine is activated by the OM anchored lipoprotein LpoB, which spans the periplasm to interact with the UB2H domain of PBP1B. In line with our model, it was previously hypothesized that LpoB activates PBP1B depending on the size of the pores in PG to couple PG growth with cell growth (Typas *et al*., 2012). Hence, apart from its role in the synthesis of 'normal PG' (with 4-3 cross-links) during cell elongation and division, the PBP1B-LpoB system has a second role in PG repair together with LdtD, producing PG with 3-3 cross-links.

PBP1A/LpoA are able to complement the loss of PBP1B/LpoB in normal growth, but they cannot compensate for the stress related function of PBP1B/LpoB with LptD. PBP1B/LpoB, LdtD and the DD-CPase PBP5 enabled an *E. coli* mutant strain to grow in the presence of an otherwise lethal concentration of ampicillin, producing exclusively 3-3 cross-links without the need for 4-3 cross-links (Hugonnet *et al*., 2016). PBP1B/LpoB (and not PBP1A/LpoA) promoted the recovery of PG-less L-form cells of *E. coli* to the walled state, generating a PG layer *de novo* (Ranjit *et al*., 2017). These observations and our own work highlight the versatility of the

PBP1B/LpoB PG synthase/regulator pair, which is used by the cell in different processes and circumstances.

LdtD is induced in response to Cpx activating conditions, leading to enhanced 3-3 cross-links (Bernal-Cabas *et al*., 2015; Delhaye *et al*., 2016), and consistent with its major protective role upon LPS export defects. The housekeeping LdtE and LdtF might have a similar function in PG repair during the transition from exponential growth into stationary phase when the LPS transport gradually ceases as cells stop growing. This idea is consistent with their expression profile and the accumulation of 3-3 cross-links in stationary phase. It remains to be seen if LdtE and LdtF work in concert with specific PG synthases/hydrolases to synthesize and remodel PG locally.

In summary, we discovered a new role of 3-3 cross-links in the PG as a mean to locally fortify the sacculus after envelope-spanning macromolecular complexes disassemble, to 'repair' areas with reduced cross-linkage. This functional connection between envelope machineries and the PG synthetic apparatus is an example of the elegant and versatile mechanisms bacteria employ to maintain the integrity of their essential cell envelope under a variety of growth conditions.

Material and Methods

Bacterial strains, plasmids and growth conditions

Bacterial strains and plasmids used in this work are listed in Supplementary Tables 1 and 2. Primers used are listed in Supplementary Table 3. Routinely, cells were grown aerobically at 37°C or 30°C in LB-Lennox medium (10 g/L tryptone, 5 g/L yeast extract, 5 g/L NaCl) (Difco). When required, antibiotics or inducers were added: ampicillin (100 µg/mL), chloramphenicol (25 µg/mL), kanamycin (25 µg/mL), arabinose (0.2% wt/vol), IPTG (0.1 mM). For *lptC* depletion, bacteria were harvested from cultures with an OD_{600} of 0.2 by centrifugation, washed twice with LD and diluted 100-fold in LD with or without arabinose. Cell growth was monitored by OD_{600} measurements and viability was determined by quantifying the colony forming units (CFU).

The phenotypes of *araB*p*lptC* and isogenic *ldt*s mutant derivatives were summarized as the slope of each growth curve between minutes 180 and 390 (related to Fig. 1F). Each slope was calculated as the regression line based on the data points identified by *y*-values (expressed as absorbance at 600 nm) and *x*-values (time, expressed in hours) using excel functions.

Construction of *E. coli* deletion or depletion strains

Deletion strains were obtained by moving *kan*-marked alleles from the Keio *E. coli* single-gene knockout library (Baba *et al*., 2006) by P1 phage transduction (Silhavy *et al*., 1984). Afterward, the *kan* cassette was removed by pCP20-encoded Flp recombinase to generate unmarked deletions with a FRT-site scar sequence (Datsenko and Wanner, 2000). The removal of the *kan* gene was verified by colony PCR. Strains

with multiple deletions were generated by sequential P1 transduction and *kan* cassette removal. *LptC* depletion strains were obtained by moving the *kan araC araB*p-*lptC* allele from BB-3 (Sperandeo *et al*., 2006) into selected mutants by P1 transduction. Depletion strains were selected on media containing kanamycin and 0.2% arabinose. The insertion of the cassette was verified by PCR.

Construction of plasmids

pGS121 and pGS124 were constructed by cloning *ldtE* and *ldtF* into the *Eco*RI/*Hind*III restriction sites of pGS100 (Sperandeo *et al*., 2006). pGS123 was constructed by cloning *ldtD* into *Eco*RI/*Xba*I restriction sites of pGS100. Primers used for genes cloning are listed in Supplementary Table 3. To assess transcriptional activity the promoter regions of *ldtE*, *ldtD* and *ldtF* genes were cloned into the *lacZ* vector pRS415 (Simons *et al*., 1987). For this, the promoter region of each *ldt* gene was amplified by PCR using primers listed in Supplementary Table 3 and cloned into *EcoR*I/*Bam*HI (*ldtE*p and *ldtD*p) or *EcoR*I/*Sma*I (*ldtF*p) restriction sites of pRS415. Each cloned region contained at least 600 bp upstream and 150 bp downstream of the start codon of each gene to include putative regulatory elements.

For pET28a-His6-LdtF, *ldtF* was cloned starting from position 58 downstream the ATG codon, into *Nde*I/*Xho*I pET28a, eliminating the putative signal sequence. The correct nucleotide sequences of inserts were verified (Eurofins Genomics).

pAMS01(LdtE) and pAMS02(LdtF) were constructed using the Gibson assembly method (Gibson *et al*., 2009) by cloning *ldtE* and *ldtF* into pJEH12(LdtD) (Hugonnet *et al*., 2016), respectively. Primers used for gene cloning are listed in Supplementary Table 3.

Overexpression plasmids and purification of proteins

Purification of PBP6a. DNA encoding for PBP6a (residues 28-400) from *E. coli* BW25113 was amplified by PCR and cloned into pET28a(+) using *Nde*I and *Xho*I. PBP6a was overexpressed in *E. coli* LOBSTR-BL21(DE3) (Kerafast) cells grown overnight at 37°C in 2 L of TB-autoinduction medium supplemented with 4 g lactose, 1 g glucose, 10 mM $MgCl_2$ and 10 mM $MgSO_4$ (Studier, 2005). Cells were harvested by centrifugation for 15 min at 4500 rpm and 14°C. The resulting cell pellet was resuspended in 50 ml buffer A (25 mM HEPES/NaOH pH 7.5, 100 mM NaCl) supplemented with 1 mM phenylmethyl sulfonyl fluoride (Sigma Aldrich), 1× protease inhibitor cocktail (Sigma Aldrich) and desoxyribonuclease I (Sigma Aldrich). Cells were broken by sonication and centrifuged for 1 h at 130,000×*g* and 4 °C. The resulting pellet was resuspended in buffer B (25 mM HEPES/NaOH pH 7.5, 1 M NaCl, 2 mM $MgCl_2$ 10% glycerol) supplemented with 1% CHAPS (Anatrace) and incubated under continuous stirring overnight at 4°C. Insoluble material was removed by centrifugation for 1 h at 130,000×*g* at 4°C. The supernatant was recovered, mixed with 1 ml Ni-NTA Superflow (Qiagen) preequilibrated in buffer B (supplemented with 0.5% CHAPS and 5 mM imidazole) and incubated under continuous gentle stirring for 3 h at 4°C. Ni-NTA agarose was poured in a gravity flow column, washed 5 times with 20 column volume (CV) buffer B (supplemented with 0.5% CHAPS and increasing concentrations of imidazole, 10-50 mM). PBP6a was eluted with buffer B supplemented with 0.5% CHAPS and 300 mM imidazole. Eluted protein was dialysed against 2 L dialysis buffer (25 mM HEPES/NaOH, 500 mM NaCl, 10% glycerol, 0.1% CHAPS, 10 mM EDTA). The protein was further purified by size exclusion chromatography on a HiLoad 16/60 Superdex 200 (GE

Healthcare) column using size exclusion buffer (25 mM HEPES/NaOH, 300 mM NaCl, 10% glycerol, 0.1% CHAPS) and a flowrate of 1 ml/min. Purity was determined by SDS-PAGE and combined fractions were concentrated and stored in aliquots at -80°C.

Purification of LdtD. *E. coli* LOBSTR-BL21(DE3) (Kerafast) cells were transformed with pETMM82, a plasmid encoding for LdtD carrying an N-terminal DsbC-His6-tag followed by a TEV-protease cleavage site (Hugonnet *et al*., 2016), and grown at 30°C in 1 L TB medium (Tartof, 1987) (supplemented with 5 mM $MgCl_2$ and 5 mM $MgSO_4$) until OD600 0.3. LdtD overexpression was induced by adding IPTG (Generon) to a final concentration of 0.5 mM. The temperature was decreased to 16°C and cells were incubated for 19 h. Cells were harvested by centrifugation for 15 min at 4,500 rpm and 14°C. The resulting cell pellet was resuspended in 60 ml buffer A (20 mM Tris pH 8.0, 1 M NaCl, 10 mM imidazole) supplemented with 1 mM phenylmethyl sulfonyl fluoride (Sigma Aldrich), 1× protease inhibitor cocktail (Sigma Aldrich) and desoxyribonuclease I (Sigma Aldrich). Cells were broken by sonication and centrifuged for 1 h at 130,000×*g* at 4°C. The supernatant was recovered, mixed with 0.5 ml Ni-NTA Superflow (Qiagen) preequilibrated in buffer A (supplemented with 10 mM imidazole) and incubated under continuous gentle stirring at 4°C. After 1.5 h another 0.5 ml of Ni-NTA Superflow (Qiagen) was added and incubated for 1.5 h. The suspension was poured in a gravity flow column and washed 2 times with 20 CV buffer B (20 mM Tris/HCl pH 7.0, 150 mM NaCl) supplemented with 20 mM imidazole, 5 mM ATP and 1 mM $MgCl_2$ to remove tightly bound chaperone proteins. After 3 more washing steps with 20 CV of buffer B each (2× 40 mM imidazole, 1× 50 mM imidazole), the protein was

eluted with buffer B supplemented with 300 mM imidazole and glycerol was added to the elution fractions to a final concentration of 10%. The protein was dialysed against 2× 2 L dialysis buffer 1 (25 mM Tris pH 7.0, 300 mM NaCl, 10% glycerol) for 1 h each at 4°C. The protein solution was supplemented with 5 mM β-mercaptoethanol (Sigma Aldrich), 10 U/ml TEV-protease (Promega) and dialysed against 1 L of dialysis buffer 2 (25 mM Tris pH 7.0, 300 mM NaCl, 5 mM β-mercaptoethanol, 10% glycerol) for 1 h and against an additional 1 L overnight at 4°C.

The sample was mixed with 1 ml of Ni-NTA-agarose preequilibrated in dialysis buffer 2 containing 50 mM of imidazole and incubated for 2-3 h at 4°C under gentle stirring. The suspension was poured in a gravity flow column and the DsbC-His-tag free protein present in the flow through was further purified by size exclusion chromatography on a HiLoad 26/60 Supedex 200 (GE Healthcare) column using size exclusion buffer (25 mM Tris/HCl pH 7.5, 300 mM NaCl, 10% glycerol) and a flowrate of 1 ml/min. Purity was determined by SDS-PAGE and combined fractions were concentrated and stored in aliquots at -80°C.

Purification of His-PBP1A and PBP1A. PBP1A was purified according to a published procedure (Born *et al*., 2006) with modifications. *E. coli* LOBSTR-BL21(DE3) (Kerafast) cells carrying the plasmid pTK1Ahis were grown in 2 L of LB medium (Miller, 1972) at 30°C until an optical density (578 nm) of 0.5 was reached. IPTG (1 mM) was added and the cells were grown for 3 h, chilled on ice for 15 min, harvested by centrifugation for 20 min at 5,000 rpm and 4^0C. The cell pellet was resuspended in 140 ml of Buffer I (25 mM HEPES/NaOH pH 7.5, 1 M NaCl, 1 mM EGTA, 10% glycerol) supplemented with 1 mM phenylmethyl sulfonyl fluoride (Sigma Aldrich), 1× protease inhibitor cocktail (Sigma Aldrich) and

desoxyribonuclease I (Sigma Aldrich). Cells were broken by sonication and the soluble fraction was removed after ultracentrifugation for 1 h at 130,000×*g* and 4°C. The membrane pellet was resuspended in extraction buffer (25 mM HEPES/NaOH pH 7.5, 5 mM $MgCl_2$, 1 M NaCl, 20% glycerol, 2% Triton X-100) with continuous stirring overnight at 4°C. Insoluble material was removed by centrifugation for 1 h at 130,000×*g* at 4°C. The supernatant containing the solubilised membrane fraction was diluted with the same volume of IMAC dilution buffer (25 mM HEPES/NaOH pH 7.5, 1 M NaCl, 40 mM imidazole, 20% glycerol) and applied to a 5 mL HisTrap HP column using an ÄKTA PrimePlus. The column was washed with IMAC wash buffer (25 mM HEPES/NaOH pH 7.5, 500 mM NaCl, 50 mM imidazole, 20% glycerol, 0.2% reduced Triton X-100), and PBP1A was eluted with the elution buffer (25 mM HEPES/NaOH pH 7.5, 500 mM NaCl, 400 mM imidazole, 20% glycerol, 0.2% reduced Triton X-100). Fractions containing His-PBP1A were pooled. For the removal of the His-tag, 16 units of thrombin (restriction grade, Novagen) were added and the sample was dialysed in 3 × 1 l of cleavage buffer (20 mM HEPES/NaOH pH 7.5, 500 mM NaCl, 10% glycerol).

Purification of MepM. The protein was purified as described in (Singh *et al*., 2012) with modifications. Briefly, 2 L of LB medium (Miller, 1972) were inoculated with strain BL21(DE3) pET21b-*yebA* and protein expression was induced by addition of IPTG at a final concentration of 50 µM. Cells were incubated for 2 h at 25°C, harvested by centrifugation and resuspended in lysis buffer (25 mM Tris/HCl pH 7.5, 300 mM NaCl, 10% glycerol). The first purification step was performed on HisTrap HP column (GE healthcare) preequilibrated with wash buffer (25 mM Tris/HCl pH 7.5, 300 mM NaCl, 20 mM imidazole). Protein was eluted in the same buffer

supplemented with 300 mM imidazole. Samples containing protein of interest were dialysed against 25 mM HEPES/NaOH pH 7.5, 300 mM NaCl, 10% glycerol overnight at 4°C. Dialysed samples were concentrated using Vivaspin 6 columns and applied to a HiLoad 16/60 Superdex 200 (GE healthcare) size exclusion column at a flowrate of 1 ml/min using the same buffer. The purified protein was stored in aliquots at -80 °C.

Other proteins. PBP1B and PBP1B(TP*) were purified as described in (Typas *et al*., 2010), LpoB was purified as described in (Egan *et al*., 2014), PBP5 was purified as described in (Peters *et al*., 2016).

Protein-protein interactions

Pull-down experiments were performed as described (Gray *et al*., 2015) using proteins at 2 μM concentration. Microscale thermophoresis (MST) experiments were carried out with a Monolith NT.115 instrument (NanoTemper GmbH, Germany). LdtD was labelled with the Monolith NT.115 Protein Labelling Kit RED-NHS according to the manufactory instructions. MST experiments were performed with serial dilution series of PBP1A or PBP1B and constant concentration of labelled LdtD in 20 mM HEPES/NaOH pH 7.5, 150 mM NaCl, 0.2 % Triton X-100, using premium capillaries, an LED-Power of 20% and an MST-Power of 40%. Changes in normalised fluorescence caused by the local temperature gradient were analysed by the MO.Affinity Analysis v2.1.2 software.

MepM digest of sacculi from BW25113Δ6LDT

Sacculi from BW25113Δ6LDT were prepared as described in (Glauner *et al*., 1988). MepM digest was carried out in a final volume of 200 µl containing 25 mM HEPES/NaOH pH 7.5, 150 mM NaCl, 0.05% Triton X-100, 750 µg sacculi using a final concentration of MepM of 2 µM. The sample was incubated overnight at 37°C. Then the reaction mixture was heated for 10 min at 100°C and centrifuged for 20 min. The supernatant containing disaccharide-tetrapeptide chains was collected and stored at 2-8°C.

LdtD activity assay with disaccharide-tetrapeptide chains or PG sacculi

Assays were carried out in a final volume of 50 µl containing 25 mM Tris/HCl pH 7.5, 100 mM NaCl, 10 mM $MgCl_2$, 0.1% Triton X-100, and 2 µM LdtD. Fifteen µl of peptidoglycan or 20 µl of disaccharide-tetrapeptide chains were added and the reaction mixture was incubated at 37°C overnight. The reaction was stopped by boiling the samples for 10 min.

Coupled PG synthesis - LDT assay

Coupled assays were carried out in a final volume of 50 µl containing 25 mM HEPES/NaOH pH 7.5, 175 mM NaCl, 10 mM $MgCl_2$, 0.1% Triton X-100, radioactively labelled lipid II (10,000 dpm), 15 µl of PG from BW25113Δ6LDT and 2 µM of each protein as needed (LdtD, PBP1B-TP*, LpoB, PBP6 and/or PBP5). The reaction mixture was incubated for 4 h at 37°C. The reaction was stopped by boiling the samples for 10 min.

LDTs expression for HPLC analysis

BW25113Δ6LDT strain was transformed with pJEH12(LdtD), pAMS01(LdtE), pAMS02(LdtF) or an empty plasmid (pSAV057; Alexeeva *et al*., 2010) . Empty BW25113Δ6LDT was used as control. The same strain was also co-transformed with pJEH12(LdtD) and pGS124 or pAMS02(LdtF) and pGS121. A single transformant was used to inoculate 5 mL of Antibiotic Broth (AB) (Sigma Aldrich) overnight at 37°C. A 1:1000 dilution was performed in fresh AB cultures (400 mL each, in duplicate) from the overnight cultures. Samples were grown at 37°C and expression of LDTs was carried out with 50 μM IPTG when OD_{600} was 0.2. After reaching the late exponential phase (OD_{600} 0.8), samples were cooled in ice and harvested by centrifugation at 4°C. The cell pellet was resuspended in 6 ml ice-cold water and dropped slowly into 6 ml boiling 8% SDS water solution. Samples were boiled for 60 minutes.

HPLC analysis

Samples were centrifuged for 20 minutes and the supernatant recovered and adjusted to pH 4 with 20% phosphoric acid. HPLC analysis was carried out as described in (Bertsche *et al*., 2005). Muropeptides were detected by online radioactivity detector and absorbance at 205 nm.

Imaging and image analysis

Microscopy images were obtained with a Nikon Eclipse Ti microscope through a 100× 1.45 oil objective and photometric/Cool-SNAP-HQ2 camera or with a Zeiss Axiovert 200M microscope through a 63× 1.45 oil objective coupled to a AxioCam Mrm device 290 camera (Zeiss). Cells at different time points, as indicated by arrows

in the figures, were collected from a total amount corresponding to an OD of 4, and a 1:10 ratio of fixation solution (fixation solution: formaldehyde 37% - glutaraldehyde 25% in PBS) was added. Cells were incubated for 30 min at 37°C with shaking, washed with PBS and resuspended in 500 µl of PBS. A cell suspension (5 µl) was spotted onto an agarose-coated glass slide (1% agarose), the sample was covered with a glass coverslip. To stain cell membranes, SynaptoRed C2M or FM5-95 was added to agarose solution to a final concentration of 2 µg/ml.

β-galactosidase assay

β-galactosidase specific activity was measured from a total number of cells corresponding to an OD_{600} of 8 as previously described (Martorana *et al*., 2011).

Acknowledgements

We thank Alexander Egan and Katharina Peters (Newcastle University) for providing proteins, Mohammed Terrak (University of Liège) for the expression plasmid for PBP1B(S510A) and Rick Lewis (Newcastle University) for critical reading of the manuscript. A.P., W.V. and T.d.B were supported by the European Commission via the International Training Network Train2Target (No. 721484). W.V. received support from the Wellcome Trust (101824/Z/13/Z). T.d.B. and W.V. received support from the NAPCLI project within the JPI AMR programme (ZonMW project 60-60900-98-207; MR/N501840/1).

References

Alexeeva, S., Gadella, T.W., Jr., Verheul, J., Verhoeven, G.S., and den Blaauwen, T. (2010). Direct interactions of early and late assembling division proteins in *Escherichia coli* cells resolved by FRET. Mol Microbiol *77*, 384-398. doi: 10.1111/j.1365-2958.2010.07211.x.

Baba, T., Ara, T., Hasegawa, M., Takai, Y., Okumura, Y., Baba, M., Datsenko, K.A., Tomita, M., Wanner, B.L., and Mori, H. (2006). Construction of *Escherichia coli* K-12 in-frame, single-gene knockout mutants: the Keio collection. Mol Syst Biol *2*, 2006 0008. doi: 10.1038/msb4100050

Banzhaf, M., van den Berg van Saparoea, B., Terrak, M., Fraipont, C., Egan, A., Philippe, J., Zapun, A., Breukink, E., Nguyen-Disteche, M., den Blaauwen, T.*, et al.* (2012). Cooperativity of peptidoglycan synthases active in bacterial cell elongation. Mol Microbiol *85*, 179-194. doi: 10.1111/j.1365-2958.2012.08103.x

Baquero, M.R., Bouzon, M., Quintela, J.C., Ayala, J.A., and Moreno, F. (1996). *dacD*, an *Escherichia coli* gene encoding a novel penicillin-binding protein (PBP6b) with DD-carboxypeptidase activity. J Bacteriol *178*, 7106-7111.

Battesti, A., Majdalani, N., and Gottesman, S. (2011). The RpoS-mediated general stress response in *Escherichia coli*. Annu Rev Microbiol *65*, 189-213. doi: 10.1146/annurev-micro-090110-102946.

Bernal-Cabas, M., Ayala, J.A., and Raivio, T.L. (2015). The Cpx envelope stress response modifies peptidoglycan cross-linking via the L,D-transpeptidase LdtD and the novel protein YgaU. J Bacteriol *197*, 603-614. doi: 10.1128/JB.02449-14

Bertsche, U., Breukink, E., Kast, T., and Vollmer, W. (2005). In vitro murein peptidoglycan synthesis by dimers of the bifunctional transglycosylase-transpeptidase PBP1B from *Escherichia coli*. J Biol Chem *280*, 38096-38101. doi: 10.1074/jbc.M508646200

Biarrotte-Sorin, S., Hugonnet, J.E., Delfosse, V., Mainardi, J.L., Gutmann, L., Arthur, M., and Mayer, C. (2006). Crystal structure of a novel beta-lactam-insensitive peptidoglycan transpeptidase. J Mol Biol *359*, 533-538. doi.org/10.1016/j.jmb.2006.03.014

Born, P., Breukink, E., and Vollmer, W. (2006). In vitro synthesis of cross-linked murein and its attachment to sacculi by PBP1A from *Escherichia coli*. J Biol Chem *281*, 26985-26993. doi: 10.1074/jbc.M604083200

Braun, M., and Silhavy, T.J. (2002). Imp/OstA is required for cell envelope biogenesis in *Escherichia coli*. Mol Microbiol *45*, 1289-1302. doi: 10.1046/j.1365-2958.2002.03091.x

Chng, S.S., Gronenberg, L.S., and Kahne, D. (2010a). Proteins required for lipopolysaccharide assembly in *Escherichia coli* form a transenvelope complex. Biochemistry *49*, 4565-4567. doi: 10.1021/bi100493e.

Chng, S.S., Ruiz, N., Chimalakonda, G., Silhavy, T.J., and Kahne, D. (2010b). Characterization of the two-protein complex in *Escherichia coli* responsible for lipopolysaccharide assembly at the outer membrane. Proc Natl Acad Sci U S A *107*, 5363-5368. doi: 10.1073/pnas.0912872107

Datsenko, K.A., and Wanner, B.L. (2000). One-step inactivation of chromosomal genes in *Escherichia coli* K-12 using PCR products. Proc Natl Acad Sci U S A *97*, 6640-6645. doi: 10.1073/pnas.120163297

Delhaye, A., Collet, J.F., and Laloux, G. (2016). Fine-Tuning of the Cpx Envelope Stress Response Is Required for Cell Wall Homeostasis in *Escherichia coli*. MBio *7*, e00047-00016. doi: 10.1128/mBio.00047-16.

Demchick, P., and Koch, A.L. (1996). The permeability of the wall fabric of *Escherichia coli* and *Bacillus subtilis*. J Bacteriol *178*, 768-773.

Egan, A.J., Biboy, J., van't Veer, I., Breukink, E., and Vollmer, W. (2015). Activities and regulation of peptidoglycan synthases. Philos Trans R Soc Lond B Biol Sci *370,* 0150031. doi: 10.1098/rstb.2015.0031

Egan, A.J., Jean, N.L., Koumoutsi, A., Bougault, C.M., Biboy, J., Sassine, J., Solovyova, A.S., Breukink, E., Typas, A., Vollmer, W., and Simorre, J.P. (2014). Outer-membrane lipoprotein LpoB spans the periplasm to stimulate the peptidoglycan synthase PBP1B. Proc Natl Acad Sci U S A *111*, 8197-8202. doi: 10.1073/pnas.1400376111

Freinkman, E., Chng, S.S., and Kahne, D. (2011). The complex that inserts lipopolysaccharide into the bacterial outer membrane forms a two-protein plug-and-barrel. Proc Natl Acad Sci U S A *108*, 2486-2491. doi: 10.1073/pnas.1015617108.

Freinkman, E., Okuda, S., Ruiz, N., and Kahne, D. (2012). Regulated assembly of the transenvelope protein complex required for lipopolysaccharide export. Biochemistry *51*, 4800-4806. doi: 10.1021/bi300592c.

Ghosh, A.S., and Young, K.D. (2003). Sequences near the Active Site in Chimeric Penicillin Binding Proteins 5 and 6 Affect Uniform Morphology of *Escherichia coli*. J Bacteriol *185*, 2178-2186. doi: 10.1128/JB.185.7.2178-2186.2003

Gibson, D.G., Young, L., Chuang, R.Y., Venter, J.C., Hutchison, C.A., 3rd, and Smith, H.O. (2009). Enzymatic assembly of DNA molecules up to several hundred kilobases. Nat Methods *6*, 343-345. doi: 10.1038/nmeth.1318

Glauner, B., Holtje, J.V., and Schwarz, U. (1988). The composition of the murein of *Escherichia coli*. J Biol Chem *263*, 10088-10095.

Goffin, C., and Ghuysen, J.M. (1998). Multimodular penicillin-binding proteins: an enigmatic family of orthologs and paralogs. Microbiol Mol Biol Rev *62*, 1079-1093.

Gray, A.N., Egan, A.J., Van't Veer, I.L., Verheul, J., Colavin, A., Koumoutsi, A., Biboy, J., Altelaar, A.F., Damen, M.J., Huang, K.C*., et al.* (2015). Coordination of peptidoglycan synthesis and outer membrane constriction during *Escherichia coli* cell division. Elife *4*, e07118 doi: 10.7554/eLife.07118

Haeusser, D.P., and Margolin, W. (2016). Splitsville: structural and functional insights into the dynamic bacterial Z ring. Nat Rev Microbiol *14*, 305-319. doi: 10.1038/nrmicro.2016.26

Herlihey, F.A., Moynihan, P.J., and Clarke, A.J. (2014). The essential protein for bacterial flagella formation FlgJ functions as a beta-N-acetylglucosaminidase. J Biol Chem *289*, 31029-31042. doi: 10.1074/jbc.M114.603944.

Holtje, J.V. (1998). Growth of the stress-bearing and shape-maintaining murein sacculus of *Escherichia coli*. Microbiol Mol Biol Rev *62*, 181-203.

Hugonnet, J.E., Mengin-Lecreulx, D., Monton, A., den Blaauwen, T., Carbonnelle, E., Veckerle, C., Brun, Y.V., van Nieuwenhze, M., Bouchier, C., Tu, K., Rice, L.B., Arthur, M. (2016). Factors essential for L,D-transpeptidase-mediated peptidoglycan cross-linking and beta-lactam resistance in *Escherichia coli*. Elife *5,* e19469 doi: 10.7554/eLife.19469

Jean, N.L., Bougault, C.M., Lodge, A., Derouaux, A., Callens, G., Egan, A.J., Ayala, I., Lewis, R.J., Vollmer, W., and Simorre, J.P. (2014). Elongated structure of the outer-membrane activator of peptidoglycan synthesis LpoA: implications for PBP1A stimulation. Structure *22*, 1047-1054. doi: 10.1016/j.str.2014.04.017

Kamio, Y., and Nikaido, H. (1976). Outer membrane of Salmonella typhimurium: accessibility of phospholipid head groups to phospholipase c and cyanogen bromide activated dextran in the external medium. Biochemistry *15*, 2561-2570.

Kuru, E., Lambert, C., Rittichier, J., Till, R., Ducret, A., Derouaux, A., Gray, J., Biboy, J., Vollmer, W., VanNieuwenhze, M., Brun, Y.V., Sockett, R.E. (2017). Fluorescent D-amino-acids reveal bi-cellular cell wall modifications important for *Bdellovibrio bacteriovorus* predation. Nat Microbiol. *2,* 1648-1657. doi: 10.1038/s41564-017-0029-y

Le Brun, A.P., Clifton, L.A., Halbert, C.E., Lin, B., Meron, M., Holden, P.J., Lakey, J.H., and Holt, S.A. (2013). Structural characterization of a model gram-negative bacterial surface using lipopolysaccharides from rough strains of *Escherichia coli*. Biomacromolecules *14*, 2014-2022. doi: 10.1021/bm400356m

Magnet, S., Bellais, S., Dubost, L., Fourgeaud, M., Mainardi, J.L., Petit-Frere, S., Marie, A., Mengin-Lecreulx, D., Arthur, M., and Gutmann, L. (2007). Identification

of the L,D-transpeptidases responsible for attachment of the Braun lipoprotein to *Escherichia coli* peptidoglycan. J Bacteriol *189*, 3927-3931. doi: 10.1128/JB.00084-07

Magnet, S., Dubost, L., Marie, A., Arthur, M., and Gutmann, L. (2008). Identification of the L,D-transpeptidases for peptidoglycan cross-linking in *Escherichia coli*. J Bacteriol *190*, 4782-4785. doi: 10.1128/JB.00025-08

Mainardi, J.L., Fourgeaud, M., Hugonnet, J.E., Dubost, L., Brouard, J.P., Ouazzani, J., Rice, L.B., Gutmann, L., and Arthur, M. (2005). A novel peptidoglycan cross-linking enzyme for a beta-lactam-resistant transpeptidation pathway. J Biol Chem *280*, 38146-38152. DOI 10.1074/jbc.M507384200

Mainardi, J.L., Legrand, R., Arthur, M., Schoot, B., van Heijenoort, J., and Gutmann, L. (2000). Novel mechanism of beta-lactam resistance due to bypass of DD-transpeptidation in *Enterococcus faecium*. J Biol Chem *275*, 16490-16496. doi: 10.1074/jbc.M909877199

Mainardi, J.L., Morel, V., Fourgeaud, M., Cremniter, J., Blanot, D., Legrand, R., Frehel, C., Arthur, M., Van Heijenoort, J., and Gutmann, L. (2002). Balance between two transpeptidation mechanisms determines the expression of beta-lactam resistance in *Enterococcus faecium*. J Biol Chem *277*, 35801-35807. doi: 10.1074/jbc.M204319200

Martorana, A.M., Motta, S., Di Silvestre, D., Falchi, F., Dehò, G., Mauri, P., Sperandeo, P., and Polissi, A. (2014). Dissecting *Escherichia coli* outer membrane biogenesis using differential proteomics. PLoS One *9*, e100941. doi: 10.1371/journal.pone.0100941

Martorana, A.M., Sperandeo, P., Polissi, A., and Deho, G. (2011). Complex transcriptional organization regulates an *Escherichia coli* locus implicated in lipopolysaccharide biogenesis. Res Microbiol *162*, 470-482. doi: 10.1016/j.resmic.2011.03.007

Miller, J.H. (1972). Experiments in molecular genetics. Cold Spring Harbor Laboratory, Cold Spring Harbor, New York.

Narita, S., and Tokuda, H. (2009). Biochemical characterization of an ABC transporter LptBFGC complex required for the outer membrane sorting of lipopolysaccharides. FEBS Lett *583*, 2160-2164. doi: 10.1016/j.febslet.2009.05.051

Neidhardt, F.C., and Umbarger, H.E. (1996). Chemical Composition of *Escherichia coli*. p. 13-16 *In* Neidhardt F.C. (ed) *Escherichia coli* and *Salmonella*: Cellular and Molecular Biology. ASM Press.

Nelson, D.E., and Young, K.D. (2000). Penicillin binding protein 5 affects cell diameter, contour, and morphology of *Escherichia coli*. J Bacteriol *182*, 1714-1721. doi: 10.1128/JB.182.6.1714-1721.2000

Nelson, D.E., and Young, K.D. (2001). Contributions of PBP 5 and DD-carboxypeptidase penicillin binding proteins to maintenance of cell shape in *Escherichia coli*. J Bacteriol *183*, 3055-3064. doi: 10.1128/JB.183.10.3055-3064.2001

Nikaido, H. (2003). Molecular Basis of Bacterial Outer Membrane Permeability Revisited. Microbiol Mol Biol Rev *67*, 593-656. doi: 10.1128/MMBR.67.4.593-656.2003

Okuda, S., Freinkman, E., and Kahne, D. (2012). Cytoplasmic ATP hydrolysis powers transport of lipopolysaccharide across the periplasm in *E. coli*. Science *338*, 1214-1217. doi: 10.1126/science.1228984

Okuda, S., Sherman, D.J., Silhavy, T.J., Ruiz, N., and Kahne, D. (2016). Lipopolysaccharide transport and assembly at the outer membrane: the PEZ model. Nat Rev Microbiol *14*, 337-345. doi: 10.1038/nrmicro.2016.25

Paradis-Bleau, C., Markovski, M., Uehara, T., Lupoli, T.J., Walker, S., Kahne, D.E., and Bernhardt, T.G. (2010). Lipoprotein cofactors located in the outer membrane activate bacterial cell wall polymerases. Cell *143*, 1110-1120. doi: 10.1016/j.cell.2010.11.037

Pazos, M., Peters, K., and Vollmer, W. (2017). Robust peptidoglycan growth by dynamic and variable multi-protein complexes. Curr Opin Microbiol *36*, 55-61. doi: 10.1016/j.mib.2017.01.006

Peters, K., Kannan, S., Rao, V.A., Biboy, J., Vollmer, D., Erickson, S.W., Lewis, R.J., Young, K.D., and Vollmer, W. (2016). The Redundancy of Peptidoglycan Carboxypeptidases Ensures Robust Cell Shape Maintenance in *Escherichia coli*. MBio *7,* e00819-16. doi:10.1128/mBio.00819-16

Pisabarro, A.G., de Pedro, M.A., and Vazquez, D. (1985). Structural modifications in the peptidoglycan of *Escherichia coli* associated with changes in the state of growth of the culture. J Bacteriol *161*, 238-242.

Polissi, A., and Georgopoulos, C. (1996). Mutational analysis and properties of the *msbA* gene of *Escherichia coli*, coding for an essential ABC family transporter. Mol Microbiol *20*, 1221-1233. doi: 10.1111/j.1365-2958.1996.tb02642.x

Raetz, C.R., and Whitfield, C. (2002). Lipopolysaccharide endotoxins. Annu Rev Biochem *71*, 635-700. doi:10.1146/annurev.biochem.71.110601.135414

Ranjit, D.K., Jorgenson, M.A., and Young, K.D. (2017). PBP1B Glycosyltransferase and Transpeptidase Activities Play Different Essential Roles during the De Novo Regeneration of Rod Morphology in *Escherichia coli*. J Bacteriol *199,* e00612-16. doi: 10.1128/JB.00612-16

Ruiz, N., Gronenberg, L.S., Kahne, D., and Silhavy, T.J. (2008). Identification of two inner-membrane proteins required for the transport of lipopolysaccharide to the outer membrane of *Escherichia coli*. Proc Natl Acad Sci U S A *105*, 5537-5542. doi: 10.1073/pnas.0801196105

Sanders, A.N., and Pavelka, M.S. (2013). Phenotypic analysis of *Eschericia coli* mutants lacking L,D-transpeptidases. Microbiology *159*, 1842-1852. doi: 10.1099/mic.0.069211-0.

Sathiyamoorthy, K., Vijayalakshmi, J., Tirupati, B., Fan, L., and Saper, M.A. (2017). Structural analyses of the *Haemophilus influenzae* peptidoglycan synthase activator LpoA suggest multiple conformations in solution. J Biol Chem *292*, 17626-17642. doi: 10.1074/jbc.M117.804997

Sheikh, J., Hicks, S., Dall'Agnol, M., Phillips, A.D., and Nataro, J.P. (2001). Roles for Fis and YafK in biofilm formation by enteroaggregative *Escherichia coli*. Mol Microbiol *41*, 983-997. doi: 10.1046/j.1365-2958.2001.02512.x

Silhavy, T.J., Kahne, D., and Walker, S. (2010). The bacterial cell envelope. Cold Spring Harb Perspect Biol *2*, a000414. doi: 10.1101/cshperspect.a00041

Silhavy, T.J., M. L. Berman, and Enquist, L.W. (1984). Experiments with gene fusions. C.S.H. ColdSpringHarborLaboratory, N.Y.

Simons, R.W., Houman, F., and Kleckner, N. (1987). Improved single and multicopy *lac*-based cloning vectors for protein and operon fusions. Gene *53*, 85-96. doi.org/10.1016/0378-1119(87)90095-3

Singh, S.K., SaiSree, L., Amrutha, R.N., and Reddy, M. (2012). Three redundant murein endopeptidases catalyse an essential cleavage step in peptidoglycan synthesis of *Escherichia coli* K12. Mol Microbiol *86*, 1036-1051. doi: 10.1111/mmi.12058

Sperandeo, P., Cescutti, R., Villa, R., Di Benedetto, C., Candia, D., Dehò, G., and Polissi, A. (2007). Characterization of *lptA* and *lptB*, two essential genes implicated in lipopolysaccharide transport to the outer membrane of *Escherichia coli*. J Bacteriol *189*, 244-253. doi:10.1128/JB.01126-06

Sperandeo, P., Lau, F.K., Carpentieri, A., De Castro, C., Molinaro, A., Dehò, G., Silhavy, T.J., and Polissi, A. (2008). Functional analysis of the protein machinery required for transport of lipopolysaccharide to the outer membrane of *Escherichia coli*. J Bacteriol *190*, 4460-4469. doi: 10.1128/JB.00270-08

Sperandeo, P., Martorana, A.M., and Polissi, A. (2017a). Lipopolysaccharide biogenesis and transport at the outer membrane of Gram-negative bacteria. Biochim Biophys Acta *1862*, 1451-1460. doi: 10.1016/j.bbalip.2016.10.006

Sperandeo, P., Martorana, A.M., and Polissi, A. (2017b). The lipopolysaccharide transport (Lpt) machinery: A nonconventional transporter for lipopolysaccharide assembly at the outer membrane of Gram-negative bacteria. J Biol Chem *292*, 17981-17990. doi: 10.1074/jbc.R117.802512

Sperandeo, P., Pozzi, C., Dehò, G., and Polissi, A. (2006). Non-essential KDO biosynthesis and new essential cell envelope biogenesis genes in the *Escherichia coli yrbG-yhbG* locus. Res Microbiol *157*, 547-558. doi:10.1016/j.resmic.2005.11.014

Sperandeo, P., Villa, R., Martorana, A.M., Samalikova, M., Grandori, R., Dehò, G., and Polissi, A. (2011). New insights into the Lpt machinery for lipopolysaccharide transport to the cell surface: LptA-LptC interaction and LptA stability as sensors of a properly assembled transenvelope complex. J Bacteriol *193*, 1042-1053. doi: 10.1128/JB.01037-10

Studier, F.W. (2005). Protein production by auto-induction in high density shaking cultures. Protein Expr Purif *41*, 207-234.

Tartof, K.D.H., C.A. (1987). Improved media for growing plasmid and cosmid clones. Bethesda Res Lab Focus *9*.

Typas, A., Banzhaf, M., Gross, C.A., and Vollmer, W. (2012). From the regulation of peptidoglycan synthesis to bacterial growth and morphology. Nat Rev Microbiol *10*, 123-136. doi: 10.1038/nrmicro267

Typas, A., Banzhaf, M., van den Berg van Saparoea, B., Verheul, J., Biboy, J., Nichols, R.J., Zietek, M., Beilharz, K., Kannenberg, K., von Rechenberg, M.*, et al.* (2010). Regulation of peptidoglycan synthesis by outer-membrane proteins. Cell *143*, 1097-1109. doi: 10.1016/j.cell.2010.11.038

Vanderlinde, E.M., Strozen, T.G., Hernandez, S.B., Cava, F., and Howard, S.P. (2017). Alterations in Peptidoglycan Cross-Linking Suppress the Secretin Assembly Defect Caused by Mutation of GspA in the Type II Secretion System. J Bacteriol *199*. e00617-16. doi: 10.1128/JB.00617-16

Vazquez-Laslop, N., Lee, H., Hu, R., and Neyfakh, A.A. (2001). Molecular sieve mechanism of selective release of cytoplasmic proteins by osmotically shocked Escherichia coli. J Bacteriol *183*, 2399-2404. doi:10.1128/JB.183.8.2399-2404.2001

Villa, R., Martorana, A.M., Okuda, S., Gourlay, L.J., Nardini, M., Sperandeo, P., Dehò, G., Bolognesi, M., Kahne, D., and Polissi, A. (2013). The *Escherichia coli* Lpt transenvelope protein complex for lipopolysaccharide export is assembled via conserved structurally homologous domains. J Bacteriol *195*, 1100-1108. doi: 10.1128/JB.02057-12.

Vollmer, W., Blanot, D., and de Pedro, M.A. (2008). Peptidoglycan structure and architecture. FEMS Microbiol Rev *32*, 149-167. doi: 10.1111/j.1574-6976.2007.00094.x

Wu, T., McCandlish, A.C., Gronenberg, L.S., Chng, S.S., Silhavy, T.J., and Kahne, D. (2006). Identification of a protein complex that assembles lipopolysaccharide in the outer membrane of *Escherichia coli*. Proc Natl Acad Sci U S A *103*, 11754-11759. doi:10.1073/pnas.0604744103

Zhou, Z., White, K.A., Polissi, A., Georgopoulos, C., and Raetz, C.R. (1998). Function of *Escherichia coli* MsbA, an essential ABC family transporter, in lipid A and phospholipid biosynthesis. J Biol Chem *273*, 12466-12475. doi: 10.1074/jbc.273.20.12466

Figure legends

Figure 1. LDTs prevent cell lysis upon defective OM assembly. Cells of the *araB*p*lptC* conditional strain (**A, B**) and the isogenic mutants deleted for *ldtD*, *ldtE* and *ldtF* (**C, D**) were grown in the presence of 0.2% arabinose to an OD_{600} of 0.2, harvested, washed three times and resuspended in an arabinose-supplemented (+ Ara) or arabinose-free (no Ara) medium. (**A**, **C**) Growth was monitored by OD_{600} measurements (upper panels) and by determining CFU (lower panels). At t = 120, 210 and 270 min (arrows) samples were imaged (**B**, *araB*p*lptC*; **D**, isogenic mutant deleted for *ldtD*, *ldtE* and *ldtF*). Phase contrast images are on the top and fluorescence images are on the bottom. Scale bars, 3 μm. (**E**) PG sacculi purified from *araBplptC* cells grown in the presence of arabinose or after 210 min (2) or 270 min (3) growth in the absence of arabinose, were digested with cellosyl and the muropeptide composition was determined by HPLC. The graph shows the relative abundance of TetraTetra (with 4-3 cross-links) and TetraTri(3-3) muropeptides. The latter significantly increased upon depletion of *lptC*. (**F**) Cells of the *araBplptC* conditional strain and isogenic mutants deleted for every *ldt* gene alone or in all possible combinations were grown in an arabinose-free medium as indicated above. Growth phenotypes are summarized as the slope of growth curves measured between 180 and 390 min. Positive and negatives values indicate cell growth and cell lysis, respectively. The values are the means ± standard deviation (SD) from three independent experiments. The mean slope calculated from growth curves in arabinose-supplemented medium for *araBplptC* conditional strain and isogenic *ldt* mutants was 0,56 ±0,03. *Ldt* genes are indicated by their capital letters.

Figure 2. Ectopic expression of LdtD and LdtE-LdtF results in 3-3 cross-links. (**A**) Muropeptide profiles of BW25113Δ6LDT cells containing either no plasmid, empty plasmid, or plasmid with *ldtD*, *ldtE*, *ldtF*, *ldtE-ldtF* or *ldtD-ldtF*, grown in the presence of inducer. (**B**) Structures of major peaks numbered in the top chromatogram in panel A. LDT products are muropeptides containing 3-3 cross-links (peaks 4-7), tripeptides (peaks 1, 5 and 7) and glycine at position 4 (Gly4, peaks 2 and4). G, *N*-acetylglucosamine; M(r), *N*-acetylmuramitol; L-Ala, L-alanine; D-Glu, D-glutamic acid; D-Ala, D-alanine; *m*-DAP, *meso*-diaminopimelic acid.

Figure 3. The *ldtD* promoter is activated under envelope stress conditions. Wild-type BW25113 ($lptC^{+}$) and isogenic mutants deleted for every *ldt* alone and in all possible combinations were transformed with plasmids expressing *ldtD*p-*lacZ* (**A**) *ldtE*p-*lacZ* (**B**) or *ldtF*p-*lacZ* (**C**) fusions. Cells were grown in LD medium. β-galactosidase specific activity was calculated from cells collected at 120 min (OD_{600}~ 0.2), 180 min (OD_{600} ~ 0.8) and 210 min (OD_{600} ~ 2.0) min (light grey bars for each strain, left side). The *araB*p*lptC* conditional strain and its mutant derivatives were transformed with plasmids expressing *ldtD*p-*lacZ* (**A**) *ldtE*p-*lacZ* (**B**) or *ldtF*p-*lacZ* (**C**). Cells were grown with 0.2% arabinose to an OD_{600} of 0.2, harvested, washed three times and resuspended in an arabinose-supplemented (+ Ara) or arabinose-free (- Ara) medium. Samples for determination of β-galactosidase specific activity were collected at the time point at which the strains cultivated under non-permissive conditions arrested growth and 30 and 60 min afterwards (shown as dark grey bars for each strain in the +Ara and no Ara conditions). The values are the means ± SD of at least three independent experiments. All mutants were also transformed with the void plasmid

and the mean of β-galactosidase specific activity calculated from cells grown in any condition was 249±30 (min^{-1} mg^{-1}). *Ldt* genes are indicated by their capital letters.

Figure 4. The GTase activity of PBP1B is required to prevent cell lysis upon defective OM assembly. Cultures of *araB*p*lptC* Δ*mrcA* (**A**) or *araB*p*lptC* Δ*mrcB* (**C**) lacking PBP1A and PBP1B, respectively, were grown with 0.2% arabinose to an OD_{600} of 0.2, harvested, washed three times and resuspended in an arabinose-supplemented (+ Ara) or arabinose-free (no Ara) medium. Cell growth was then monitored by OD_{600} measurements. At t = 120 min, 210 min and 270 min (arrows) samples from *araB*p*lptC* Δ*mrc*A (**B**) and *araB*p*lptC* Δ*mrc*B (**D**) were collected for imaging. Phase contrast images are shown on the top and fluorescence images on the bottom. Scale bars, 3 μm. (**E**) Complementation of the *araB*p*lptC* Δ*mrcB* lysis phenotype by ectopic expression of wild type *mrcB* (GT^+TP^+), *mrcB* with mutated GTase (GT*), TPase (TP*) or both (TP*GT*). All mutants were grown in the presence of 0.2% arabinose at 30°C to an OD_{600} of 0.2, harvested, washed three times and resuspended in an arabinose-free medium. The growth of *araB*p*lptC* Δ*mrcB* in arabinose-supplemented medium is shown as control. Cell growth was monitored by OD_{600} measurements.

Figure 5. The DD-CPase PBP6a prevents cell lysis upon defective OM assembly. Cells of *araB*p*lptC* Δ*dacA* (**A**) or *araB*p*lptC* Δ*dacC* (**C**) lacking PBP5 and PBP6a, respectively, were grown in the presence of 0.2% arabinose to an OD_{600} of 0.2, harvested, washed three times and resuspended in an arabinose-supplemented (+Ara) or arabinose-free (no Ara) medium. Cell growth was then monitored by OD_{600} measurements. At t = 120 min, 210 min and 270 min (arrows) samples from

*araB*p*lptC* Δ*dacA* (**B**) and *araB*p*lptC* Δ*dacC* (**D**) were collected for imaging. Phase contrast images are on the top and fluorescence images are on the bottom. Scale bars, 3 μm.

Figure 6. LdtD interacts with PBP1B and not PBP1A. (**A**) Coomassie-stained SDS-PAGE gel showing the pull-down of proteins to Ni^{2+}-NTA beads. LdtD bound to the beads and was present in the elution fraction E only in the presence of oligohistidine-tagged PBP1B, and not in the presence of oligohistidine-tagged LpoB, oligohistidine-tagged PBP1A or in the absence of another protein. A, applied sample. (**B**) Microscale thermophoresis curves showing that LdtD interacts with PBP1B and not with PBP1A. The K_D value for the LdtD-PBP1B interaction is indicated. The values are mean ± SD of three independent experiments

Figure 7. LdtD shows LD-TPase activity with different PG substrates. (**A**) HPLC chromatograms showing the formation of TetraTri(3-3) dimers by LdtD incubated with glycan chains harboring monomeric tetrapeptides (DS-tetra chains) or PG from BW25113Δ6LDT lacking all six *ldt* genes. Samples were digested with cellosyl, reduced with sodium borohydride before HPLC analysis. (**B**) HPLC chromatograms obtained from samples upon incubating radioactive labeled lipid II, PG from BW25113Δ6LDT and the proteins indicated to the right. Samples were digested with cellosyl, reduced with sodium borohydride and subjected to HPLC analysis with detection of both UV signal (black traces) and radioactivity (red traces). PBP1B (TP*), PBP1B with an inactive transpeptidase site due to the replacement of Ser-510 by Ala. (**C**) Proposed structures of muropeptides present in the fractions in panels A and B. G, *N*-acetylglucosamine; M, *N*-acetylmuramic acid; M(r), *N*-acetylmuramitol;

M-*P*, N-acetylmuramic acid-1-phosphate; L-Ala, L-alanine; D-Glu, D-glutamic acid; D-Ala, D-alanine; *m*-DAP, *meso*-diaminopimelic acid.

Figure 8. Role of a PG repair machine. Left panel: The Lpt machine transverses the PG layer that has been locally opened to allows the formation of the transenvelope protein bridge and transport of the bulky LPS molecules. The standard cross-links in PG are of the 4-3 type (black line). Right panel: upon LptC depletion the Lpt machine disassembles, the LptA component is degraded and LPS molecules remain in the outer leaflet of the CM. PBP1B-LpoB, LdtD and PBP6a work in concert to repair the PG, synthesizing it locally with 3-3 cross-links (red line). Components of the Lpt machine are colored blue and indicated by their capital letters. G and M: *N*-acetylglucosamine and *N*-acetylmuramic acid residues, respectively. Amino acids of the stem peptide are indicated as colored hexagons: L-Ala, yellow; D-Glu, green; *meso*-Dap, red; D-Ala, yellow.

Table 1. Summary of the level of 3-3 cross-links in PG and growth phenotype of single and multiple *ldt* mutant strains with or without depletion of LPS export.

Gene present			3-3 Cross-linkage / Phenotype in strain				
			lptC^{+}	*araBplptC*			
				+ Arabinose		no Arabinose	
ldtD	*ldtE*	*ldtF*	3-3 CL (area %)[1]	Growth	3-3 CL (area %)[1]	Growth	3-3 CL (area %)[1]
+	+	+	3.0	normal	1.7	arrest	7.5
-	+	+	3.2	normal	2.4	lysis	6.1
+	-	+	2.9	normal	1.9	lysis	6.0
+	+	-	2.9	normal	1.9	lysis	8.4
-	-	+	2.2	normal	1.9	lysis	-[3]
-	+	-	n.d.[2]	normal	n.d.	lysis	n.d.
+	-	-	2.4	normal	8.2	arrest	8.4
-	-	-	n.d.	normal	n.d.	lysis	n.d.

[1] Sum of the percentages of all muropeptides with 3-3 cross-links (CL) in the muropeptide profile. See Supplementary Table 4 for complete data on the muropeptide composition.
[2] n.d. (not detected), 3-3 cross-linked muropeptides were below detection limit.
[3] not determined because the *lptC*-depleted cells lysed rapidly preventing reliable peptidoglycan analysis.

Figure 1

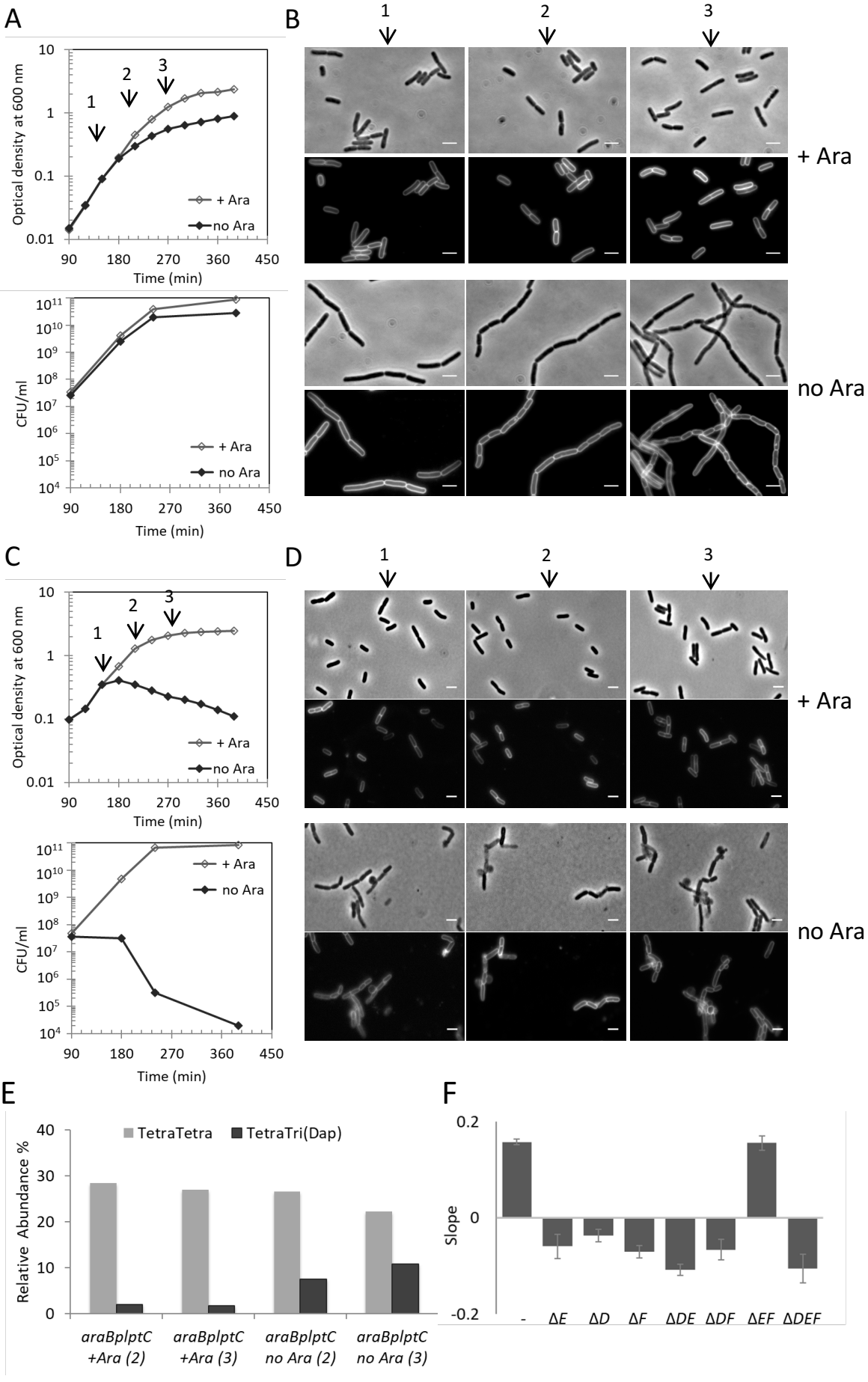
A
B
C
D
E
F
Optical density at 600 nm
Time (min)
CFU/ml
+ Ara
no Ara
1
2
3
Relative Abundance %
TetraTetra
TetraTri(Dap)
araBplptC +Ara (2)
araBplptC +Ara (3)
araBplptC no Ara (2)
araBplptC no Ara (3)
Slope
-
ΔE
ΔD
ΔF
ΔDE
ΔDF
ΔEF
ΔDEF

Figure 2

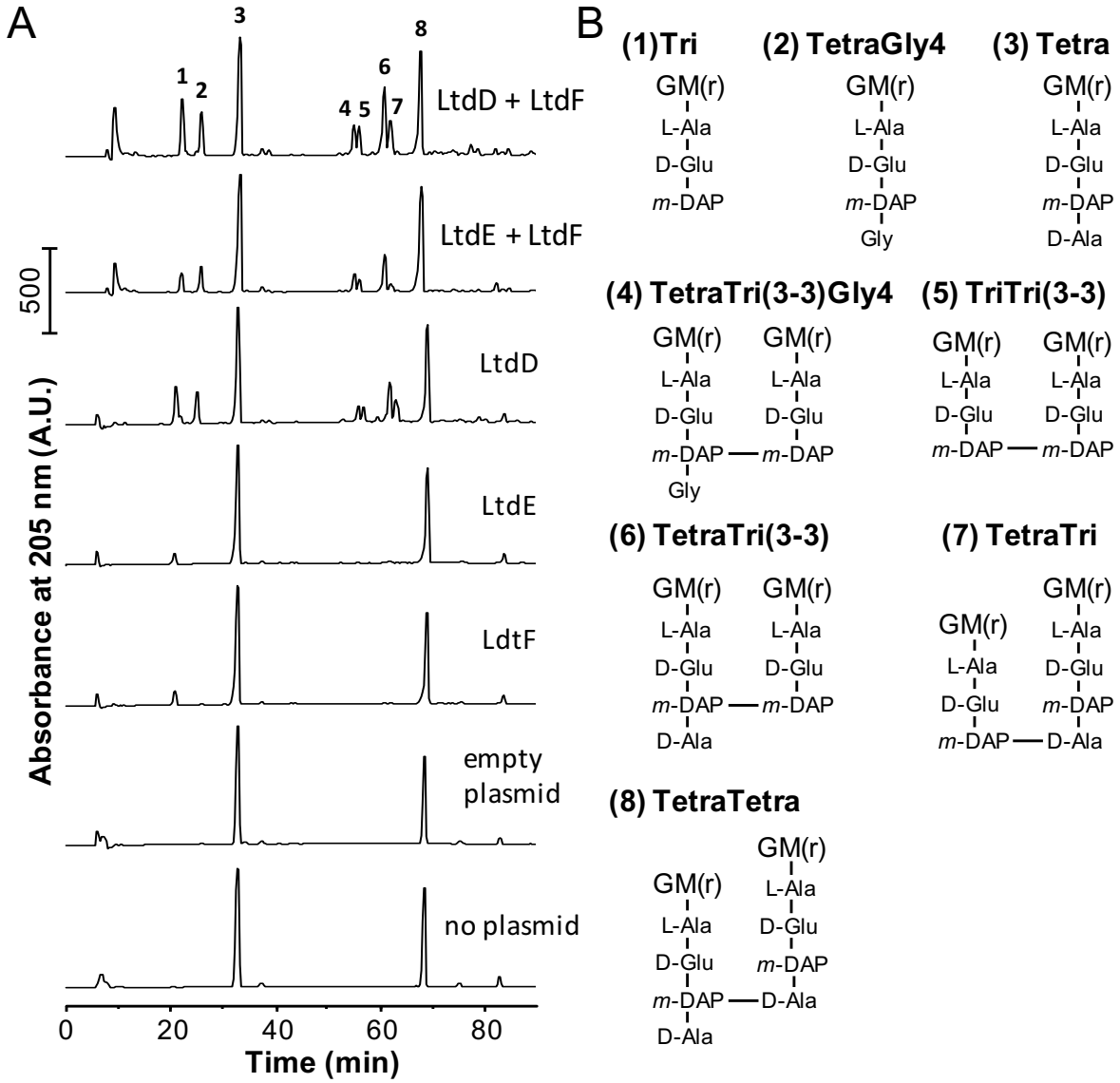
A
1
2
3
4
5
6
7
8
LtdD + LtdF
LtdE + LtdF
LtdD
LtdE
LdtF
empty plasmid
no plasmid
500
Absorbance at 205 nm (A.U.)
0
20
40
60
80
Time (min)
B
(1)Tri
(2) TetraGly4
(3) Tetra
(4) TetraTri(3-3)Gly4
(5) TriTri(3-3)
(6) TetraTri(3-3)
(7) TetraTri
(8) TetraTetra
GM(r)
L-Ala
D-Glu
m-DAP
Gly
D-Ala

Figure 3

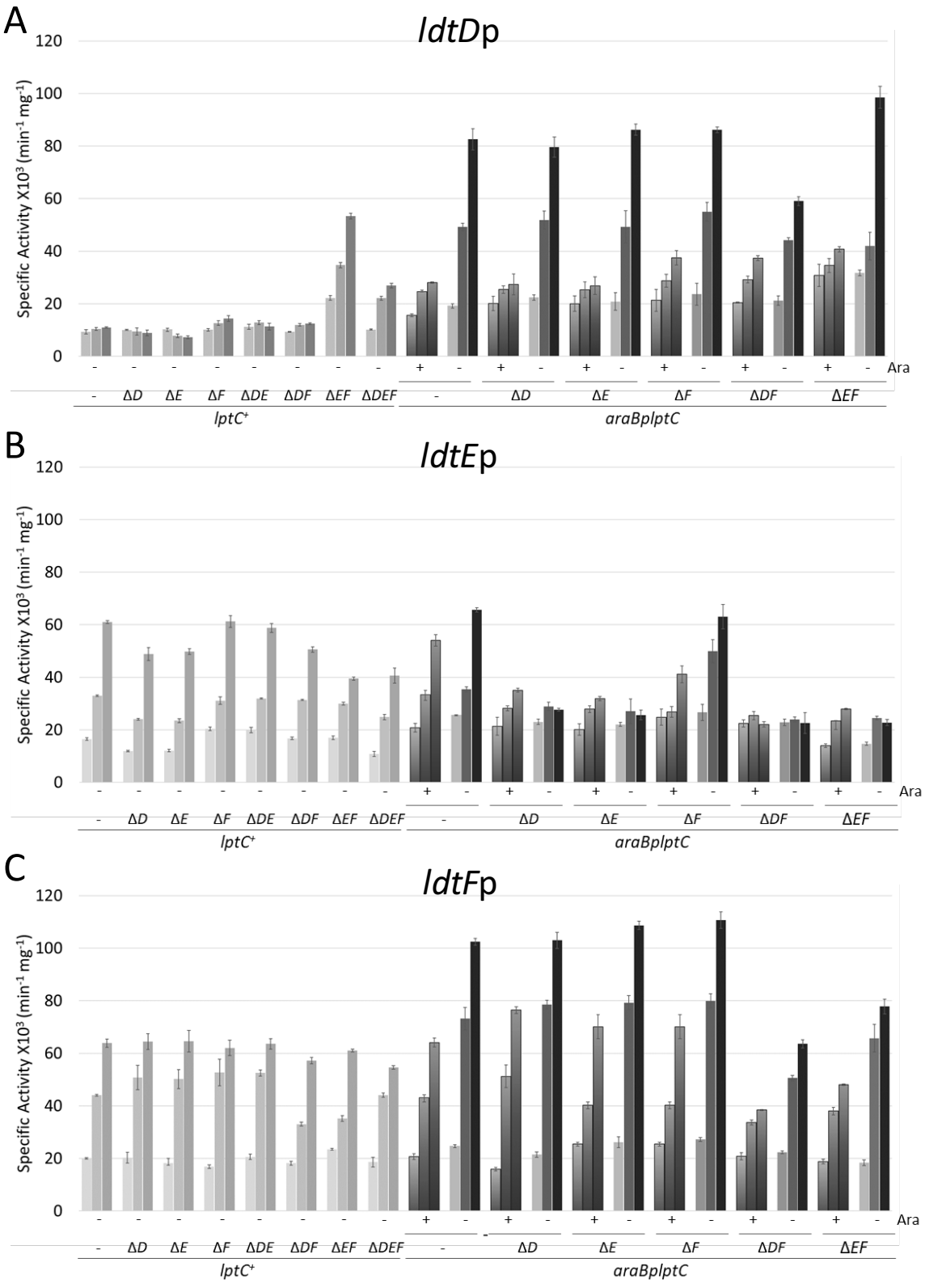
A
ldtDp
B
ldtEp
C
ldtFp
Specific Activity X10³ (min⁻¹ mg⁻¹)
0
20
40
60
80
100
120
Ara
- ΔD ΔE ΔF ΔDE ΔDF ΔEF ΔDEF
lptC+
araBplptC
ΔD ΔE ΔF ΔDF ΔEF

Figure 4

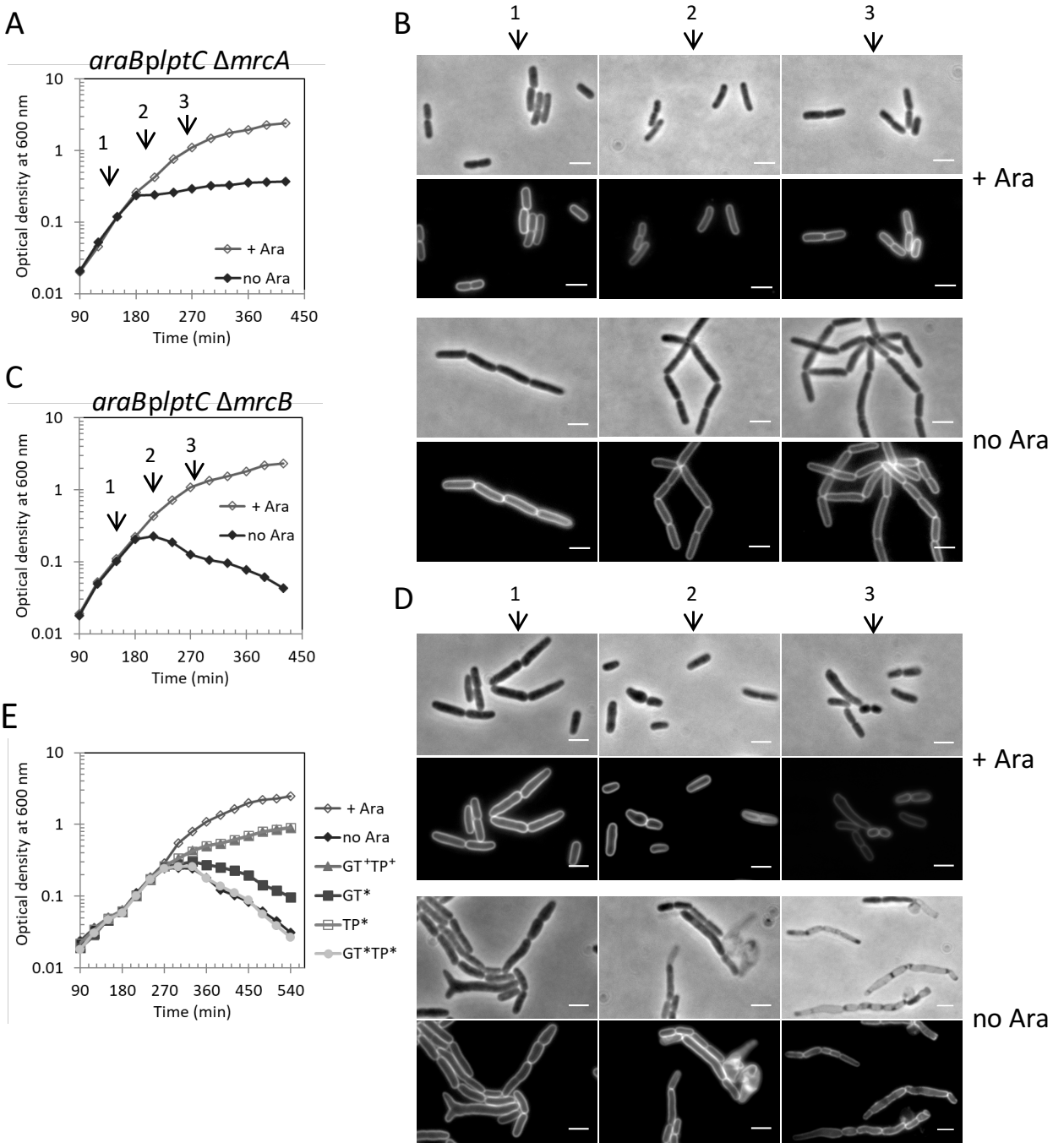
A
araBplptC ΔmrcA
Optical density at 600 nm
Time (min)
+ Ara
no Ara
B
1
2
3
+ Ara
no Ara
C
araBplptC ΔmrcB
D
E
GT+TP+
GT*
TP*
GT*TP*

Figure 5

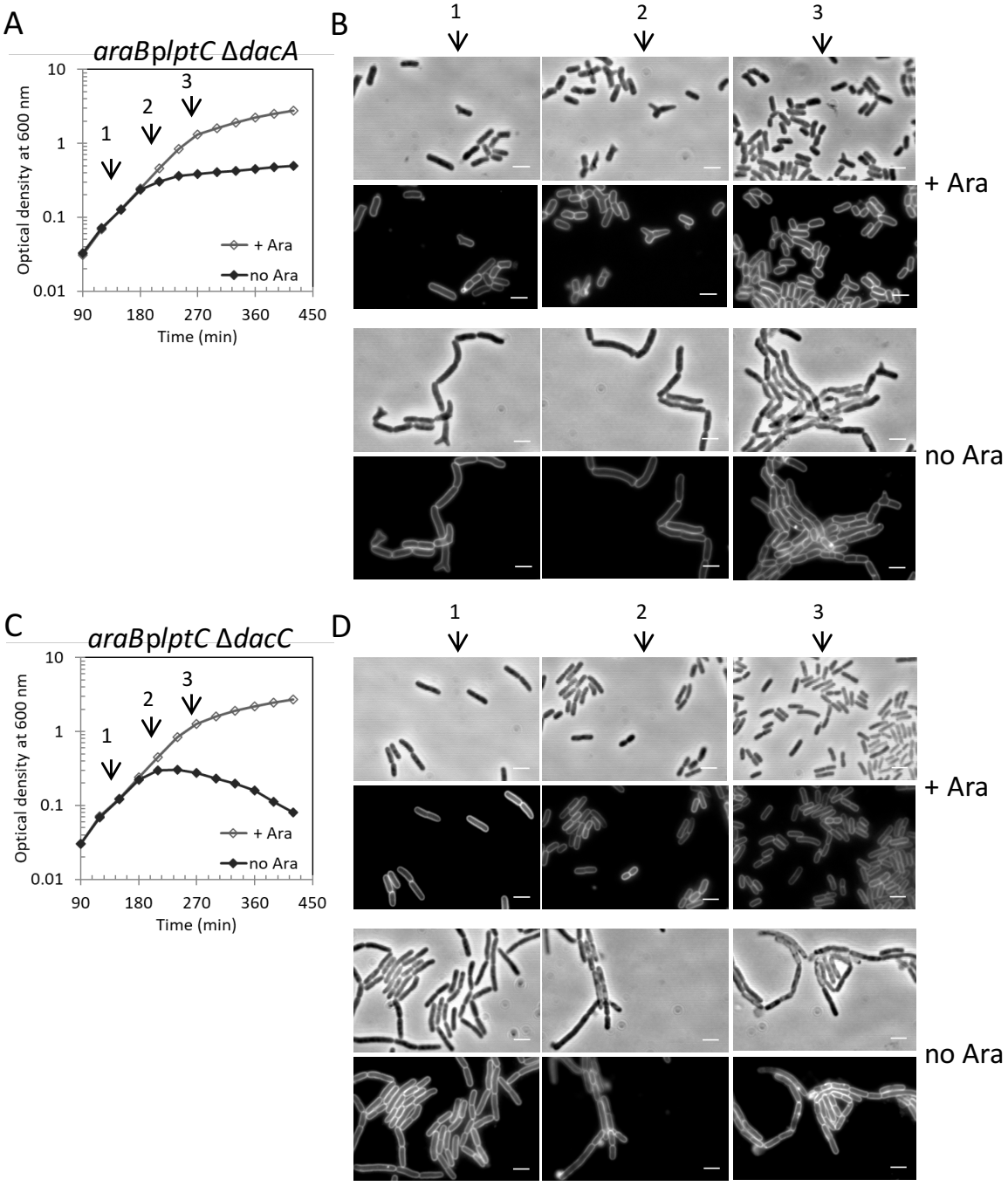
A
araBplptC ΔdacA
Optical density at 600 nm
10
1
0.1
0.01
90
180
270
360
450
Time (min)
1
2
3
+ Ara
no Ara
B
1
2
3
+ Ara
no Ara
C
araBplptC ΔdacC
Optical density at 600 nm
10
1
0.1
0.01
90
180
270
360
450
Time (min)
1
2
3
+ Ara
no Ara
D
1
2
3
+ Ara
no Ara

Figure 6

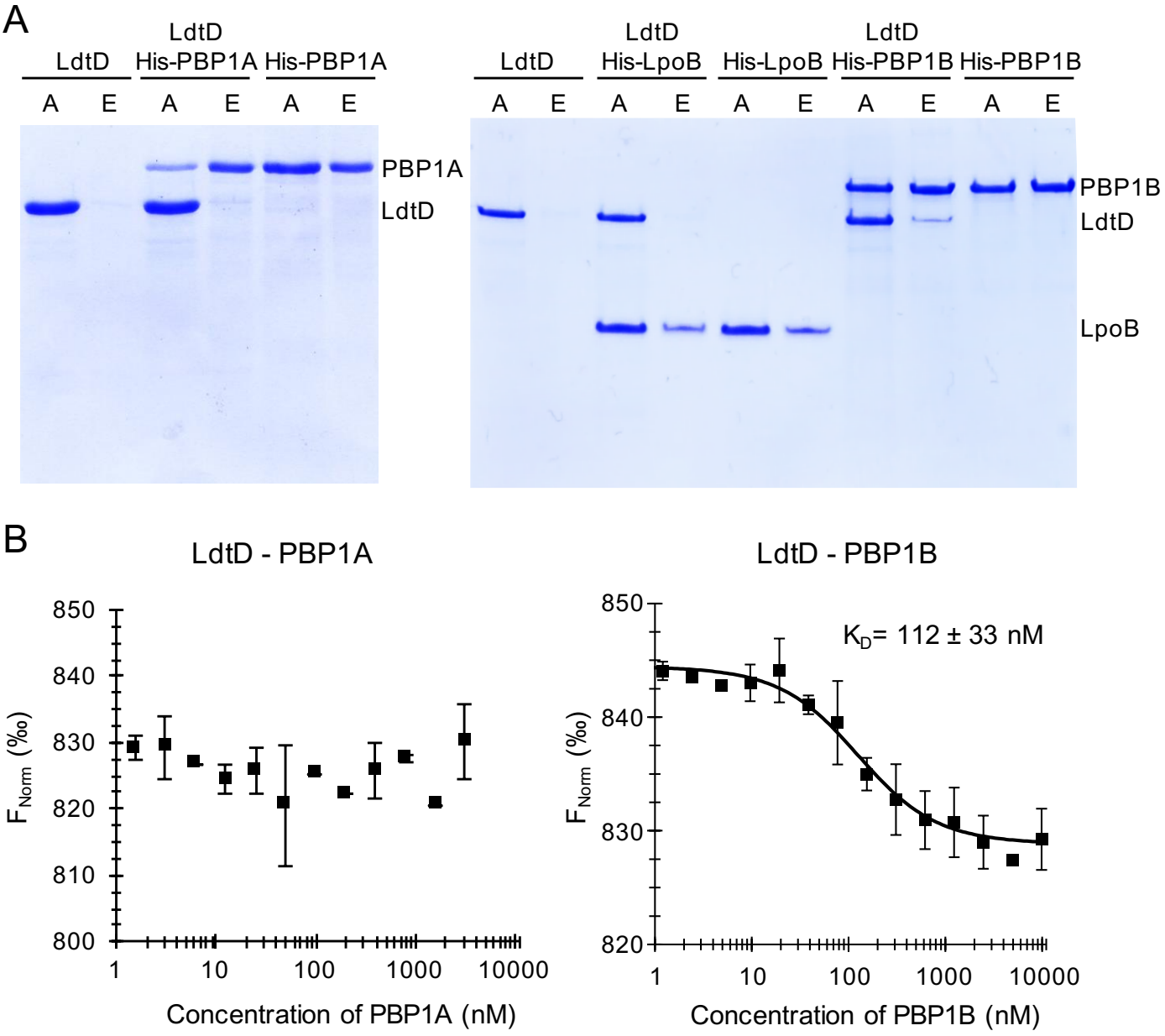
A
LdtD
LdtD
His-PBP1A
His-PBP1A
A E A E A E
PBP1A
LdtD
LdtD
His-LpoB
His-LpoB
LdtD
His-PBP1B
His-PBP1B
A E A E A E A E A E
PBP1B
LdtD
LpoB
B
LdtD - PBP1A
850
840
830
820
810
800
F_Norm (‰)
1
10
100
1000
10000
Concentration of PBP1A (nM)
LdtD - PBP1B
K_D= 112 ± 33 nM
850
840
830
820
F_Norm (‰)
1
10
100
1000
10000
Concentration of PBP1B (nM)

Figure 7

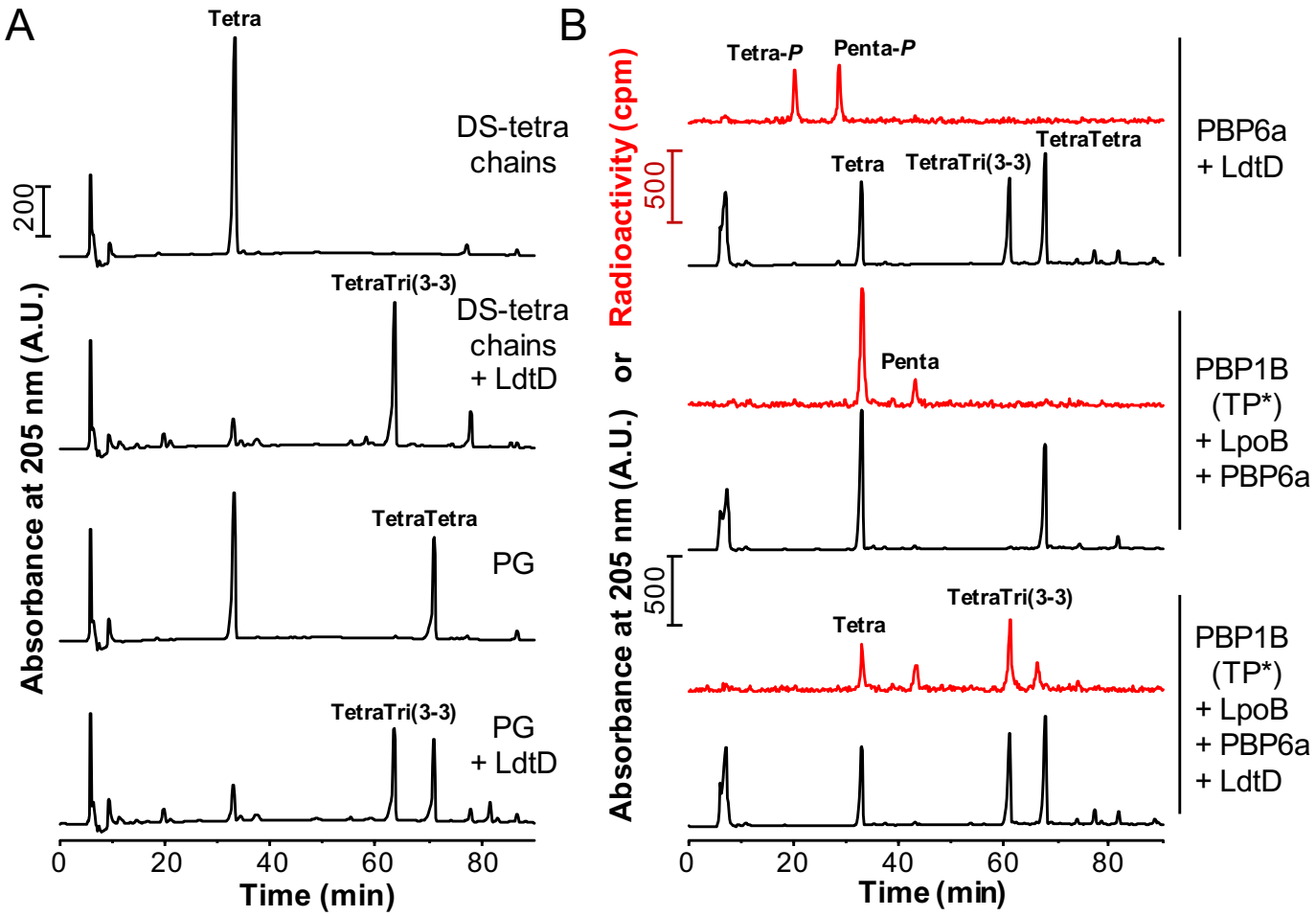
A
Tetra
DS-tetra chains
200
TetraTri(3-3)
DS-tetra chains + LdtD
TetraTetra
PG
TetraTri(3-3)
PG + LdtD
Absorbance at 205 nm (A.U.)
0
20
40
60
80
Time (min)
B
Tetra-P
Penta-P
Tetra
TetraTri(3-3)
TetraTetra
PBP6a + LdtD
500
Penta
PBP1B (TP*) + LpoB + PBP6a
TetraTri(3-3)
Tetra
PBP1B (TP*) + LpoB + PBP6a + LdtD
Radioactivity (cpm) or Absorbance at 205 nm (A.U.)
Time (min)

C

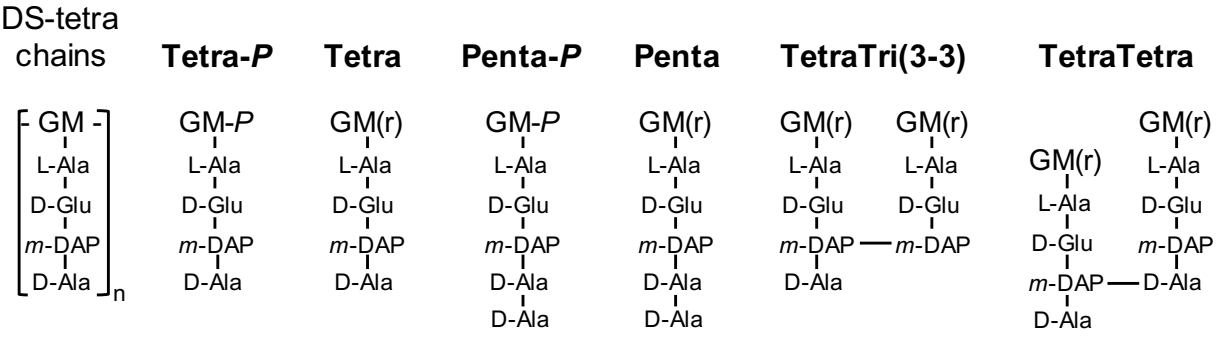
DS-tetra chains
Tetra-P
Tetra
Penta-P
Penta
TetraTri(3-3)
TetraTetra
GM
L-Ala
D-Glu
m-DAP
D-Ala
n
GM-P
GM(r)

Figure 8

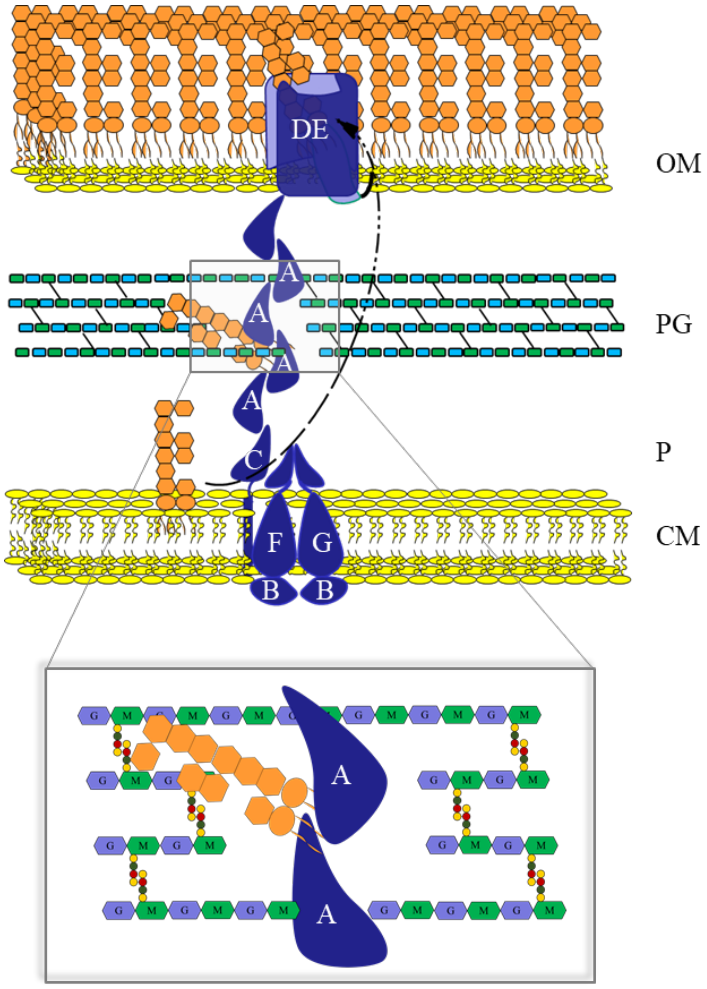
DE
OM
A
A
A
PG
A
C
P
F
G
B
B
CM
A
A

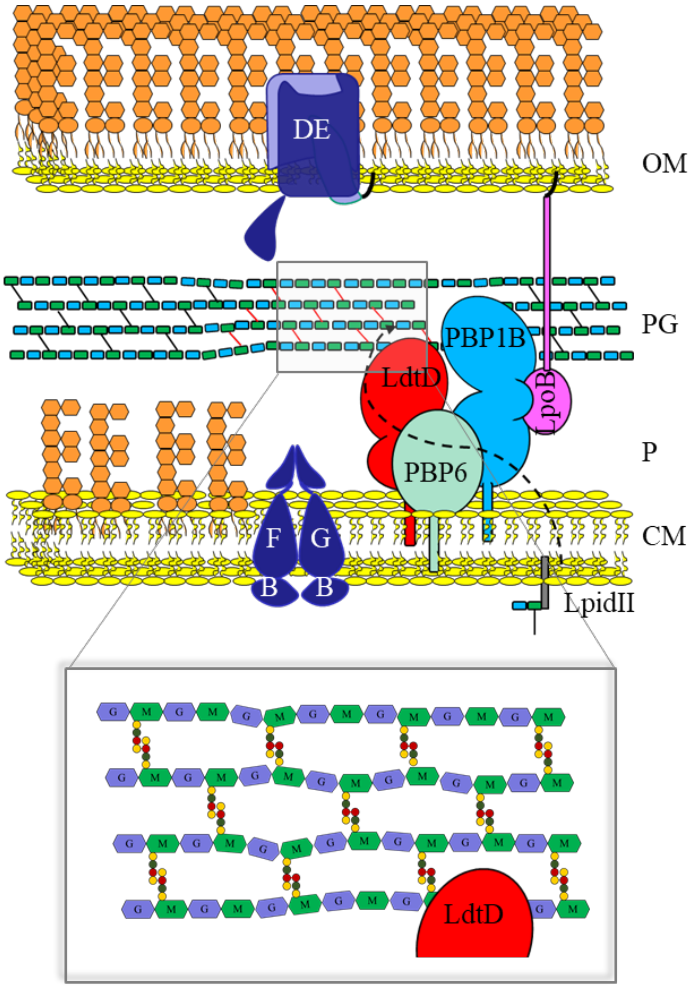
DE
OM
PBP1B
LdtD
LpoB
PG
PBP6
P
F
G
B
B
CM
LpidII
LdtD

Supplemental Information

Peptidoglycan remodeling enables *E. coli* to survive severe outer membrane assembly defect

Niccolò Morè[1], Alessandra M. Martorana[1#], Jacob Biboy[2#], Christian Otten[2], Matthias Winkle[2], Alejandro Montón Silva[3], Lisa Atkinson[2], Hamish Yau[2], Eefjan Breukink[4], Tanneke den Blaauwen[3], Waldemar Vollmer[2*], and Alessandra Polissi[1*]

[1] Dipartimento di Scienze Farmacologiche e Biomolecolari, Università degli Studi di Milano, Milano, Italy.

[2] The Centre for Bacterial Cell Biology, Institute for Cell and Molecular Biosciences, Newcastle University, Newcastle upon Tyne, United Kingdom.

[3] Bacterial Cell Biology and Physiology, Swammerdam Institute for Life Sciences, University of Amsterdam, Amsterdam, The Netherlands.

[4] Membrane Biochemistry and Biophysics, Department of Chemistry, Faculty of Science, Utrecht University, Padualaan 8, 3584 CH Utrecht, The Netherlands.

[#] contributed equally.

*For Correspondence:

Alessandra Polissi: Dipartimento di Scienze Farmacologiche e Biomolecolari, Università degli Studi di Milano, Via Balzaretti 9, 20133 Milano, Italy;

Email: alessandra.polissi@unimi.it; Phone: +39 (02) 503 18205; Fax:

Waldemar Vollmer: The Centre for Bacterial Cell Biology, Institute for Cell and Molecular Biosciences, Newcastle University, Richardson Road, Newcastle upon Tyne, NE2 4AX, United Kingdom; Email: w.vollmer@ncl.ac.uk; Phone: +44 (0) 191 208 3216; Fax: +44 (0) 191 208 3205.

Supplemental Information

Supplementary Table 1: Bacterial strains.

Supplementary Table 2: Plasmids.

Supplementary Table 3: Oligonucleotides.

Supplementary Table 4: Muropeptide composition of *ldt* and *mrcB* mutant strains with or without (separate file) depletion of *lptC*.

Supplemnetary Figure 1: Peptidoglycan cross-linking reactions.

Supplementary Figure 2: Deletion of *ldtD* and *ldtE* in the *araB*p*lptC* conditional strain compromises cell viability under non-permissive conditions.

Supplementary Figure 3: Phenotypes of wild type BW25113 (*lptC*$^{+}$) and *araB*p*lptC* conditional strains lacking *ldtF*.

Supplementary Figure 4: Growth profiles and cell imaging of *araB*p*lptC* Δ*ldtD* Δ*ldtF*, *araB*p*lptC* Δ*ldtD* Δ*ldtE* and *araB*p*lptC* Δ*ldtE* Δ*ldtF*.

Supplementary Figure 5: The simultaneous deletion of *ldtA*, *ldtB* and *ldtC* in the *araB*p*lptC* conditional strain does not impact on cell viability under non-permissive conditions.

Supplementary Figure 6: *LdtE* and *ldtF* are RpoS regulated genes.

Supplementary Figure 7: The PBP1B activator LpoB prevents lysis in *lptC*-depleted cells.

Supplementary Figure 8: LdtD is active during *in vitro* PG synthesis in the presence of PBP1B(TP*), LpoB and PBP5.

Supplementary Table 1. Bacterial Strains.

Strain	Relevant Genotype or Features	Source or Reference
AMM05	BW25113 Δ*ldtD*::frt	This work
AMM06	BW25113 Δ*ldtE*::frt	This work
AMM07	BW25113 Δ*ldtE*::frt Δl*dtD*::frt	This work
AMM10	BB-3 Δ*ldtD*::frt	This work
AMM11	BB-3 Δ*ldtE*::frt	This work
AMM12	BB-3 Δ*ldtD*::frt Δ*ldtE*::frt	This work
AMM14	BB-3 Δ*ldtA*::frt Δ*ldtB*::frt Δ*ldtC*::frt	This work
AMM24	BW25113 Δ*ldtF*::frt	This work
AMM25	BW25113 Δ*ldtD*::frt Δ*ldtF*::frt	This work
AMM26	BW25113 Δ*ldtE*::frt Δ*ldtF*::frt	This work
AMM28	BW25113 Δ*ldtD*::frt Δ*ldtE*::frt Δ*ldtF*::frt	This work
AMM30	BB-3 Δ*ldtF*::frt	This work
AMM31	BB-3 Δ*ldtD*::frt Δ*ldtF*::frt	This work
AMM32	BB-3 Δ*ldtE*::frt Δ*ldtF*::frt	This work
AMM33	BB-3 Δ*ldtA*::frt Δ*ldtB*::frt Δ*ldtC*::frt Δ*ldtD*::frt Δ*ldtE*::frt Δ*ldtF*::frt	This work
AMM34	BB-3 Δ*ldtD*::frt Δ*ldtE*::frt Δ*ldtF*::frt	This work
AMM36	BW25113 Δ*rpoS*:: frt	This work
AMM51	BW25113 Δ*mrcA*::frt	This work
AMM52	BW25113 Δ*mrcB*::frt	This work
AMM53	BW25113 Δ*dacA*::frt	This work
AMM54	BW25113 Δ*dacC*::frt	This work
AMM55	BW25113 Δ*lpoB*::frt	This work
AMM56	BW25113 Δ*cpoB*::frt	This work
AMM60	BB-3 Δ*mrcA*::frt	This work
AMM61	BB-3 Δ*mrcB*::frt	This work
AMM62	BB-3 Δ*dacA*::frt	This work
AMM63	BB-3 Δ*dacC*::frt	This work
AMM64	BB-3 Δ*lpoB*::frt	This work
AMM65	BB-3 Δ*cpoB*::frt	This work
BB-3	BW25113 Φ(*kan araC araB*p*lptC*)1	(Sperandeo et al., 2006)
BL21(DE3)	F– *ompT hsdS*B(rB– mB–) *gal dcm* (DE3)	Novagen
BW25113	*lacI*^{q} *rrnB*$_{T14}$ Δ*lacZ*$_{WJ16}$ *hsdR514* Δ*araBAD*$_{AH33}$ Δ*rhaBAD*$_{LD78}$	(Datsenko and Wanner, 2000)
BW25113Δ6LDT	*lacI*^{q} *rrnB*$_{T14}$ Δ*lacZ*$_{WJ16}$ *hsdR514* Δ*araBAD*$_{AH33}$ Δ*rhaBAD*$_{LD78}$ *ΔycbB ΔerfK ΔycfS ΔybiS ΔynhG ΔyafK*	(Kuru et al., 2017)
DH5α	Δ(*argF-lac169*) ϕ80 *dlacZ58*(M15) *glnV44*(AS) λ^{-} *rfbD1 gyrA96 recA1 endA1 spoT1 thi-1 hsdR17*	(Hanahan, 1983)
JW0732	BW25113 Δ*cpoB*::*kan*	(Baba et al., 2006)
JW0803	BW25113 Δ*ldtB*790::*kan*	(Baba et al., 2006)
JW0908	BW25113 Δ*ldtD*742::*kan*	(Baba et al., 2006)
JW1668	BW25113 Δ*ldtE*753::*kan*	(Baba et al., 2006)
JW1968	BW25113 Δ*ldtA*761::*kan*	(Baba et al., 2006)
JW5820	BW25113 Δ*ldtC*775::*kan*	(Baba et al., 2006)
JW3359	BW25113 Δ*mrcA*::*kan*	(Baba et al., 2006)
JW0145	BW25113 Δ*mrcB*::*kan*	(Baba et al., 2006)
JW5157	BW25113 Δ*lpoB*::*kan*	(Baba et al., 2006)
JW0627	BW25113 Δ*dacA*::*kan*	(Baba et al., 2006)
JW0823	BW25113 Δ*dacC*::*kan*	(Baba et al., 2006)

JW5437	BW25113 Δ*rpoS*::*kan*	(Baba et al., 2006)
LOBSTR-BL21(DE3)	F– *ompT hsdS*B(rB– mB–) *gal dcm* (DE3), carries genomically modified copies of *arnA* and *slyD*	Kerafast

Supplementary Table 2. Plasmids.

Plasmids	Relevant characteristics	Source or Reference
pDACAhis	pET28a(+)derivative, for overexpression of His-PBP5	(Potluri et al., 2010)
pET28a-dacC	pET28a-dacC$^{28\text{-}400}$	This work
pGS100	pGZ119EH derivative, contains TIR sequence downstream of p*tac*, Cam^R	(Sperandeo et al., 2006)
pMN86	pET21b-yebA$^{40\text{-}440}$	(Singh et al., 2012)
pMUCα	pJFK118EH derivative, for ectopic expression of PBP1B	U. Bertsche, W. Vollmer, unpublished
pMUCα(mut)	pJFK118EH derivative, for ectopic expression of PBP1B S510A	U. Bertsche, W. Vollmer, unpublished
pMUC TG(mut)α	pJFK118EH derivative, for ectopic expression of PBP1B E233Q	U. Bertsche, W. Vollmer, unpublished
pMUC TG(mut) α(mut)	pJFK118EH derivative, for ectopic expression of PBP1B S510A E233Q	U. Bertsche, W. Vollmer, unpublished
pRS415	pBR322 derivative; harbors the entire *lac* operon without promoter; Amp^R	(Simons et al., 1987)
pRS415-p*ldtD*	pRS415 derivative; expresses LacZ from the *ldtD* promoter region	This work
pRS415-p*ldtE*	pRS415 derivative; expresses LacZ from the *ldtE* promoter region	This work
pRS415-p*ldtF*	pRS415 derivative; expresses LacZ from the *ldtF* promoter region	This work
pET28a His6-*ldtF*	pET28a derivative; expresses LdtF from the T7 promoter starting from amino acid 20 and fused at N-terminal with 6xHis tag	This work
pETMM82 *dsbC*-His6-*ldtD*	pETMM82 derivative; expresses LdtD fused at N-terminal with DsbC and a 6×His tag	(Hugonnet et al., 2016)
pJEH12(*ldtD*)	pACYC184 derivative; expresses LdtD under the IPTG-inducible *trc* promoter; Tet^R	(Hugonnet et al., 2016)
pAMS01(*ldtE*)	pACYC184 derivative; expresses LdtE under the IPTG-inducible trc promoter; Tet^R	This work
pAMS02(*ldtF*)	pACYC184 derivative; expresses LdtF under the IPTG-inducible *trc* promoter; Tet^R	This work
pSAV057	ptrc99A derivative; contains weakened -35 promotor region (TTGACA-TTTACA); p15 origin; Cam^R	(Alexeeva et al., 2010)
pGS121	pGZ119H derivative; expresses LdtE under the *tac* promoter; Cam^R	This work
pGS124	pGZ119H derivative, expresses LdtF under the *tac* promoter; Cam^R	This work

Supplementary Table 3. Primers

Primer	Sequence 5' -> 3'	Description	Used to make
AP405/39 *ldtE*-f	CCGGAATTCACCATGAAACGCGCGTCTTTCCACTC	[CCG]-[*Eco*RI]-[ACC]-[start *ldtE*; fwd]	pGS121 construction
AP407/34 *ldtE*-r	CCCAAGCTTTTACTGCGTCACGCGTAACATATTC	[CCC]-[*Hind*III]-[TTA]-[stop *ldtE*; rev]	pGS121 construction
AP458/31 *ldtF*-f	CCGGAATTCATGCGTAAAATCGCATTAATTC	[CCG]-[*Eco*RI]-[start *ldtF*; fwd]	pGS124 construction
AP460/34 *ldtF*-r	CCCAAGCTTTTATTTTGCCTCGGGGAGCGTGTAG	[CCC]-[*Hind*III]-[TTA]-[stop *ldtF*; rev]	pGS124 construction
AP475/33 *ldtD*-f	CGAGAGGAATTCGTGGTACAAAGCTGGGAAGAT	[CGAGAG]-[*Eco*RI]-[579 bp upstream of ATG of *ldtD*; fwd]	*ldtD*p cloning in pRS416
AP476/28 ldtD-r	CGCGGATCCTTTGCGTGCGGGCTTTTTC	[CGC]-[*Bam*HI]-[232 bp downstream of ATG of *ldtD*; rev]	*ldtD*p cloning in pRS416
AP477/31 *ldtE*-f	CCGAGAGGAATTCGTATTCACCGTTTGCTGGG	[CCGAGAG]-[*Eco*RI]-[601 bp upsrteam of ATG of *ldtE*; fwd]	*ldtE*p cloning in pRS415
AP478/27 *ldtE*-r	CGCGGATCCGGCGATAGTGTTATTGGC	[CGC]-[*Bam*HI]-[219 bp downstream of ATG of *ldtE*; rev]	*ldtE*p cloning in pRS415
AP490/30 *ldtF*-f	GGAATTCCATATGGGTTTGCTGGGCAGCAG	[GGAATTC]-[*Nde*I]-[starting at 58bp downstream of ATG of *ldtF*; fwd]	pET28a His6-*ldtF* cloning
AP491/29 *ldt*F-r	CCGCTCGAGTTATTTTGCCTCGGGGAGCG	[CCG]-[*Xho*I]-[stop *ldtF*; rev]	pET28a His6-*ldtF* cloning
AP538/32 *ldtF*-f	CGAGAGGAATTCGAATCAGGCAGCGGACGTAC	[CGAGAG]-[*Eco*RI]-[614 bp upstream of ATG of *ldtF*; fwd]	*ldtF*p cloning in pRS415
AP539/29 *ldtF*-r	TCCCCCCGGGCTCGCCCATTTTGACGTAG	[TCCC]-[*Sma*I]-[161 bp downstream of ATG of *ldtF*; rev]	*ldtF*p cloning in pRS416
Pbp6a-sp_for	GCGCGCCATATGGCGGAACAAACCGTTG	[GCGCGC]-[*Nde*I]-[starting at 82 bp downstream of ATG of *dacC*; fwd]	pET28a His6-*dacC* cloning
Pbp6a-sp_rev	GCGCGCCTCGAGTTAAGAGAACCAGCTGCC	[GCGCGC]-[*XhoI*]-[stop *dacC*; rev]	pET28a His6-*dacC* cloning
AMS-GA7h-F	ATTTCACACAGGAAACAGACCATGGATGAAACGC GCGTCTTTGCTTAC	[24 bp complement of pJEH12(*ldtD*)]-[start of *ldtE*; fwd]	pAMS01(*ldtE*) contruction
AMS-GA7h-R	GCATGCCTGCAGGTCGACTCTAGACTACTGCGTCA CGCGTAACATATTC	[24 bp complement of pJEH12(*ldtD*)]-[stop of *ldtE*; fwd]	pAMS01(*ldtE*) contruction
AMS-GA7a_F	ATTTCACACAGGAAACAGACCATGGATGCGTAAA ATCGCATTAATTC	[24 bp complement of pJEH12(*ldtD*)]-[start of *ldtF*; fwd]	pAMS02(*ldtF*) contruction
AMS-GA7a_R	GCATGCCTGCAGGTCGACTCTAGATTATTTTGCCT CGGGGAGCG	[24 bp complement of pJEH12(*ldtD*)]-[stop of *ldtF*; fwd]	pAMS02(*ldtF*) contruction
AMS-GA7_F	TCTAGAGTCGACCTGCAGGCATGC	pACYC plasmid linearization for Gibson; fwd	pAMS01(*ldtE*) and pAMS2(*ldtF*) contruction
AMS-GA7_R	CCATGGTCTGTTTCCTGTGTGAAATT	pACYC plasmid linearization for Gibson; rev	pAMS01(*ldtE*) and pAMS2(*ldtF*) contruction

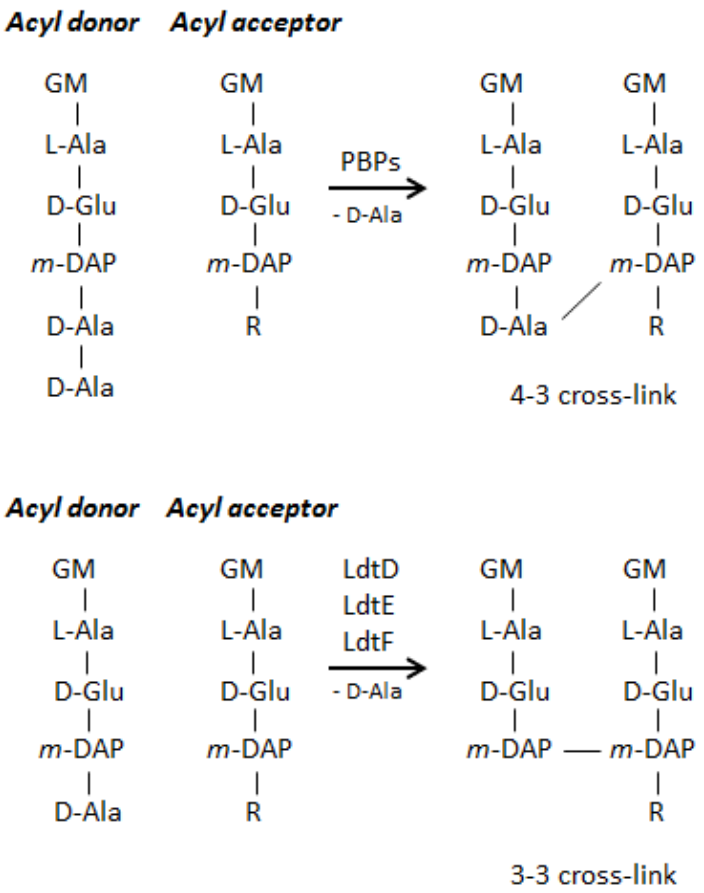

Supplementary Figure S1. Peptidoglycan cross-linking reactions catalyzed by the DD-transpeptidases (PBPs, top) and the LD-transpeptidases (LdtD, LdtE and LdtF, bottom) resulting in 4-3 and 3-3 cross-links, respectively. G, *N*-acetylglucosamine (G); M, *N*-acetylmuramic acid; R indicates H, D-Ala or D-Ala-D-Ala.

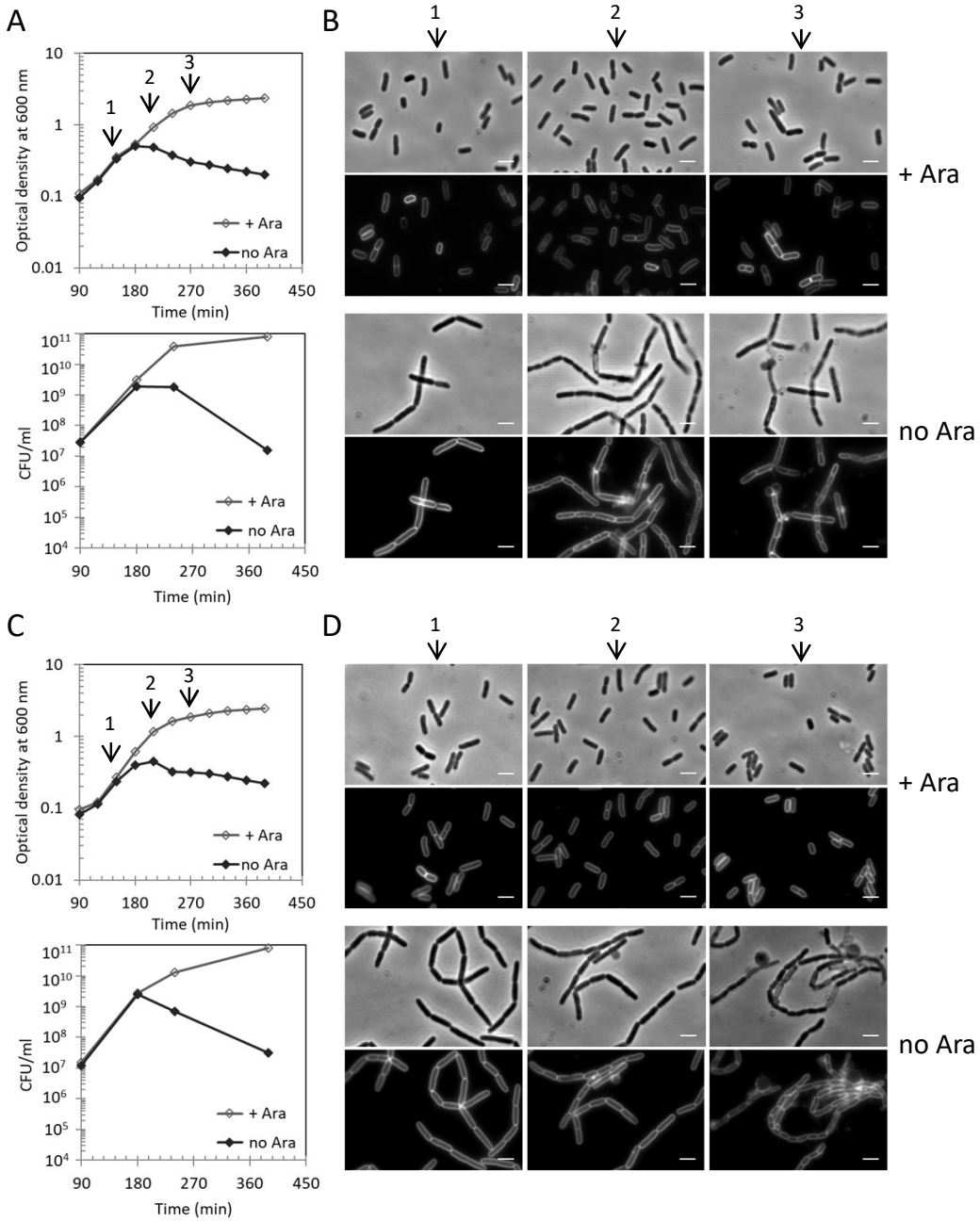

Supplementary Figure S2. Deletion of *ldtD* and *ldtE* in the *araB*p*lptC* conditional strain compromises cell viability under non-permissive conditions. Cells of *araB*p*lptC* Δ*ldtD* (**A**) and *araB*p*lptC* Δ*ldtE* (**C**) were grown in the presence of 0.2% arabinose to an OD_{600} of 0.2, harvested, washed three times and resuspended in an arabinose-supplemented (+ Ara) or arabinose-free (no Ara) medium. Cell growth was monitored by OD_{600} measurements (upper panels) and viability was assessed by determining CFU (lower panels). At t = 120 min, 210 min and 270 min (arrows), a*raB*p*lptC* Δ*ldtD* (**B**) and *araB*p*lptC* Δ*ldtE* (**D**) cells were collected for imaging. Phase contrast images are on the top and fluorescence images are on the bottom. Scale bars, 3 μm.

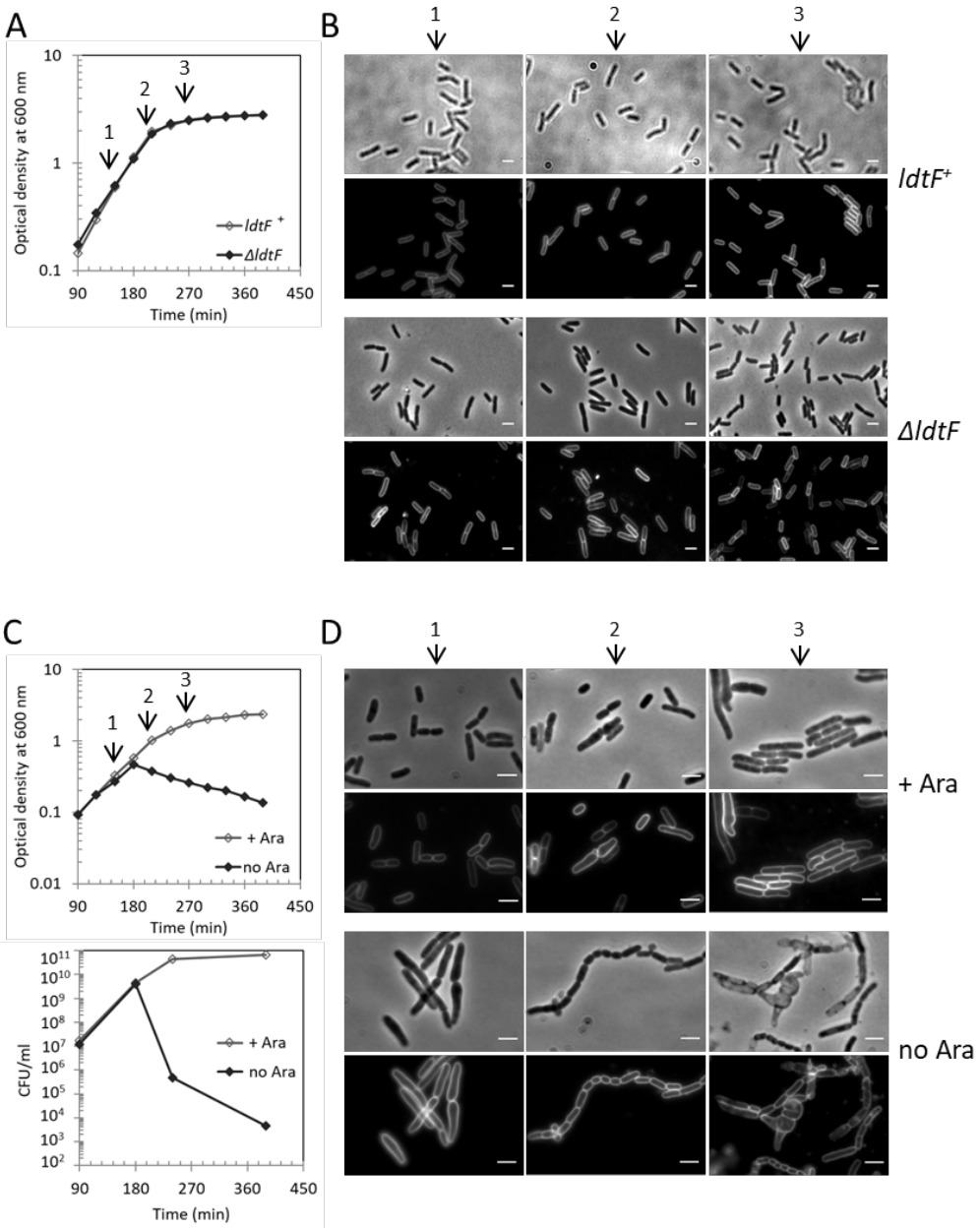

Supplementary Figure S3. Phenotypes of wild type BW25113 (*lptC*$^{+}$) and *araB*p*lptC* conditional strains lacking *ldtF*. Cells of BW25113, the isogenic Δ*ldtF* mutant (**A**) and the *araB*p*lptC* Δ*ldtF* mutant (**C**) were grown in the presence of 0.2% arabinose to an OD_{600} of 0.2, harvested, washed three times and resuspended in an arabinose-supplemented (+ Ara) or arabinose-free (no Ara) medium. Cell growth was then monitored by OD_{600} measurements (upper panels) and viability was assessed by determining the CFU (lower panels). At t = 120 min, 210 min and 270 min (arrows), BW25113 and BW25113 Δ*ldtF* (**B**) and *araB*p*lptC* Δ*ldtF* (**D**) cells were collected for imaging. Phase contrast images are on the top and fluorescence images are on the bottom. Scale bars 3 µm. *araB*p*lptC* Δ*ldtF* cells displayed morphological defects even when grown under permissive conditions.

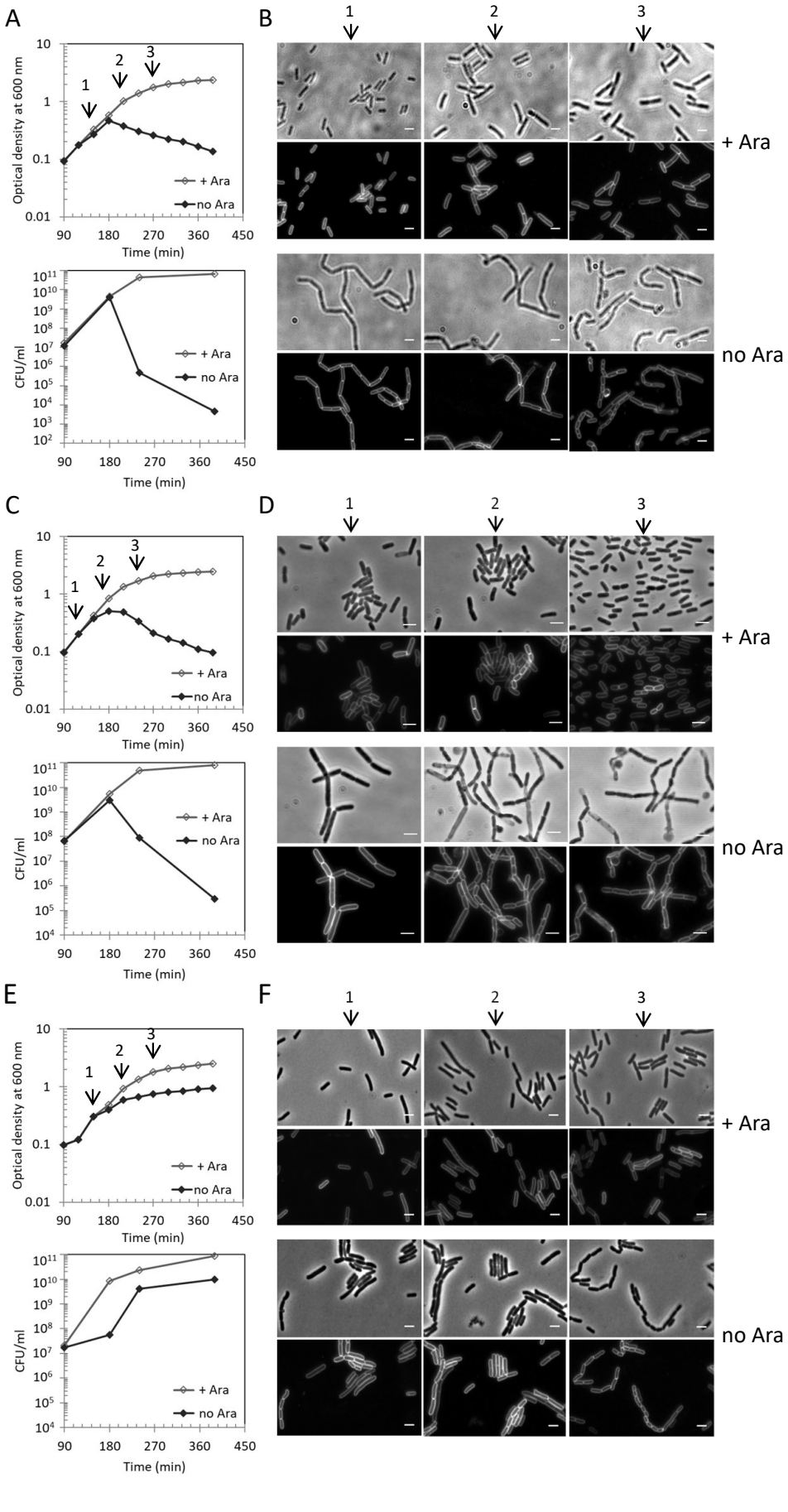
A
B
C
D
E
F
1
2
3
Optical density at 600 nm
CFU/ml
Time (min)
+ Ara
no Ara
+ Ara
no Ara

Supplementary Figure S4. Growth profiles and cell imaging of *araB*p*lptC* Δ*ldtD* Δ*ldtF*, *araB*p*lptC* Δ*ldtD* Δ*ldtE* and *araB*p*lptC* Δ*ldtE* Δ*ldtF*. Cells of *araB*p*lptC* Δ*ldtD* Δ*ldtF* (**A**, **B**), *araB*p*lptC* Δ*ldtD* Δ*ldtE* (**C**, **D**) and *araB*p*lptC* Δ*ldtE* Δ*ldtF* (**E**, **F**) were grown and imaged as described in the legend of Supplementary Figure 2. *araB*p*lptC* Δ*ldtE* Δ*ldtF* cells did not lyse under non-permissive conditions (no Ara).

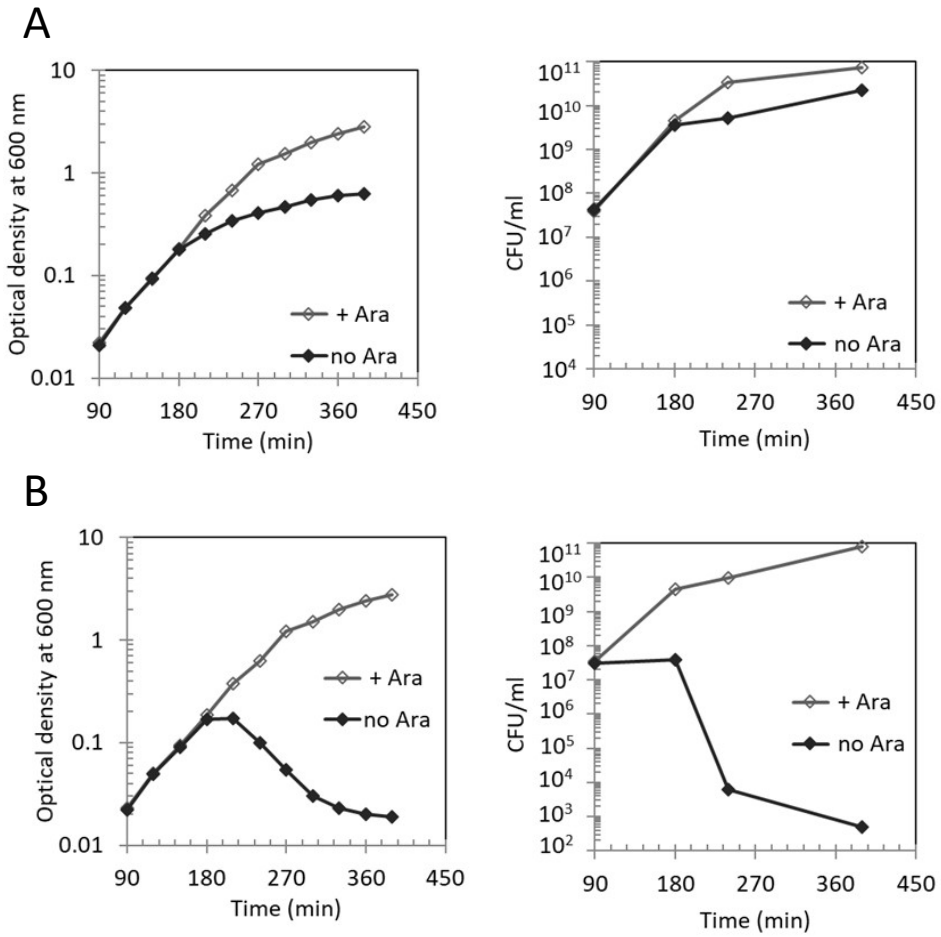

Supplementary Figure S5. The simultaneous deletion of *ldtA*, *ldtB* and *ldtC* in the *araB*p*lptC* conditional strain has no impact on cell viability under non-permissive conditions. Cells of the *araB*p*lptC* conditional strain with deletions of *ldtA*, *ldtB* and *ldtC* (**A**) and all six *ldt* genes (*ldtA*, *ldtB, ldtC*, *ldtD*, *ldtE* and *ldtF*) (**B**) were grown in the presence of 0.2% arabinose to an OD_{600} of 0.2, harvested, washed three times and resuspended in an arabinose-supplemented (+ Ara) or arabinose-free (no Ara) medium. Cell growth was then monitored by OD_{600} measurements and viability was assessed by determining the CFU.

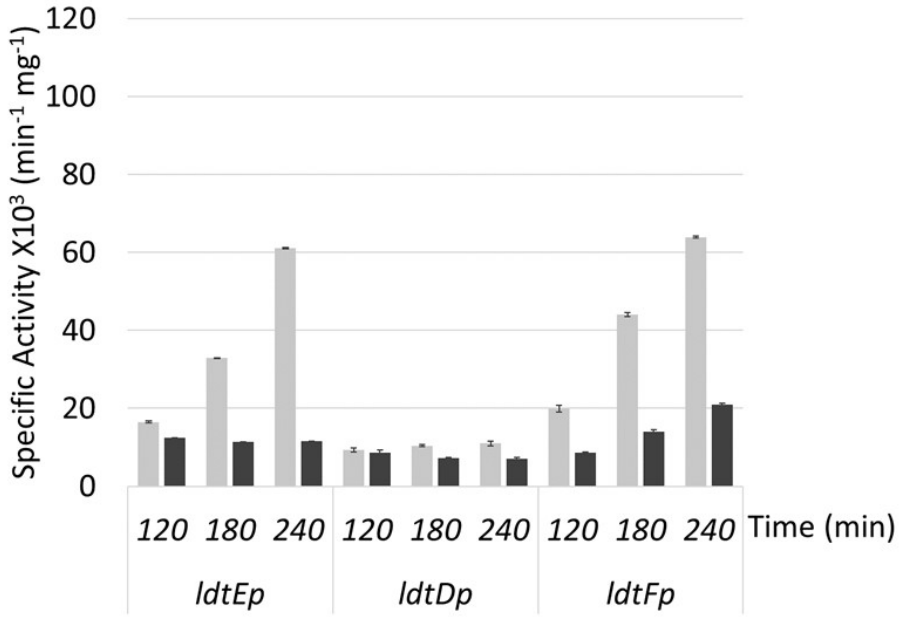

Supplementary Figure S6. *LdtE* and *ldtF* are RpoS regulated genes. BW25113 Δ*rpoS* cells carrying plasmids expressing *ldtD*p-*lacZ*, *ldtE*p-*lacZ* or *ldtF*p-*lacZ* fusions, were grown in LD broth. β-galactosidase specific activity was determined from cells collected at 120 min (OD_{600}= 0.2), 180 min (OD_{600}=0.8) and 210 min (OD_{600}=2.0). BW25113, light grey bars; BW25113Δ*rpoS*, grey bars. Note that *ldtD* expression is not affected in a Δ*rpoS* background.

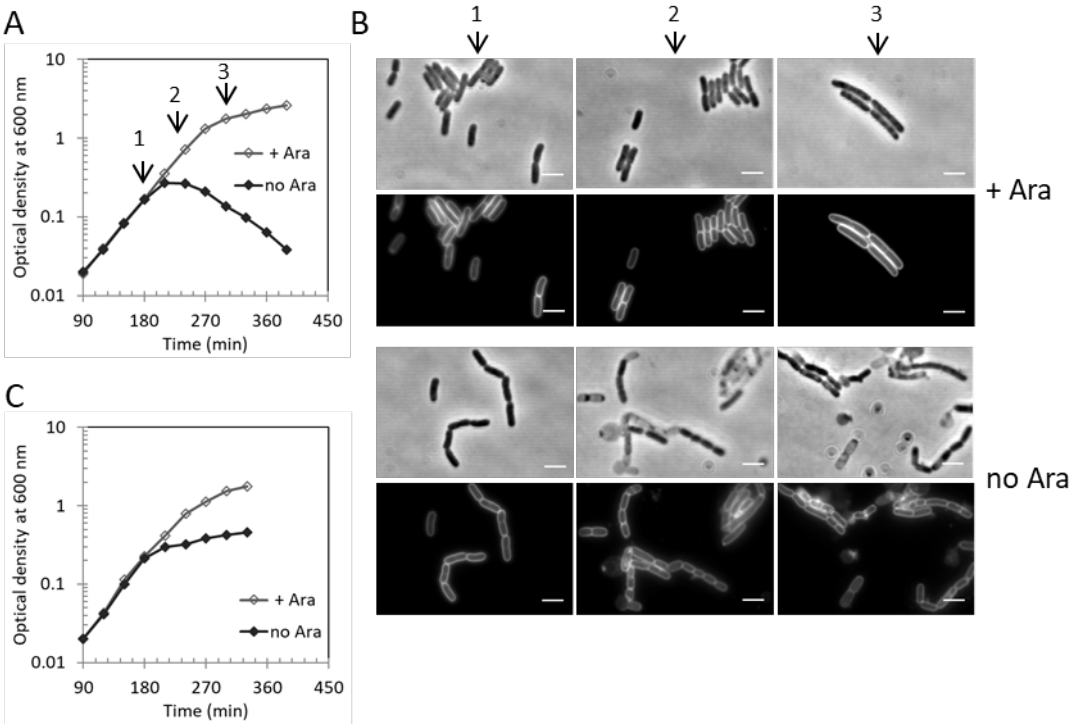

Supplementary Figure S7. Growth profiles of *araB*p*lptC* conditional strain lacking *lpoB* or *cpoB*. The PBP1B activator LpoB prevents lysis in *lptC*-depleted cells (**A, B**) whereas deletion of *cpoB* has no impact on cell viability (**C**). Cells of *araB*p*lptC* Δ*lpoB* and *araB*p*lptC* Δ*cpoB* were grown (**A, C**) and imaged (**B**) as described in the legend of Supplementary Figure 2.

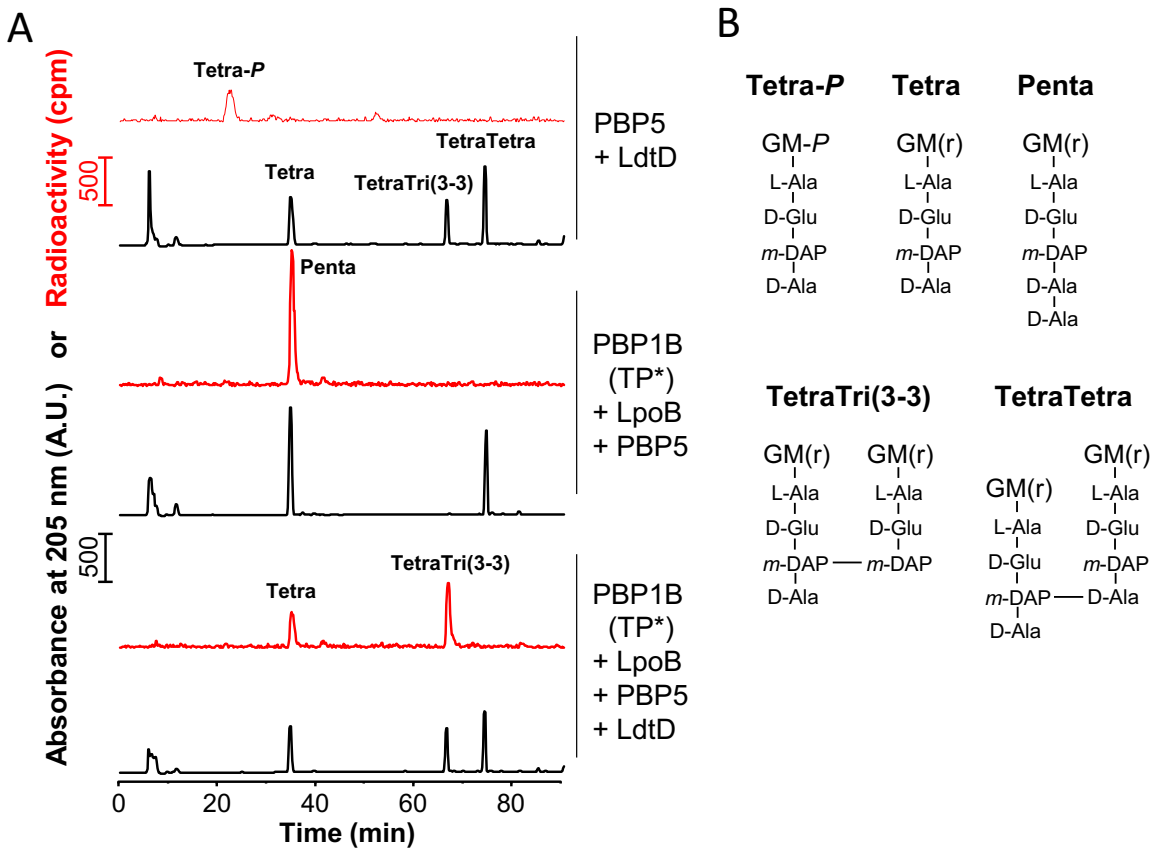

Supplementary Figure S8. LdtD is active during *in vitro* PG synthesis in the presence of PBP1B(TP*), LpoB and PBP5. (**A**) HPLC chromatograms obtained from samples containing radioactive lipid II, PG from *E. coli* BW25113ΔLDT and the proteins indicated on the right side. (**B**) Proposed structures of muropeptides shown in panel A and B. G, *N*-acetylglucosamine; M, *N*-acetylmuramic acid; M(r), *N*-acetylmuramitol; M-*P*, N-acetylmuramic acid-1-phosphate; L-Ala, L-alanine; D-Glu, D-glutamic acid; D-Ala, D-alanine; *m*-DAP, *meso*-diaminopimelic acid.

Supplemental References

Alexeeva, S., Gadella, T.W., Jr., Verheul, J., Verhoeven, G.S., and den Blaauwen, T. (2010). Direct interactions of early and late assembling division proteins in *Escherichia coli* cells resolved by FRET. Mol Microbiol *77*, 384-398.

Baba, T., Ara, T., Hasegawa, M., Takai, Y., Okumura, Y., Baba, M., Datsenko, K.A., Tomita, M., Wanner, B.L., and Mori, H. (2006). Construction of *Escherichia coli* K-12 in-frame, single-gene knockout mutants: the Keio collection. Mol Syst Biol *2*, 2006 0008.

Datsenko, K.A., and Wanner, B.L. (2000). One-step inactivation of chromosomal genes in *Escherichia coli* K-12 using PCR products. Proc Natl Acad Sci U S A *97*, 6640-6645.

Hanahan, D. (1983). Studies on transformation of *Escherichia coli* with plasmids. J Mol Biol *166*, 557-580.

Hugonnet, J.E., Mengin-Lecreulx, D., Monton, A., den Blaauwen, T., Carbonnelle, E., Veckerle, C., Brun, Y.V., van Nieuwenhze, M., Bouchier, C., Tu, K.*, et al.* (2016). Factors essential for L,D-transpeptidase-mediated peptidoglycan cross-linking and beta-lactam resistance in *Escherichia coli*. eLife *5*:e19469.

Kuru, E., Lambert, C., Rittichier, J., Till, R., Ducret, A., Derouaux, A., Gray, J., Biboy, J., Vollmer, W., VanNieuwenhze, M.*, et al.* (2017). Fluorescent D-amino-acids reveal bi-cellular cell wall modifications important for *Bdellovibrio bacteriovorus* predation. Nat Microbiol 3(2):254.

Potluri, L., Karczmarek, A., Verheul, J., Piette, A., Wilkin, J.M., Werth, N., Banzhaf, M., Vollmer, W., Young, K.D., Nguyen-Disteche, M.*, et al.* (2010). Septal and lateral wall localization of PBP5, the major D,D-carboxypeptidase of *Escherichia coli*, requires substrate recognition and membrane attachment. Mol Microbiol *77*, 300-323.

Simons, R.W., Houman, F., and Kleckner, N. (1987). Improved single and multicopy *lac*-based cloning vectors for protein and operon fusions. Gene *53*, 85-96.

Singh, S.K., SaiSree, L., Amrutha, R.N., and Reddy, M. (2012). Three redundant murein endopeptidases catalyse an essential cleavage step in peptidoglycan synthesis of *Escherichia coli* K12. Mol Microbiol *86*, 1036-1051.

Sperandeo, P., Pozzi, C., Dehò, G., and Polissi, A. (2006). Non-essential KDO biosynthesis and new essential cell envelope biogenesis genes in the *Escherichia coli yrbG-yhbG* locus. Res Microbiol *157*, 547-558.

5. Conclusions

In this study, we focused on the mechanism by which *E. coli* cells respond to severe outer membrane defects due to the block of LPS transport by remodelling PG architecture. First of all, we analyzed the structure of the PG upon block of LPS transport and found a strong increase in the non canonical 3-3 cross-linkage in the sacculus. This result represents the first evidence that Lpt machinery and PG biosynthetic apparatus are functionally connected. Until now, the sole known LDTs that in *E. coli* catalyzed this unusual cross-link were LdtD and LdtE. Using bioinformatics analysis, we found another hypothetical *ldt* gene, *ldtF*, which shares similarity with the other LDTs, so we decided to include even this new LDT in our study. We found that LdtF is an active LDT that catalyzes the formation of 3-3 crosslinks in the PG in the absence of LdtD and LdtE. Mutants deleted for the three *ldt*s are viable despite the absence of 3-3 cross-linkage, confirming that this kind of cross-link is not essential for *E. coli* survival under standard growth conditions. On the contrary, LDT activity became essential to prevent lysis in cells with defective LPS transport. We reasoned that LDTs might be essential in cells with defective LPS transport because the level of 3-3 cross-links increased in *lptC*-depletion. To better understand the role of these LDTs we deleted every *ldt* gene alone or in all possible combinations in the background of *araB*p*lptC* conditional mutant and we examined the growth phenotype and the level of 3-3 cross-links. These results suggested us that the expression of *ldtD*, *ldtE* and *ldtF* is differently regulated in the cell. To better understand how these LDTs are regulated during cell cycle and upon envelope stress, we evaluated the expression profile in wild-type background and in the conditional *araB*p*lptC* background. We observed that *ldtD*, *ldtE* and *ldtF* exhibited very different expression profiles depending on the genetic background, growth phase and growth conditions. In particular we found that LdtE and LdtF are the housekeeping LDTs that work in concert in the cell in non-stress conditions; on the contrary LdtD is exclusively expressed under stress conditions and indeed LdtD alone is able to prevent cell lysis upon LptC depletion namely when LPS transport is blocked. In literature it is already known that LdtD is induced in response to Cpx activating conditions, it should be tested that even the block of LPS transport could active the Cpx response through the activation of *ldtD*. In the last part of this work, using a combination of biochemical and genetic approaches we proved that the PG remodeling programme activated in response to envelope stress involves not only LdtD but also PBP1B, one of the two major bifunctional PG synthase, and the DD-CPase PBP6a. We

suggested that in cells where the biogenesis of the OM is defective PBP1B, LdtD and PBP6a work together to synthetize new PG strands produced by the GTase activity of PBP1B, which are trimmed by PBP6a and consequently cross-linked by LdtD. It should be tested if some other proteins are involved in this remodeling programme, maybe with some second role. However, we can hypothesize that the LPS-transport machinery requires wider pores in the PG layer, and that the PG net is opened locally, probably by some specific muramidases, to allow assembly of the Lpt machinery and rapid flow of the LPS to the cell surface. According to this hypothesis we propose that PBP1B, LdtD and PBP6a constitute a dedicated PG 'repair' machine that became essential to fill the PG holes left open by the disassembled Lpt machinery. We can conclude that the role of 3-3 cross-links is to locally fortify the sacculus after the disassembly of macromolecular complexes, filling the holes to ensure the survival of the cell. Could be interesting analyze the localization of these scar regions in the cells, maybe using D-fluorescence aminoacid or fluoresce probes, to gain more information about the localization of the Lpt machinery or the localization of this repair machine during cell cycle.

Our model implies a functional connection between Lpt machinery and PG synthetic apparatus, underlining the fact that the OM biogenesis and PG synthesis need to be finely coordinated. This work presents major new insight into the correlation between the OM and the PG, linking it with proteins involved in the repair mechanism, with the first demonstration of the essentiality of LDTs in conditions of OM damage. All together these result show us that bacteria invest a great deal in protecting their envelope, thus improving our understanding of the regulation of fundamental processes in bacteria is a key step in the development of new antibacterial, an attempt which has become more and more pressing due to the increasing prevalence of pathogens resistant to multiple compounds.

Ringraziamenti

Un sentito ringraziamento va alla Prof.ssa Alessandra Polissi, che mi ha dato l'opportunità di far parte del suo laboratorio e che con tanta pazienza e tanta disponibilità mi ha aiutato a svolgere al meglio il mio progetto di dottorato.
Un grazie particolare va ad Ale che mi ha aiutato durante tutti questi tre anni di dottorato.
Grazie anche a Paolina, Fiffi, Franco, Adelina, Giulia, Lamberto che hanno reso un piacere e non un dovere il lavoro quotidiano in laboratorio.
Grazie a tutti gli amici di Bicocca e ai colleghi di dottorato che mi hanno sempre sostenuto e hanno condiviso con me gioie e fatiche, tra birre e nottate di lavoro.
Grazie a Waldemar per avermi ospitato nel suo laboratorio e avermi permesso di svolgere al meglio il mio lavoro con continui suggerimenti e sproni. Come dimenticarsi dei ragazzi del CBCB con i quali ho condiviso fatiche e birre, un grande grazie anche a voi.
Un sentito ringraziamento va a Te, che nonostante tutto condividi con me risate e fatiche nonostante la mia terribile memoria da pesce rosso.
Grazie anche a te Sfiggi, senza di te sarebbe stato tutto più difficile e più triste.
Il grazie più sentito va a mio padre Galiano che mi ha sempre spronato a dare il massimo, a mia madre Maria che mi aiuta a tenere i piedi per terra, e infine alla mia sorellona Barbara alla quale voglio un gran bene.